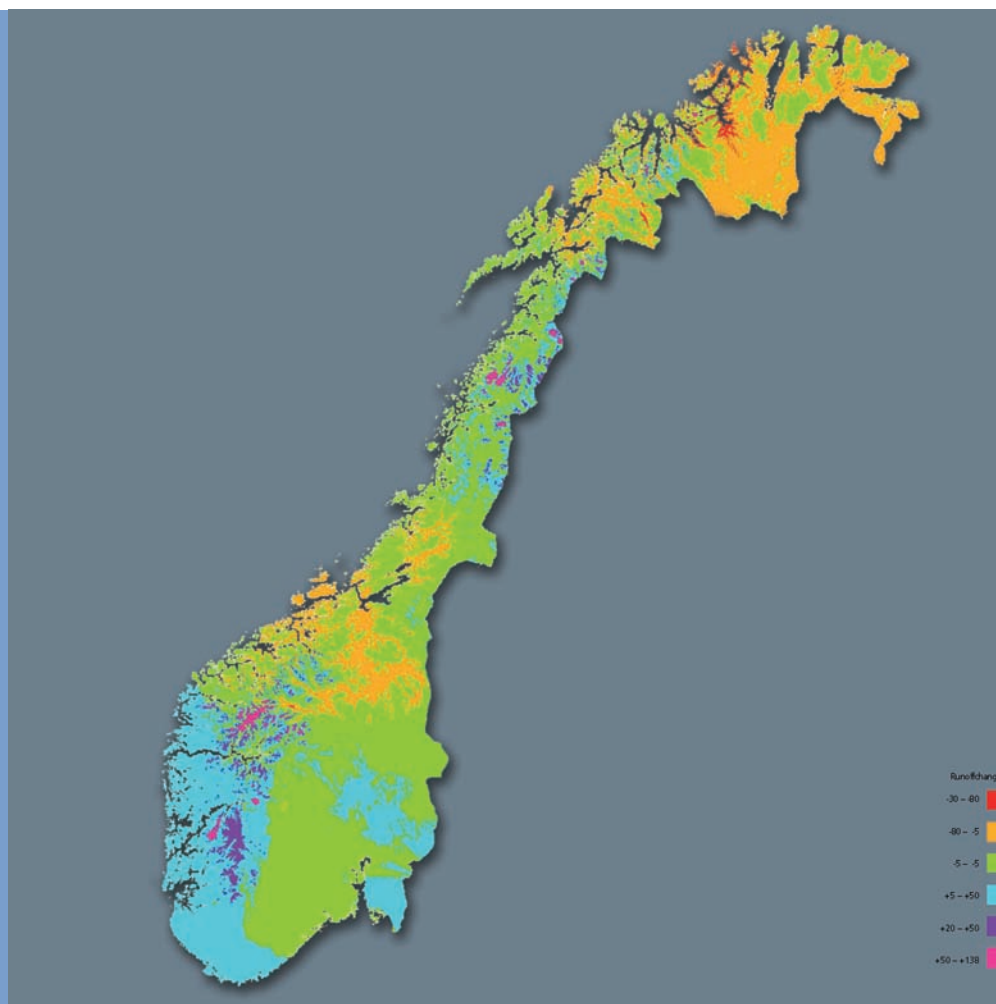# Climate change impacts on streamflow in Norway

Lars A. Roald,NVE
Stein Beldring,NVE
Torill Engen Skaugen, met.no
Eirik J. Førland, met.no
Rasmus Benestad, met.no

Runoff change

-30 – -80
-80 – -5
-5 – -5
+5 – +50
+20 – +50
+50 – +138

Climate change impacts on streamflow in Norway

Lars A. Roald, Stein Beldring, Torill Engen Skaugen, Eirik J. Førland and Rasmus Benestad

Consultancy report A no 1-2006

Climate change impacts on streamflow in Norway

Sammendrag:

Emneord: streamflow, snow, evaporation, ground water, soil moisture deficit, depth of frozen soil, climate change

Contents

Preface

The Norwegian Meteorological Institute (met.no) and the Norwegian Water Resources and Energy Directorate (NVE) have co-operated in the project "Climate change and Energy Production Potential". The project started in 2001 and is completed at the end of 2005. It has been funded by the Norwegian Electricity Industry Association (EBL) and by the Research Council of Norway (NFR) as well as by contributions from NVE and met.no.

Oslo, January 2006

Morten Johnsrud
Director Hydrology Department

Svein Taksdal
Section manager, Data Section

4

Summary

Scenarios are developed for the mean and seasonal streamflow and other water balance elements for Norway for the period 2071-2100 based on dynamically downscaled series of temperature and precipitation based on the most recent scenarios from RegClim. The scenarios are based on projections based on both the HadAm3H- and the ECHAM4/OPYC3 Global Climate Models under emission scenarios A2 and B2. The projection of possible future streamflow and the other water balance elements are simulated by the Gridded Water Balance Model. The results are presented both on countrywide maps and in more detail for 25 basins. The changes are given relative to the most recent normal period 1961-1990. The report discusses also possible changes in the occurrence of floods and implications of possible changes in the year to year variability for future energy production.

1 Introduction

Global warming of the surface temperature with approximately 0.6 °C has been observed the last 100 years. Different emission scenarios project a further increase of global temperature between 1 °C to 5 °C (Cubash et al., 2001). Globally averaged water vapour concentrations, evaporation and precipitation are projected to increase. At regional scale both increases and decreases in precipitation are projected. The projections of the development of precipitation, however, are even more uncertain than for temperature (Benestad, 2002).

Climate scenarios are produced by Atmospheric-Ocean General Circulation Models (AOGCMs). The spatial resolution of AOGCMs is quite coarse, typically about 3° or 4° in latitude and from 4° to 10° in longitude. The regional and local details of the climate at that scale are lost. As stated by Wood et al (2004); "A minimum standard of any useful downscaling method for hydrological applications needs the historic (observed) conditions to be reproducible". Different downscaling methods are developed to overcome this problem, dynamically, empirically or these two techniques in combination (e.g. Giorgi et al., 2001), to obtain higher resolution for regions or at site locations.

The focus in impact assessments due to climate change is increasing. A regional pattern with focus on a shift in the future climate compared to present may be satisfactory for some assessments. When studying the hydrological cycle, however, these difficulties are huge (Bronstert, 2004; Wood et al., 2004). The limitations of the AOGCMs rainfall estimates is well known, and different methods has been used to omit the problem; the delta change, or perturbation method has been widely used (Middelkoop et al., 2001; Reynard et al, 2001, Lettenmaier et al., 1999). Because of the uncertainty connected to the scenarios, especially to precipitation estimates, the focus in climate-change impact studies on water resources in Scandinavia has mainly been on the mean changes on a national or regional level (Roald et al., 2002; Sælthun et al., 1998). In the present study, analyses have been performed on hydrological scenarios with focus on shift in hydrological regime and droughts versus floods. To be able to do so, an empirical adjustment method has been used to tailor the climate scenarios to station level (Engen-Skaugen, 2004).

This report presents projected changes in various water balance elements for the Norwegian mainland and in more detail for 21 Norwegian basins examined and summarised in Engen-Skaugen et al (2005) and for four additional basins in mountainous areas in South Norway. The report summarises possible changes in the occurrence and severity of floods in addition to describe possible changes in the annual and seasonal averages. The projected changes in the occurrence and severity of droughts will be reported later based on further analysis in the project Climate and Energy.

The report is divided into nine Chapters. Chapter 2 gives an overview of the location and basins characteristics of 25 basins included in the study. Chapter 3 presents the climate scenarios used to produce scenarios of the water balance model. The hydrological model and the subsequent analysis of the model results are presented in Chapter 4. Chapter 5 gives an overview of projected changes in the streamflow. The model produces also scenarios of other water balance elements presented in Chapter 6. Chapter 7 describes uncertainties in the scenarios, in Chapter 8 the results are discussed with conclusions summarised in Chapter 9.

The report is a part of the study 'Climate Change and Energy Production Potential' funded by EBL kompetanse AS. The Nordic research programme 'Climate and Energy' (CE) has developed streamflow scenarios based on an alternative downscaling technique developed by the Rossby Center

at SMHI in Sweden. These scenarios include some additional basins, which were not included in the study described in this report. Some comparisons are made between preliminary results of the CE-project and the results of the EBL-project.

2 Study area

The study described in Roald et al (2002) was based on simulation of the streamflow in 48 natural basins since it relied on the use of HBV-models calibrated separately for each basin. The scenario series were intended to be used as input data for the energy production model, which relies on a different set of mostly regulated basins.

The current study examines possible changes over the entire Norwegian mainland with special focus on changes in 25 basins selected to give a countrywide set of basins of special interest to the hydropower industry and which are more suited for providing input data to the Energy production model. The basins include some coastal basins of less interest for hydropower production in order to obtain a better regional coverage over Norway. The basins are listed in Table 2.1. Table 2.2 gives some characteristics of each basin. The location of the basins is shown in Figure 2.1.

Table 2.1   Overview of basins included in the EBL-study.

Station no.	Name	River	Basin area km^2	From	To
311.6	Nybergsund	Trysilelv	4410	1908	DD.
2.142	Knappom	Flisa	1625	1916	DD.
2.111	Aursunden	Glomma	835	1923	DD.
2.13	Sjodalsvatn	Sjoa	474	1930	DD.
15.79	Orsjoren	Numedalslågen	1154	1982	DD.
16.19	Møsvatn	Måna	1506	1909	DD.
18.10	Gjerstad	Gjerstadelv	235	1980	DD.
20.2	Austenå	Tovdalselv	286	1924	DD.
20.3	Flaksvatn	Tovdalselv	1794	1899	DD.
26.20	Årdal	Sira	76	1970	DD.
26.21	Sandvatn	Sira	28	1970	DD.
27.26	Hetland	Bjerkreimselv	70	1915	DD.
257.257	Lyse krv	Lyse	309		
41.1	Stordalsvatn	Etneelv	127	1912	DD.
48.5	Reinsnosvatn	Austdøla	118	1917	DD.
50.1	Hølen	Kinso	229	1923	DD.
83.2	Viksvatn	Gaular	505	1902	DD.
104.23	Vistdal	Visa	66	1975	DD.
107.3	Farstad	Farstadelv	24	1965	DD.
109.9	Risefoss	Driva	738	1933	DD.
123.20	Rathe	Nidelv	3061	1902	DD.
123.31	Kjelstad	Garbergelv	141	1912	DD.
151.15	Nervoll	Vefsna	650	1968	DD.
167.3	Kobbvatn	Kobbelv	386	1916	DD.
212.10	Masi	Alta	5693	1966	DD.

Table 2.2 Selected characteristics of the basins.

Station no.	Name	Elevations			Basin characteristics (%)				
		Bottom	Median	Top	Forest	Mountain	Lakes	Bogs	Glaciers
311.6	Nybergsund	353	783	1748	44.78	26.26	8.4	11.6	0
2.142	Knappom	170	411	808	77.96	0	1.4	16.48	0
2.111	Aursunden	685	847	1567	34.04	32.72	12.1	10.04	0
2.13	Sjodalsvatn	940	1467	2362	5.25	71.2	9.3	1.03	9.22
15.79	Orsjoren	951	1229	1539	1.55	79.59	12.9	4.6	0
16.19	Møsvatn	890	1256	1628	6	76	12.8	5	0.02
18.10	Gjerstad	49	315	658	81.25	2.8	3.4	5.05	0
20.2	Austenå	288	763	1146	61.87	20.28	11.9	5.59	0
20.3	Flaksvatn	19	358	1146	74.44	6.45	7.7	7.89	0
26.20	Årdal	113	479	750	38.16	24.68	9	2.25	0
26.21	Sandvatn	306	472	572	44.25	35.16	10	8.84	0
27.26	Hetland	23	188	555	12.58	60.52	6.1	3.32	0
41.1	Stordalsvatn	51	685	1297	24.95	58.5	10.7	0.96	0
48.5	Reinsnosvatn	595	1234	1637	9.42	76.34	6.6	0.54	1.18
50.1	Hølen	120	1276	1686	1.85	88.38	0	0.32	0.35
83.2	Viksvatn	145	841	1636	22.5	57.32	9.5	1.07	4.72
104.23	Vistdal	47	736	1525	31.93	55.09	2.3	4.1	0.13
107.3	Farstad	11	56	764	19.83	13.62	4.7	8.85	0
109.9	Risefoss	556	1347	2284	6.84	83.91	1.9	1.22	0.37
123.20	Rathe	13	679	1572	37.8	30.16	6.7	14.07	0
123.31	Kjelstad	173	581	1166	42.62	35.82	2.1	14.75	0
151.15	Nervoll	345	827	1692	25.86	55.16	0	4.93	1.78
167.3	Kobbvatn	8	680	1512	15.51	63.09	13.9	0.56	0
212.10	Masi	272	451	1085	35.75	1.51	7	16	0
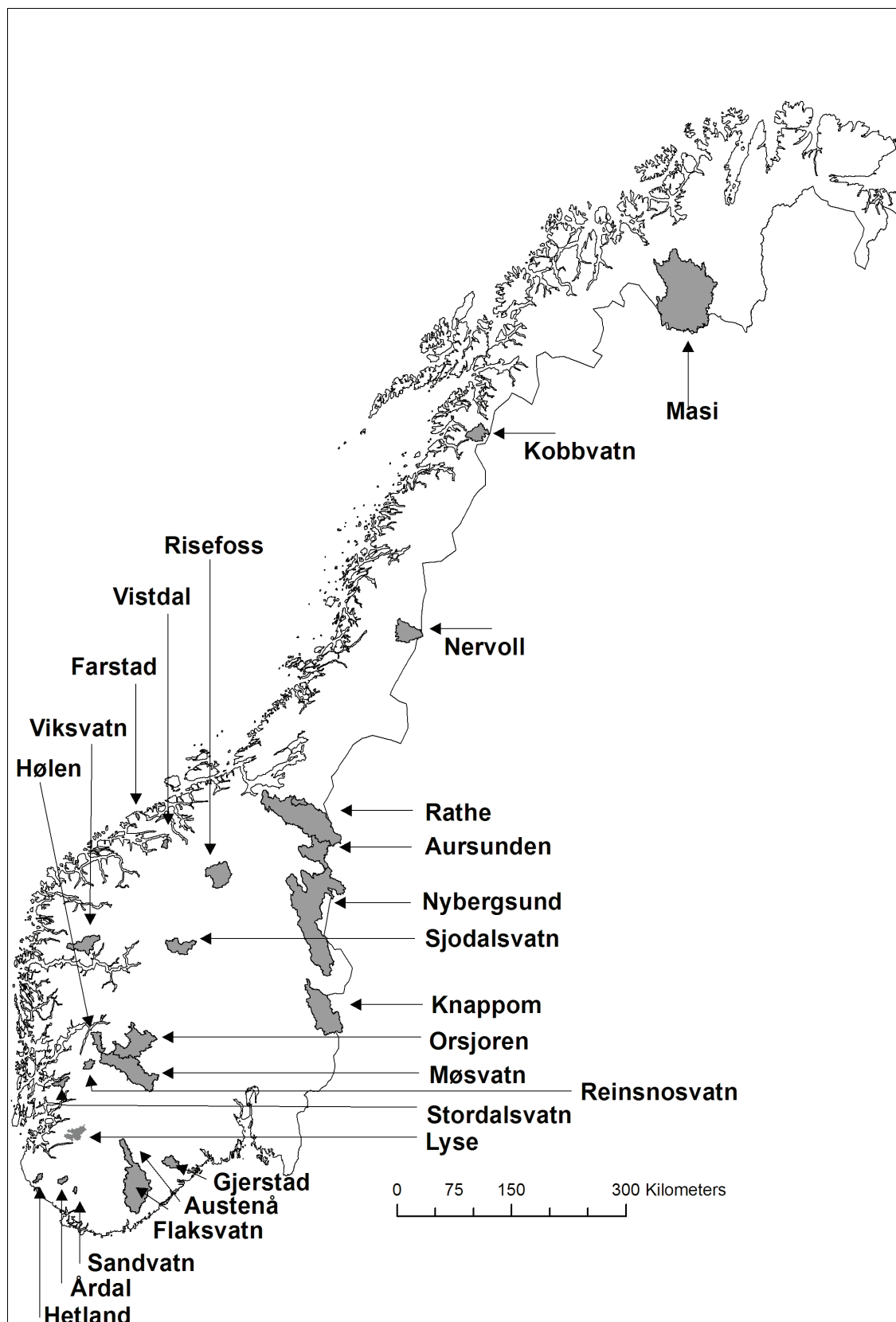
Figure 2.1   Location of the 25 basins included in the study. The Kjelstad basin is a small sub-basin within the much larger Rathe basin.

3 Climate change scenarios

3.1 Choice of models and scenarios

Two different AOGCMs are used in the study; the ECHAM4/OPYC3 model developed at the Max Planck institute (MPI) in Hamburg with the GSDIO integration (Roeckner et al., 1999) and HadAm3H model developed at the Hadley centre in UK (Gordon et al., 2000). The spatial resolution of AOGCMs is typically ~300 * 300 km^2. Thus, to obtain reliable estimates of the climate at specific regions in Norway, downscaling is necessary. Results from AOGCMs are dynamically downscaled with the regional climate model HIRHAM (Bjørge et al., 2000). HIRHAM is similar to the model used at MPI and the Danish Meteorological Institute (DMI) and is based on the dynamics of the weather forecast model HIRLAM, which is operationally used at the Norwegian Meteorological Institute (met.no) and the physics of ECHAM4. HIRHAM has a spatial resolution of ~55 *55 km^2. The resulting physical parameters have a 6 hourly time resolution and there is consistency between the parameters.

HIRHAM is run with one control period and one scenario period. The control run is one realisation of today's climate, representing the present climate. The estimated day-to-day variability is thus not comparable with observed data, the mean monthly values and standard deviation based on daily values should however be comparable. The models were run with different emission scenarios IS92a, A2 and B2 (Cubash et al., 2001). Up to 2050 IS92a gives slightly lower increase in global temperature than A2 and B2. Up to 2100 IS92a and B2 gives approximately 2.5 °C increase in global temperature while A2 is giving an increase of 3.5 °C. ECHAM4/OPYC3 is run with emission scenario B2, and the UK model, HadAm3H, is run with SRES emission scenarios A2 and B2 up to 2100. The model runs have different control periods and scenario periods (Table 3.1).

Table 3.1   The Atmospheric-Ocean General Circulation Models (AOGCSs) and emission scenarios used with respective control and scenario period.

Model	Emission scenario	Control period	Scenario period
ECHAM4/OPYC3	IS92a	1980-1999	2030-2049
ECHAM4/OPYC3	B2	1961-1990	2071-2100
HadAm3	A2	1961-1990	2071-2100
HadAm3	B2	1961-1990	2071-2100

The scenarios presented in Roald et al (2002) were based on the ECHAM4/OPYC3 model and the IS92a emission scenario only. The scenarios presented in this report are based on the A2 and B2 emission scenarios for the period 2071-2100.

Daily values of at-site measurement of temperature and precipitation are traditionally used as input to the hydrological model. Estimates of temperature and precipitation are therefore interpolated from HIRHAM to selected locations. There are large difficulties using temperature and precipitation interpolated from HIRHAM as station data representing the at site location. The station altitude is wrongly represented in the model, and the number of rainy days is typically estimated too large (Frei et al., 2003). The dynamically downscaled temperature and precipitation data are therefore empirically adjusted to be representative locally. The adjustment procedure is described in Engen-Skaugen (2004).

3.2 Projected changes in temperature and precipitation in selected Norwegian basins

The hydrological model utilises data from three adjacent climate stations to assign daily time series of daily temperature and precipitation to each 1 x 1 km^2 grid cell corrected for differences in altitudes between each climate station and the cell. The mean daily temperature and precipitation can be estimated for an entire basin by averaging over all cells included in the basin. The changes in mean annual and seasonal temperature and precipitation have been calculated for eight basins. The projected changes in the temperature are shown in Figure 3.2.1.
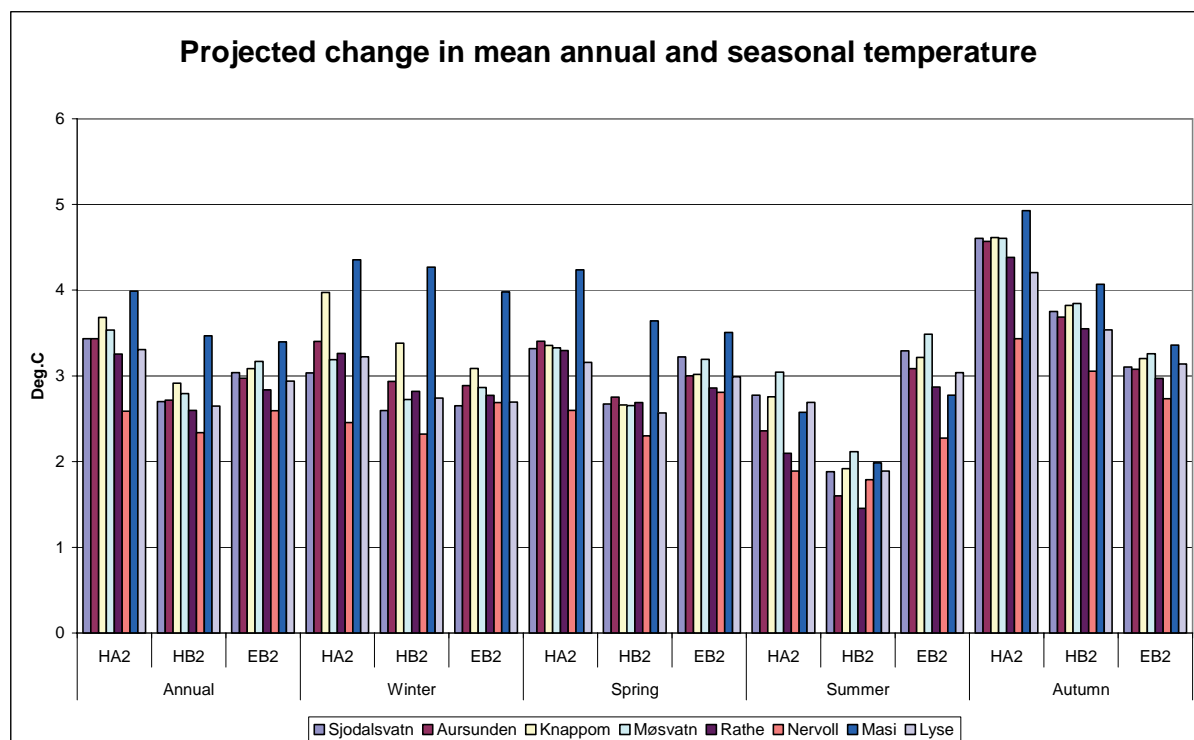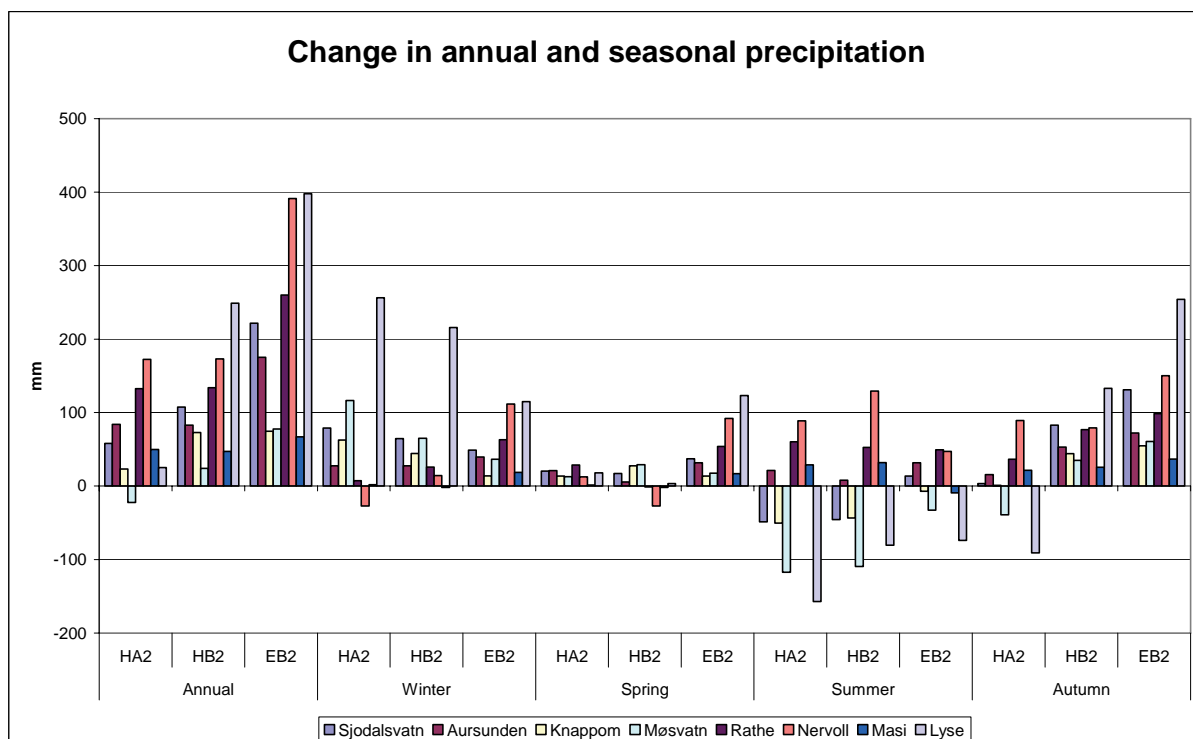

Figure 3.2.1   Projected change in the annual and seasonal basin mean temperature for eight basins in Norway from 1961-1990 to 2071-2100. HA2 and HB2 refers to scenarios A2 and B2 based on the HadAm3H-model and EB2 to scenario B2 of the ECHAM4-model.

The projected change in temperature varies 1°C between the various stations for each season and scenario with the exception of Masi in Finnmark, where the change is expected to be largest. The largest increase is in the autumn, and the smallest will occur in the summer. The HadA2- scenario gives the largest increase in all seasons, except in the summer when the ECHAM4B2- scenario is higher. The average values of the projected changes are given in Table 3.2.1 for each scenario for the mean temperature as well as for the mean maximum and minimum temperatures. The largest projected change occurs in the minimum temperature and the smallest in the maximum temperature, indicating a reduction in the mean temperature range.

The projected change in the annual and seasonal precipitation data is shown in Figure 3.2.2. The projected changes differs more depending on the region where each basin is situated. The set of basin does not include a basin on the west coast, where the projected increase is largest. The annual precipitation is increasing by 5 to 20 % in most of the basins with the largest increase according to the ECHAM4B2 – scenario. The change in the spring ranges from 10 to 40%, most in mountainous basins. The summer rainfall is reduced up to 30 % in some basins in east Norway, and increases by 10

% in some basins in the West and North Norway. The autumn precipitation increases by 15 to 25 % in the B2-scenarios, less in the A2-scenario.

Figure 3.2.2   Projected change in the annual and seasonal basin average precipitation in eight Norwegian basins from 1961-1990 to 2071-2100.
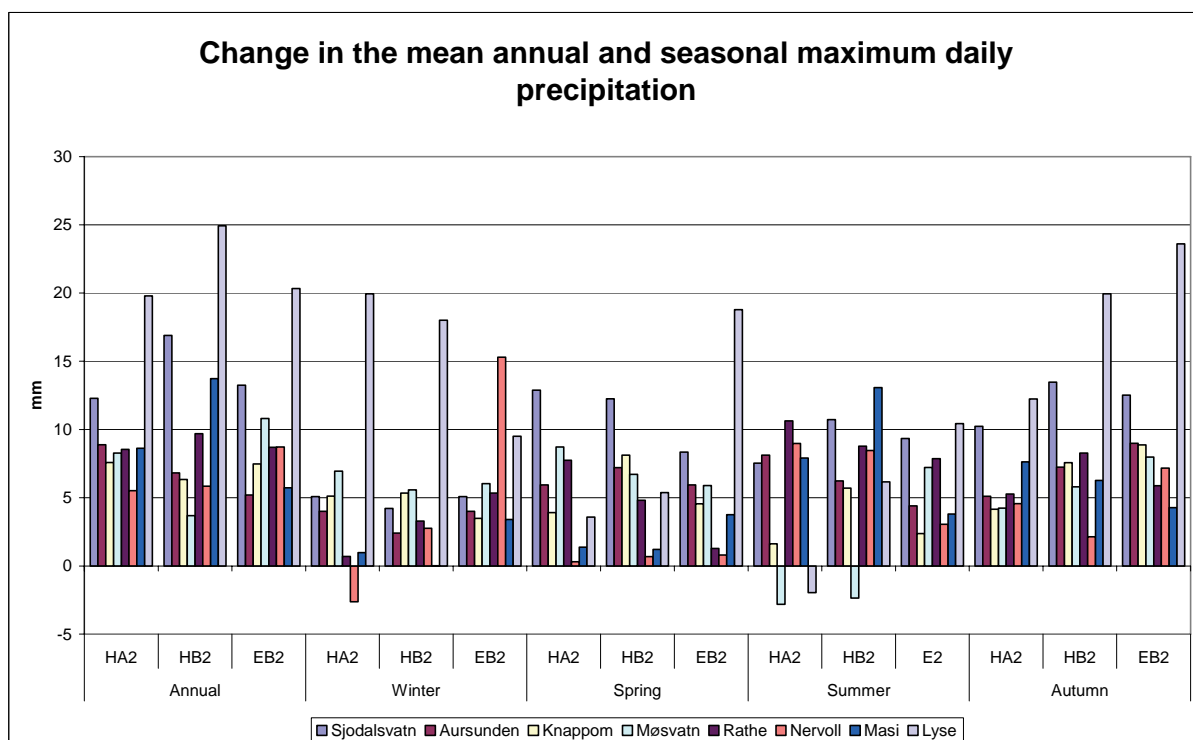
Figure 3.2.3   Projected change in the mean annual and seasonal maximum daily precipitation in eight basins from 1961-1990 to 2071-2100.

The projected change in the annual and seasonal maximum daily rainfall (Figure 3.2.3) indicates an increase of 3-25 mm in almost all basins and seasons. The large increase estimated in the Lyse basin is probably more uncertain than the estimates in the other basins.

Table 3.2.1 Projected change in the annual and seasonal mean, maximum and minimum temperatures over eight basins for three different climate scenarios from 1961-1990 to 2071-2100.

	Annual			Winter			Spring			Summer			Autumn		
	HA2	HB2	EB2	HA2	HB2	EB2	HA2	HB2	EB2	HA2	HB2	EB2	HA2	HB2	EB2
Mean temperature	3.40	2.77	3.00	3.36	2.97	2.95	3.34	2.74	3.07	2.52	1.83	3.00	4.42	3.66	3.10
Maximum temperature	2.97	1.58	3.52	1.95	2.00	3.49	3.78	2.73	3.18	2.87	1.46	3.43	3.87	2.91	3.04
Minimum temperature	7.15	6.62	6.21	7.30	6.37	6.19	5.77	4.34	4.33	2.56	2.12	2.98	6.94	5.53	5.92

4 Hydrological models

4.1 The Gridded Water Balance Model

The Gridded Water Balance model (GWB-model) (Beldring et al. 2003), a spatially distributed version of the HBV-model (Bergström, 1995), was used in this work. The model performs water balance calculations for square grid cell landscape elements characterized by their altitude and land use. Each grid cell may be divided into two land use zones with different vegetations, a lake area and a glacier area. The model is run with daily time steps, using precipitation and air temperature data as input. It has components for accumulation, sub-grid scale distribution and ablation of snow, interception storage, sub-grid scale distribution of soil moisture storage, evapotranspiration, groundwater storage and runoff response, lake evaporation and glacier mass balance. Potential evapotranspiration is a function of air temperature, however, the effects of seasonally varying vegetation characteristics are considered. The algorithms of the model were described by Bergström (1995) and Sælthun (1996). The model is spatially distributed since every model element has unique characteristics that determine its parameters, input data are distributed, water balance computations are performed separately for each model element, and finally, only those parts of the model structure which are necessary are used for each element.

A regionally applicable set of parameters was determined by calibrating the model with the restriction that the same parameter values are used for all computational elements of the model that fall into the same class for land surface properties (Beldring et al. 2002). This calibration procedure rests on the hypothesis that model elements with identical landscape characteristics have similar hydrological behaviour, and should consequently be assigned the same parameter values. The grid cells should represent the significant and systematic variations in the properties of the land surface, and representative (typical) parameter values must be applied for different classes of soil and vegetation types, lakes and glaciers (Gottschalk et al., 2001). The model was calibrated using available information about climate and hydrological processes from all gauged basins in Norway with reliable observations, and parameter values were transferred to other basins based on the classification of landscape characteristics. Several automatic calibration procedures, which use an optimization algorithm to find those values of model parameters that minimize or maximize, as appropriate, an objective function or statistic of the residuals between model simulated output and observed watershed output, have been developed. The nonlinear parameter estimation method PEST (Doherty et al., 1998) was used in this study. PEST adjusts the parameters of a model between specified lower and upper bounds until the sum of squares of residuals between selected model outputs and a complementary set of observed data are reduced to a minimum. A multi-criteria calibration strategy was applied, where the residuals between model simulated and observed monthly runoff from several basins located in areas with different runoff regimes and landscape characteristics were considered simultaneously.

The precipitation stations used in this study were classified in five exposure classes with fixed correction factors for rain, snow and mixed type precipitation according to a Nordic study (Førland et al., 1996). The precipitation data were accordingly given a simplified precipitation type classification. Precipitation and temperature values for the model grid cells were determined by inverse distance interpolation of observations from the three closest precipitation stations and the two closest temperature stations. Differences in precipitation and temperature caused by elevation were corrected by site specific precipitation-altitude gradients and fixed temperature lapse rates for days with and without precipitation, respectively. There is considerable uncertainty with regard to the variations of precipitation with altitude in the mountainous terrain of Norway. Specific precipitation-altitude

gradients were therefore determined for each of the 25 basins, and these values were used for all grid cells within a basin. Few mountain stations necessitate to use these general gradients. The precipitation-altitude gradients were reduced by 50 % for elevations above 1200 m a.s.l., as drying out of ascending air occurs in high mountain areas due to orographically induced precipitation (Daly et al., 1994). The reduction of 50 % is arbitrarily chosen, however, the height of 1200 metres is not, as this is the approximate altitude of the coastal mountain ranges in western and northern Norway. These mountains ranges release most of the precipitation associated with the eastward-migrating extratropical storm tracks that dominate the weather in Norway. The temperature lapse rates for days with and without precipitation were also determined by calibration, however, the same values were used for all grid cells.

In order to have confidence in a hydrological model, its performance must be validated. Model performance is usually evaluated by considering one or more objective statistics or functions of the residuals between model simulated output and observed watershed output. The objective functions used in this study were the Nash-Sutcliffe and bias statistics of the residuals, which have a low correlation (Węglarczyk, 1998). The Nash-Sutcliffe efficiency criterion ranges from minus infinity to 1.0 with higher values indicating better agreement. It measures the fraction of the variance of observed values explained by the model:

$$NS = 1 - \frac{\sum_{t=1}^{n} \left(q_t^{obs} - q_t^{sim} \right)^2}{\sum_{t=1}^{n} \left(q_t^{obs} - q^{mean} \right)^2}$$

where q_t^{obs} is observed watershed output at discrete times t, q_t^{sim} is the corresponding model simulations, q^{mean} is the mean of the observed values, and n is the number of data points to be matched. Bias (relative volume error) measures the tendency of model simulated values to be larger or smaller than their observed counterpart:

$$BIAS = \frac{\sum_{t=1}^{n} \left(q_t^{sim} - q_t^{obs} \right)}{\sum_{t=1}^{n} q_t^{obs}}$$

Although the Nash-Sutcliffe efficiency criterion is frequently used for evaluating the performance of hydrological models, it favours a good match between observed and modelled high flows, while sacrificing to some extent matching of below-mean flows. It is for this reason that two different measures of model performance were considered. A test of model performance in an independent period was also performed.

The distributed model was calibrated separately to produce the scenario series for each basin. Country-wide simulations were produced using a global parameter set conditioned on land surface characteristics.

4.2 Analyses of the results

The GWB-model was run both for the entire Norwegian mainland and for 25 selected basins. Annual and seasonal changes are available as GIS-covers for the streamflow as well as for other water balance elements. Daily data series were calculated for each basin for the control and the scenario periods. Data series are available for the control period based on both the HadAm3H- and the ECHAM4-model. A third control series have been calculated as well based on the Δ-change method and observed climatological data in the control period. Time series of other water balance variables were also calculated for a subset of the basins as well as for the climate series driving the model. These series are stored as time series on NVE's database HYDRA II and can be accessed by all application programs linked to the database. Appendix I comprise an overview of scenario data series currently available on HYDRA II. Overview of GIS-covers is given in Appendix II.

The changes are identified by calculating the difference or proportion of statistical properties of the scenario and the control series for each water balance element. The results can be shown both as maps of changes in the various water balance elements or graphs illustrating changes in the annual statistics and in the seasonality. The statistics examined are the mean value, standard deviation, value and time of the year for the annual maximum and minimum value. All statistics have been calculated for annual values and seasonal values. The seasons were: Winter: December-February, Spring: March-May, Summer: June-August and Autumn: September-November. The simulation of changes in the energy production is based on changes in the weekly values for selected basins. Weekly mean values have therefore been calculated for all series. This is now used in the Climate and Energy project based on streamflow scenarios based on the alternative Rossby Center Method of downscaling climate change scenarios to climate stations.

Changes in the flood series were examined by calculating and comparing flood statistics of the scenario and the control period for all 25 stations. Flood frequency analysis was applied to both series for each station and model/emission scenario. Flood quantiles was calculated for floods with return period up to 50 year based on the General Extreme Value (GEV) distribution and estimation by the Probability Weighted Moments (PWM)-method (Hosking & Wallis, 1997). The change in seasonality of the annual maximum flood can be illustrated by determining the frequency of the annual peak flood occurring per month in the control and scenario period.

Changes in the occurrence and magnitude of droughts can be performed by analysis of either time below a given threshold or on the deficit volume below the threshold. This will not be included in the present report, but will be included in a later report of the Climate and Energy project.

5 Streamflow scenarios

5.1 Introduction

The annual and seasonal streamflow in Norway varies considerable between different basins and regions, depending both on the basin size, altitude distribution and location within different regions within Norway. The GWB-model produces gridded dataset, which is utilised to produce maps of change in the mean annual streamflow over the entire Norwegian mainland. The changes in the annual and seasonal streamflow can also be shown as graphs for all 25 basins as shown in Section 5.2.

Changes in the year to year variability of the streamflow can be of greater concern for the hydropower production than moderate changes in the mean values. Section 5.3 summarises changes in the variability expressed as the CV of the annual and seasonal values of the streamflow.

The projected changes are dependent on the elevation. This has been examined for a few basins, and the results are described in Section 5.4.

The 25 basins can be grouped into a small number of regions with a similar expected response to a possible climate change. Possible changes in these regions in terms of mean streamflow and floods are described in Section 5.5.

5.2 Projected changes in the mean annual and seasonal streamflow over Norway

The mean annual runoff in Norway is shown in Figure 5.2.1 (left) for the control period. The percentage change of the mean annual runoff from the control to the scenario period is shown for the HadAM3H-model and the A2-scenario (right), and in Figure 5.2.2 for the ECHAM4-model and the B2-scenario (left) and for the HadAM3H-model and the B2-scenario (right). Figure 5.2.3 show mean annual runoff in 23 selected basins in mm per year. The mean annual runoff varies considerably over Norway because of the long mountain ranges shielding East Norway from precipitation of the prevailing westerlies. The annual runoff varies from less than 250 mm in the driest basins in the rain shadow to more than 5000 mm in the wettest basins close to some maritime glaciers.

The HadA2-scenario indicates a moderate increase in the annual runoff in West Norway and in Nordland of 9-12 % and a reduction in East and Mid Norway and in Finnmark of 5-20 %. The HadB2-scenario indicates increase of 5-20 % in large areas in West Norway and locally in Nordland and in East Norway, and decrease in Mid-Norway and in Finnmark of 2-3 %. The ECHAM4B2-scenario indicates increase of 5-20 % in all regions exposed to the west with increase of 20-128 % in mountainous basins in West Norway, Nordland and on the extreme west coast.

The differences in the B2-scenario of the two models are probably caused by natural climate variability, leading to differences in the projected pressure fields and hence dominating wind direction.
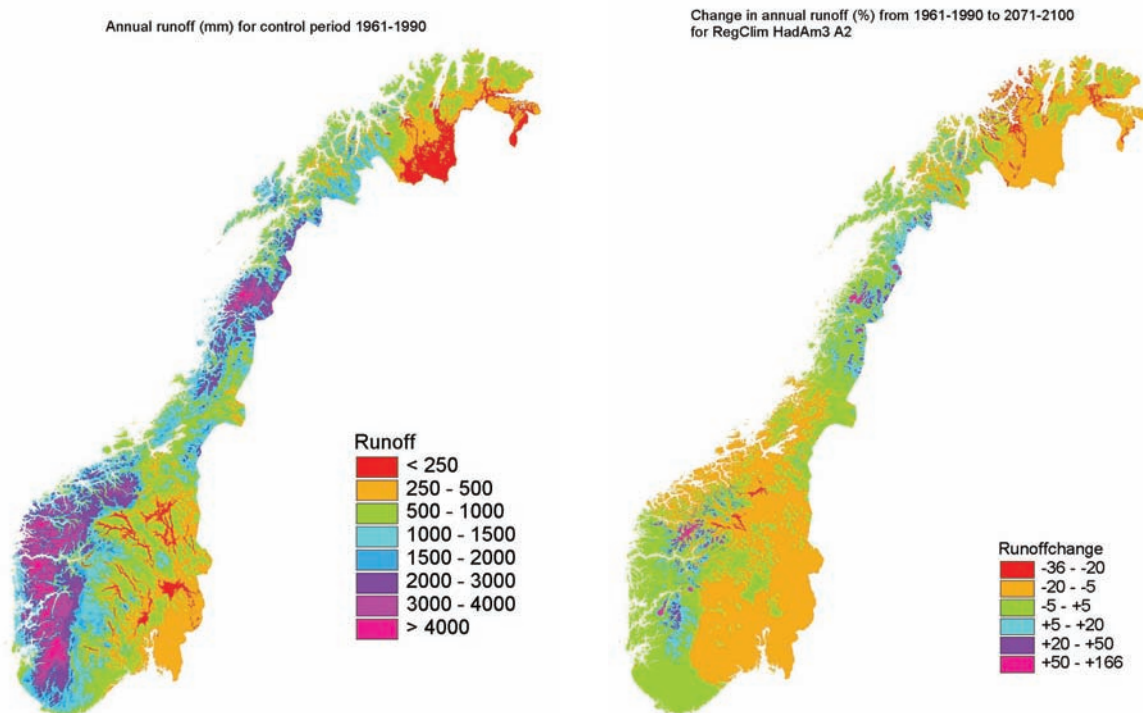
Figure 5.2.1   Annual runoff for 1961-1990 (mm) (left) and projected percentage change in runoff from 1961-1990 to 2071-2100 based on the HadAm3H-model and the A2 scenario (right).
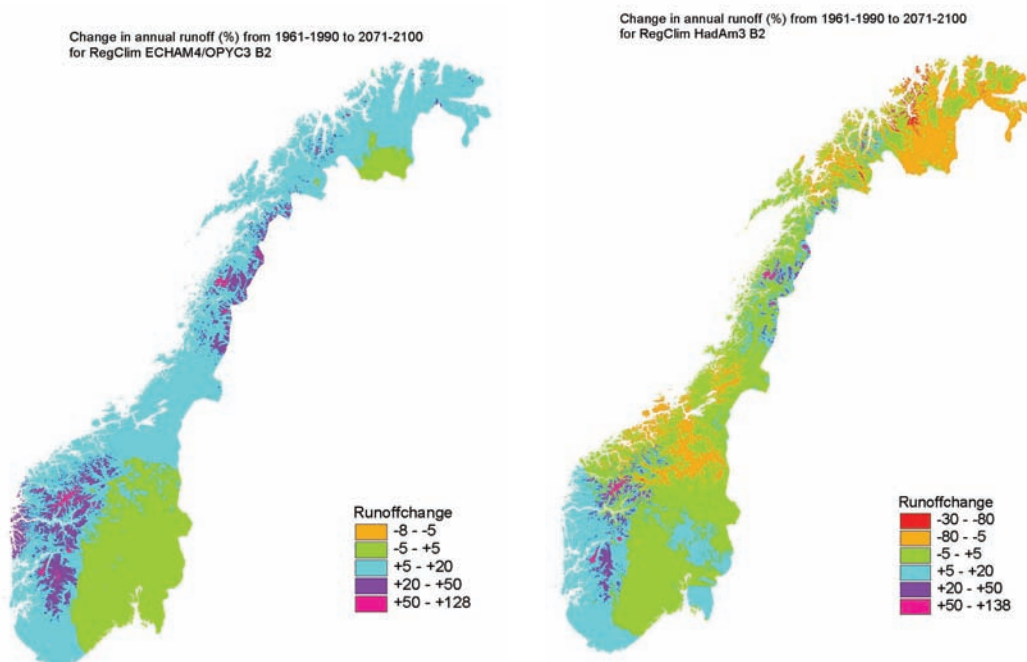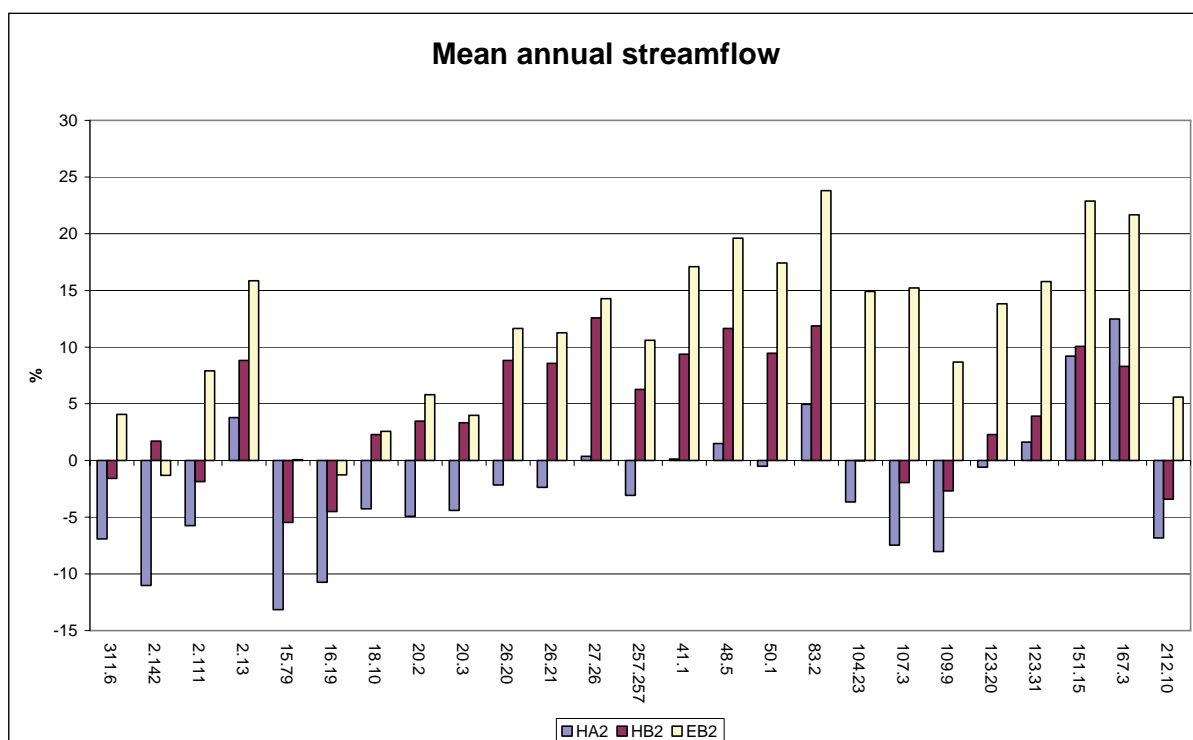

Figure 5.2.2   Projected percentage change in annual runoff from 1961-1990 to 2071-2100 based on the ECHAM4-model and the B2 scenario (left) and the HadAm3H-model and the B2 scenario (right).

19
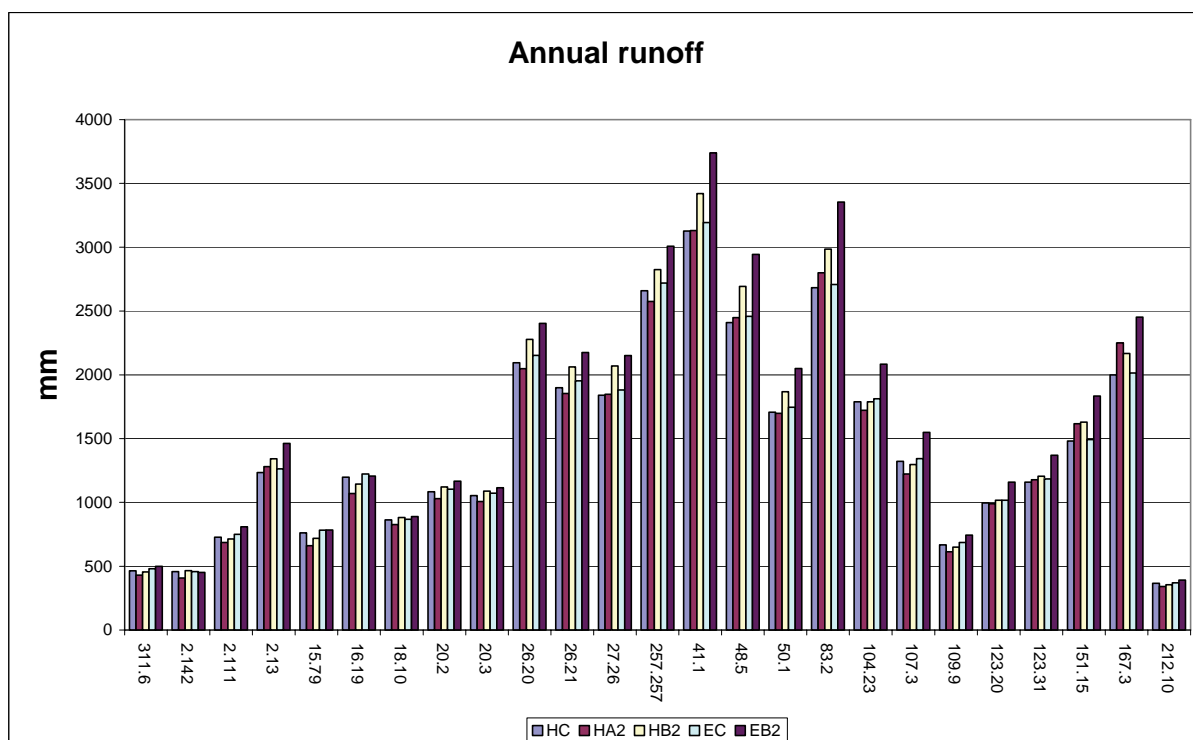
Figure 5.2.3   Annual runoff in the control period 1961-1990 (HC and EC) and in the scenario period 2071-2100 based on climate scenarios of the HadAm3H-model (HA2 and HB2) and the ECHAM4-model (EB2).

The change in the mean annual streamflow are shown in Figure 5.2.4 for the 25 basins included in the study. Each basin is identified by its station number, and the series are ordered from basins in the south east clockwise around the coast. Basins with station number 311.6 Nybergsund , 2.111 Aursunden and 2.142 Knappom are from East Norway bordering to Sweden, 2.13 Sjodalsvatn and 109.9 Risefoss are from the most alpine mountain area, 15.79 Orsjoren, 16.19 Møsvatn, 48.5 Reinsnosvatn and 50.1 Hølen are from Hardangervidda mountain plateau, 18.10 Gjerstad, 20.2 Austenå and 20.3 Flaksvatn are from the south coast or inland, 26.20 Årdal , 26.21 Sandvatn, 27.26 Hetland and 257.257 Lyse are from the south west, 41.1 Stordalsvatn and 83.2 Viksvatn are from West Norway, 104.23 Vistdal, 107.3 Farstad , 123.20 Rathe and 123.31 Kjelstad from Mid Norway, 151.15 Nervoll and 167.3 Kobbvatn are from Nordland and 212.10 Masi is from Finnmark.

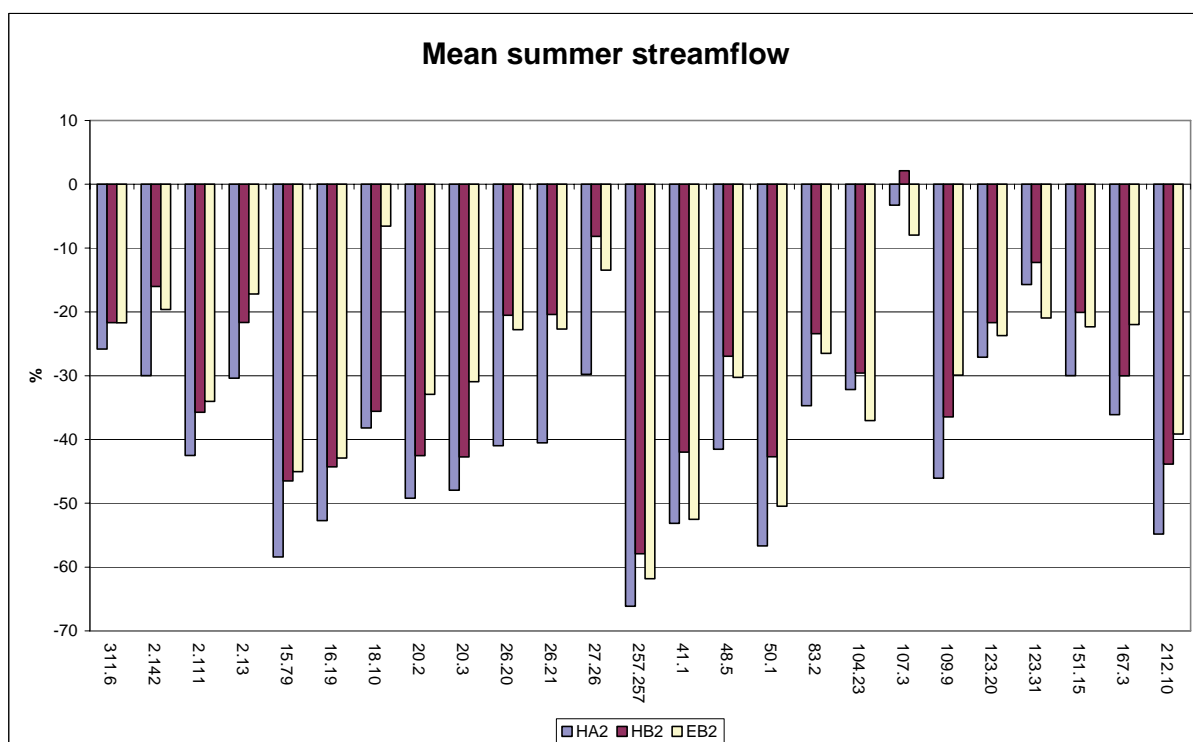**Figure 5.2.4** **Projected percentage change in the mean annual streamflow in 25 Norwegian basins from 1961-1990 to 2071-2100.**
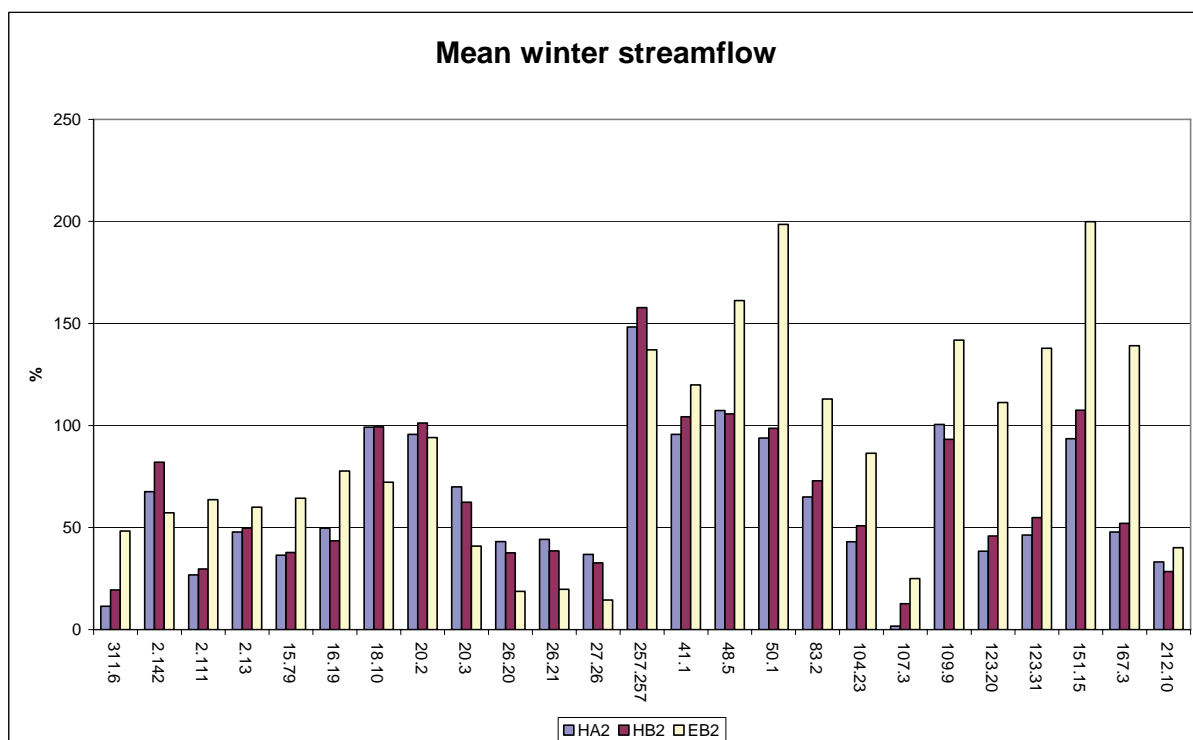
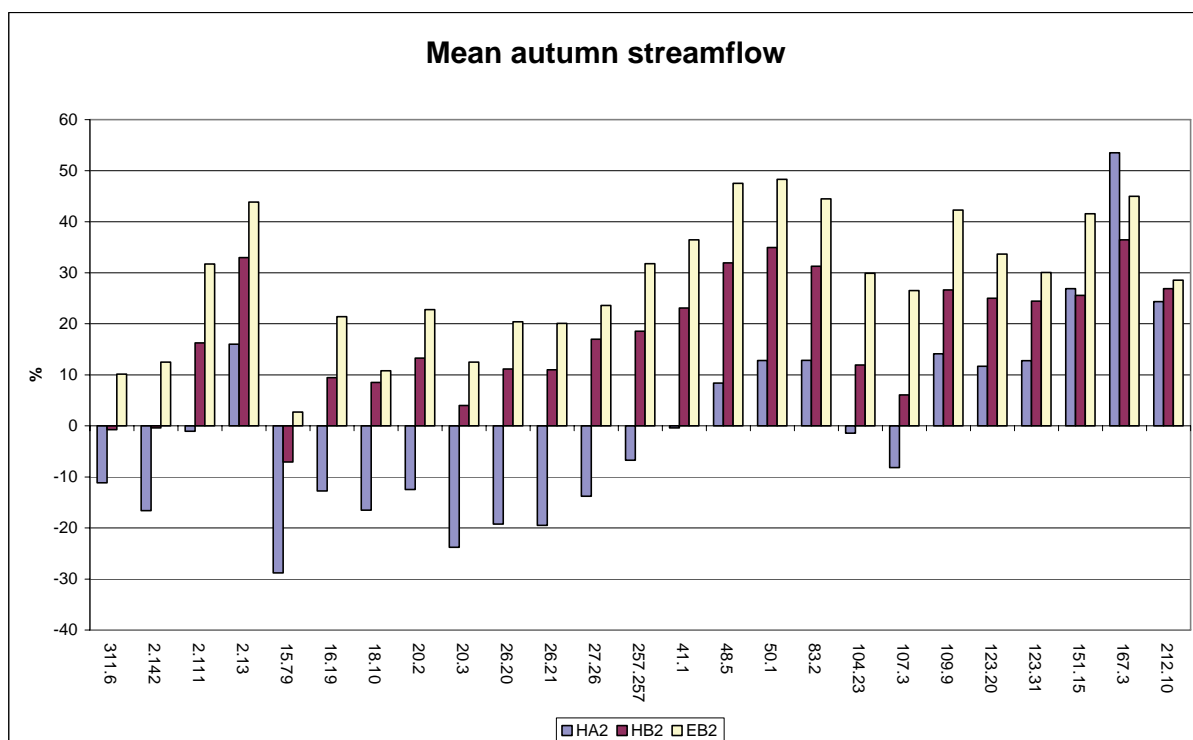
Figure 5.2.5 **Projected percentage change in the mean winter streamflow in 25 Norwegian basins from 1961-1990 to 2071-2100.**
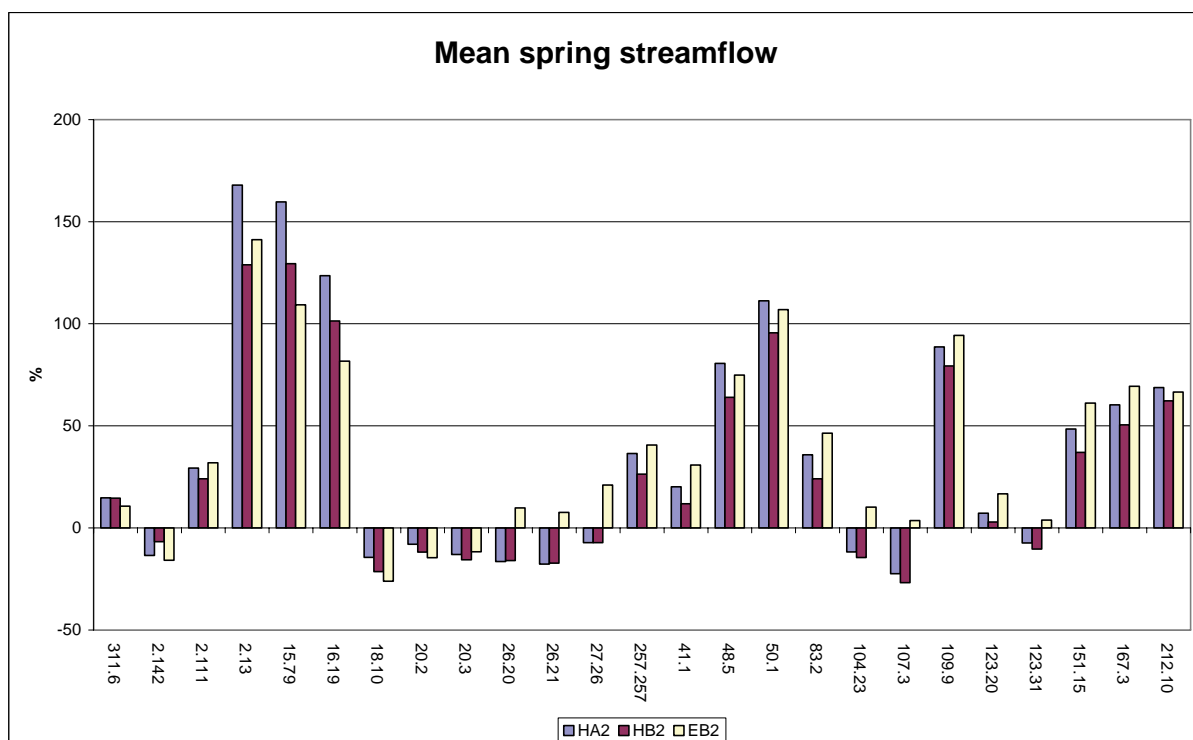
Figure 5.2.6   Projected percentage change in the mean spring streamflow in 25 Norwegian basins from 1961-1990 to 2071-2100.

Figure 5.2.7   Projected percentage change in the mean summer streamflow in 25 Norwegian basins from 1961-1990 to 2071-2100.

Mean autumn streamflow

Figure 5.2.8   **Projected percentage change in the mean autumn streamflow in 25 Norwegian basins from 1961-1990 to 2071-2100.**

The changes are more significant in the seasonal distribution over the year. Figures 5.2.5-5.2.8 show the percentage change of the four seasons.

The mean winter streamflow increase in all basins, the largest increase occurs in West Norway and in Nordland especially in the scenario based on the ECHAM4-model. The smallest increase appears in basin 107.3, which is on the extreme coast, without much snow even under the present climate. The mean spring streamflow increases by 70 to 170 % in mountainous basin and by 40 to 70 % in North Norway, all in basins with a dominant snowmelt flood in the spring or early summer. The spring streamflow decreases by 20 % in lowland basins in East Norway and on the south coast. The mean summer streamflow decreases in all basins, least in basin 107.3. The reduction ranges otherwise from 10 to 65 %, depending on the basin and the various scenarios. The mean autumn streamflow varies considerably between the two emission scenarios. The autumn streamflow is reduced in most basins in east and south by 10 to 30 %. Basins in West and North Norway will mostly have increased autumn streamflow of 7 to 55 % for the A2 scenario. The B2 emission scenario results in increased autumn streamflow in almost all basins, least in the east and south. The ECHAM4 scenarios with an increase of 10-50 % in most basins are generally higher than the scenarios of the HadAm3H-model with an increase of 5 to 35 %. This reflects the changes in the pressure fields simulated by the two models.

5.3 Projected changes in the annual and seasonal variability

The energy production of Norway is strongly dependent on the inflow to the reservoirs and the amount of water that can be utilised for energy production. The consumption of energy is fairly stable or growing based on a net annual production around 118 TWh. The annual and seasonal inflow varies, however, and can provide a production from around 140 to 85 TWh under present climate conditions. More inflow will be lost as spill given the present production and reservoir capacity. Although the average inflow will increase in most regions, large annual and seasonal variability would still cause problems for the energy supply in dry years (Killingtveit et al 2003). Possible changes in the year to year variability will therefore have consequences for the reliability of the electricity production in Norway.

The coefficient of variation (CV) of the annual and seasonal streamflow has been calculated for the control period and all scenarios to examine if large changes can be expected in a changed climate. The scenario based on the ECHAM4B2 scenario show an average decline of CV of 16 % for the annual streamflow. Only three basins show a small increase. The number of basins with increase and decline of the annual streamflow is even for the HadB2-scenario. The basins with decline in the variability are in the mountainous basins in East Norway and in the south and southwest. Basins in West and North Norway show increased annual variability. The HadA2 scenario has about as many basins with increased as reduced variability. Mountain basins in East Norway and most basins in North Norway are decreasing while most basins in West and Mid Norway are increasing by 9 to 17 % in CV.

The seasonal CV's show also some regional patterns.

Winter: Large increase in CV in many basins in the east and in mountain basins. Decrease in CV in the south and northern part of West Norway. Stronger decrease in CV is projected in most basins in the ECHAM4B2 scenario than in the HadA2 and B2.

Spring: Large decrease in CV in East Norway in all scenarios, and in mountain basins elsewhere. Increase in coastal basins.

Summer: Decrease in CV in basins in East Norway and in Mid Norway by 5 to 22 % in all scenarios. Large increases in mountain basins in the west, south and in West Norway of 15 to 100 %, especially in the A2-scenario, less in the B2-scenario. Basins in the southwest show a marginal decline in the ECHAM4-B2 scenario.

Autumn: Decline in CV in the autumn in all basins except in East Norway in the HadAm3H.A2-scenario by 0 to 44 % and in the HadAm3HB2-scenario in West and North Norway. The ECHAM4-B2 scenario shows a decrease by 6 to 30 % in Jotunheimen, Hardangervidda and in southwest and increase in most basins in West and North Norway.

There is a shift towards marginally lower minimum annual streamflow in the scenarios based on the HadAm3H-model. The ECHAM4-scenario has a shift towards higher minimum annual streamflow in all basins with an average change of 37 %.

5.4 Projected changes in different elevation bands

The seasonal distribution of the streamflow is strongly controlled by the occurrence and accumulation of snow, which again depend on the altitude. Many of the basins included in the study cover a wide range of altitudes. The total streamflow from various parts of these basins comprise contributions from different elevation bands, with large differences in the seasonality. The contribution to the total streamflow have been calculated for all elevation bands which each basins can be divided into for a subset of basins similar to previous studies presented in Sælthun et al 1998. The elevation band ranges from 0-500 m.a.s.l., 500-1000 m.a.s.l., 1000-1500 m.a.s.l. and 1500-2500 m.a.s.l. Table A1.2a and b in Appendix I give an overview of the sub-set of series and the elevation bands included in each basin.

The size of part of each basin falling within each elevation band varies enormously. It is therefore necessary to standardise data to obtain comparable values for the different elevation band. This can be done by either calculating the streamflow expressed in mm/day or standardised by the annual mean. We have chosen the second alternative in the examples shown below.
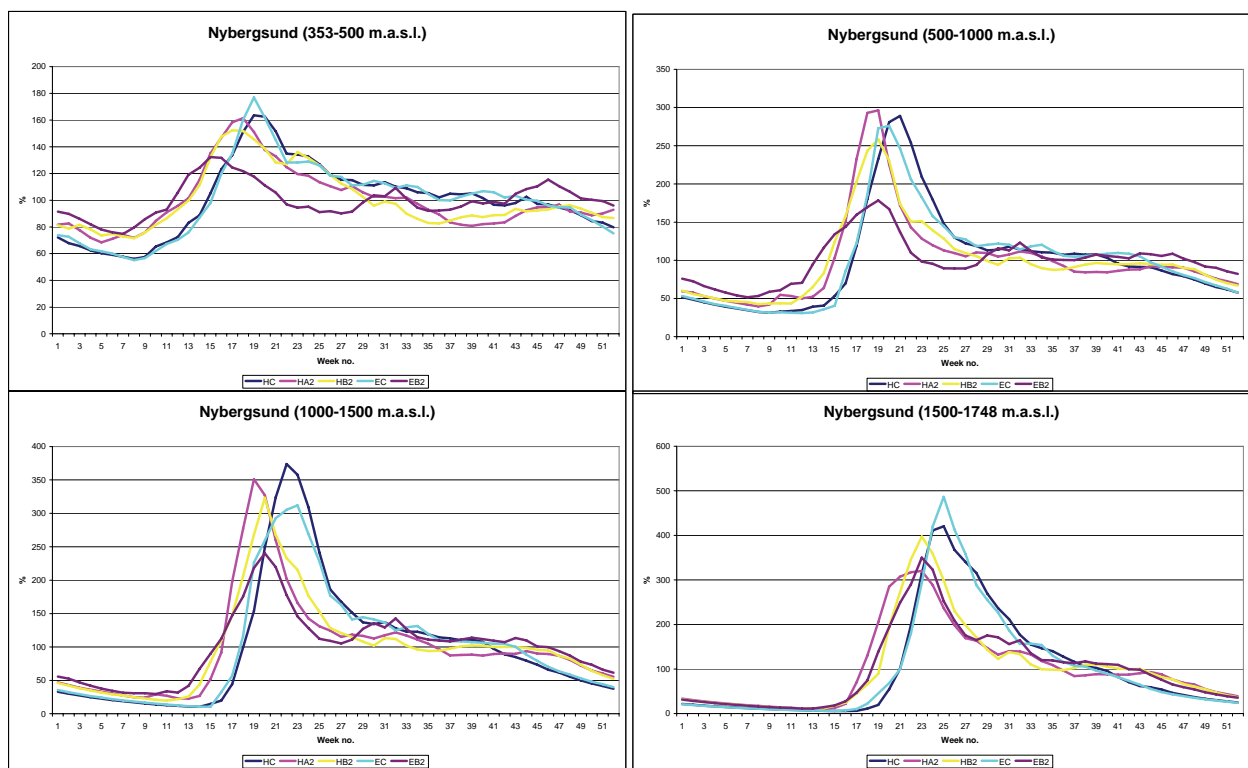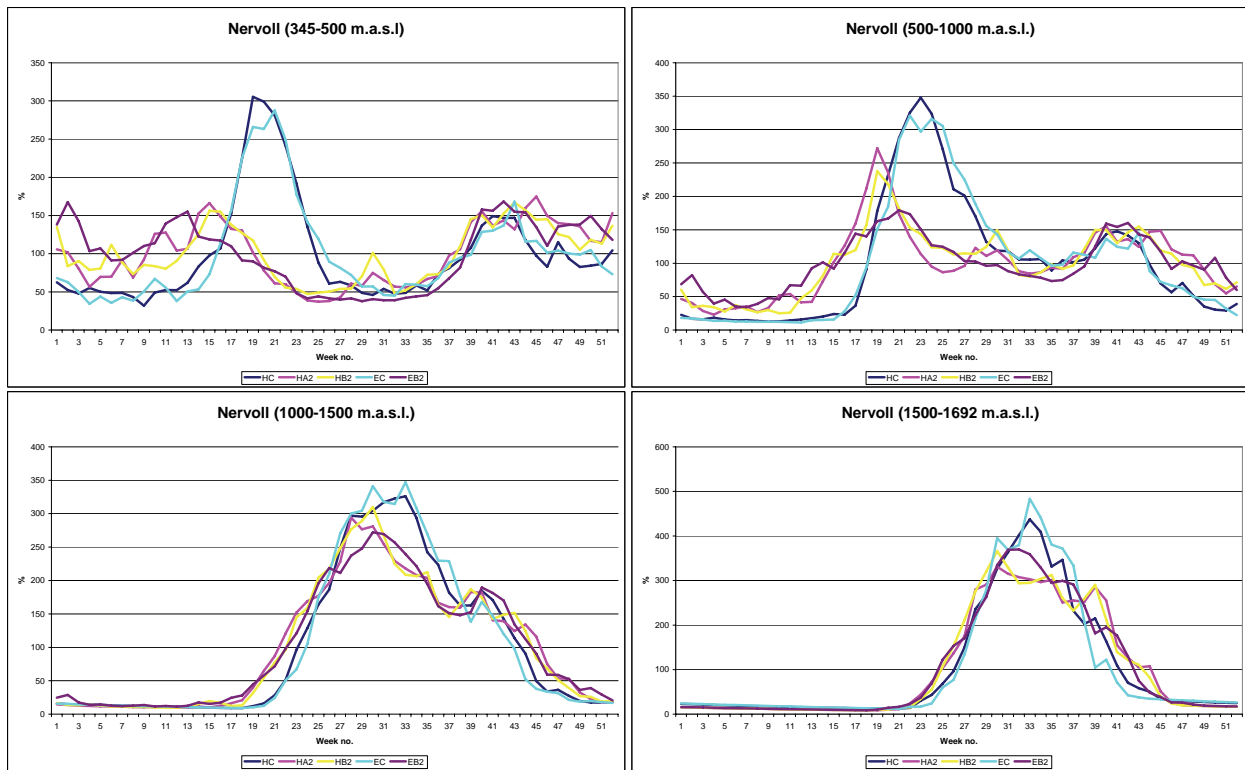

Figure 5.4.1 Weekly mean streamflow in percent of the annual mean of the control period and the scenario series for four elevation bands at Nybergsund in River Trysilelv.
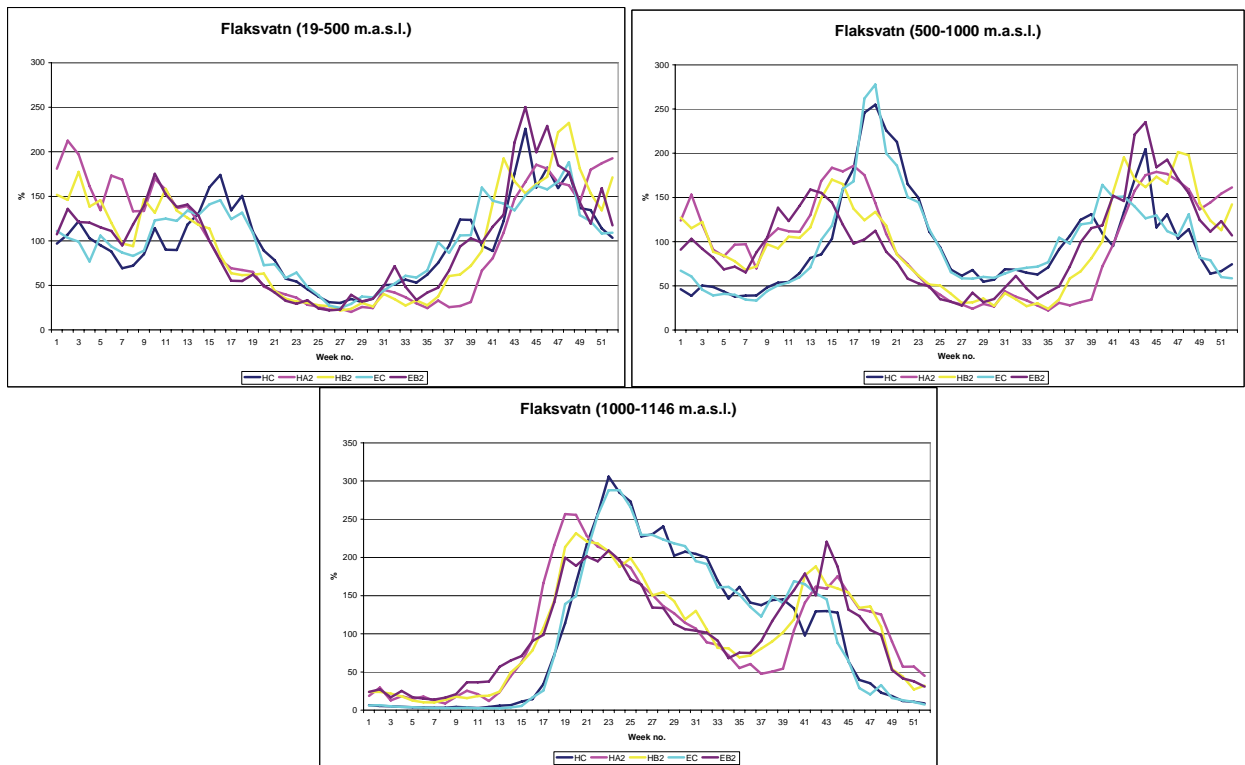
Figure 5.4.2   Weekly mean streamflow in percent of the annual mean of the control period and the scenario series for four elevation bands at Lake Flaksvatn in River Tovdalselv.
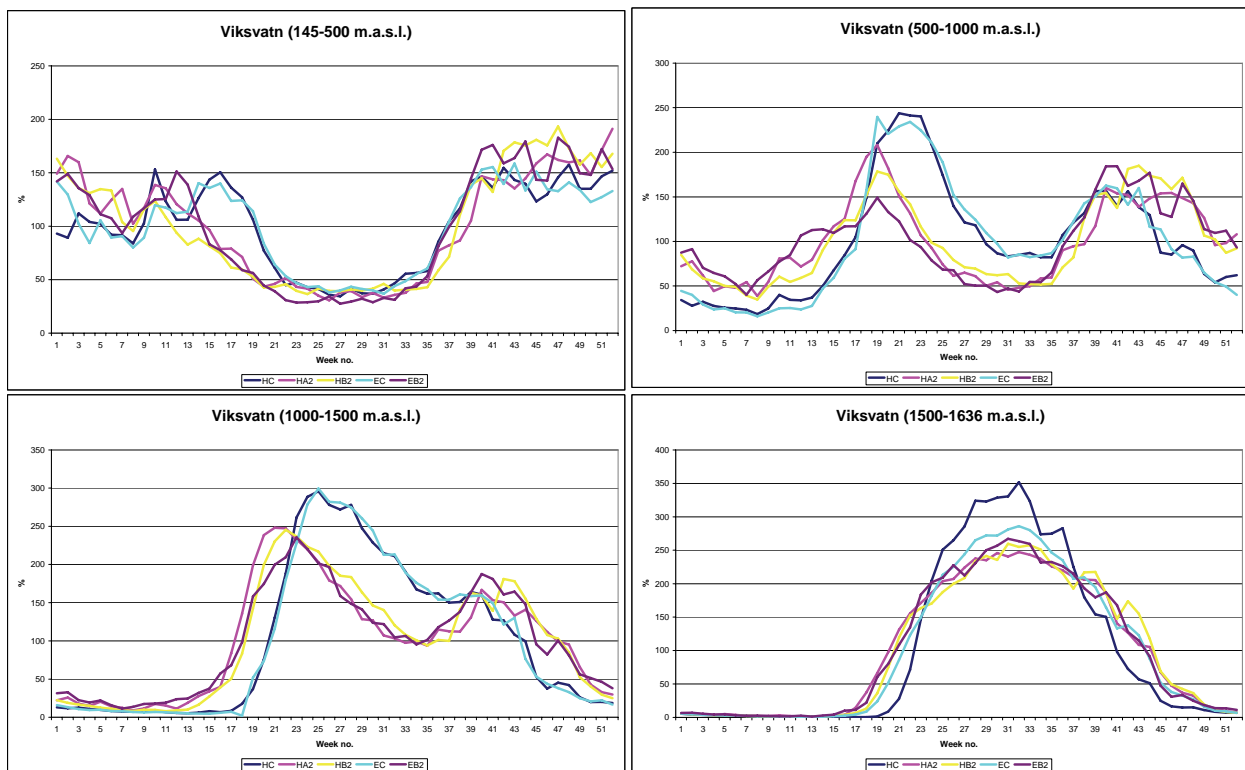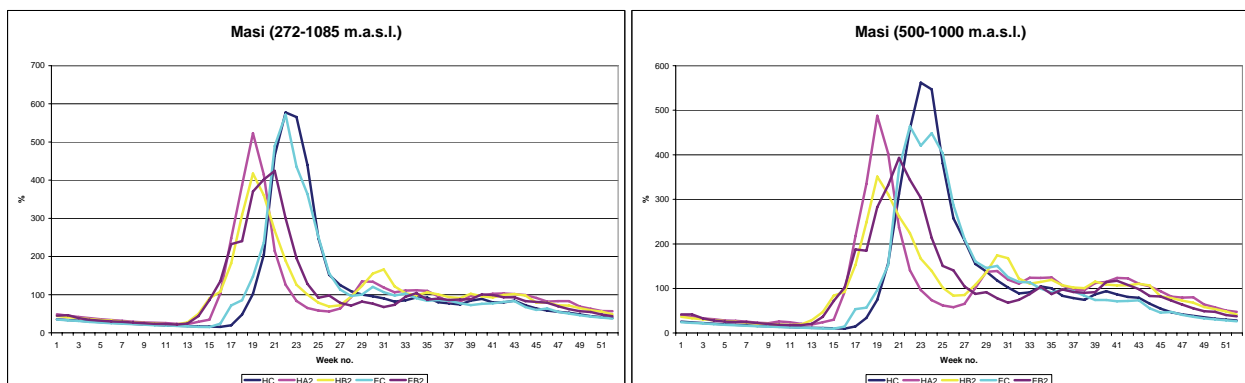

Figure 5.4.3   Weekly mean streamflow in percent of the annual mean of the control period and the scenario series for four elevation bands at Lake Viksvatn in River Gaula.

Figure 5.4.4   Weekly mean streamflow in percent of the annual mean of the control period and the scenario series for four elevation bands at Nervoll in River Vefsna.

Figure 5.4.5   Weekly mean streamflow in percent of the annual mean of the control period and the scenario series for two elevation bands at Masi in River Alta.

Figures 5.4.1 to 5.4.5 show weekly mean values for the control period (blue and turquoise) for the HadAM3H- and the ECHAM4-model respectively. The mean weekly values of the scenario period are shown for the HadA2-scenario (magenta), the HadB2 (yellow) and the ECHAMB2 (violet).

The shift from a snow melt regime with a dominant spring flood to a regime with winter and autumn flood dominance is most obvious in the lower elevation band, while the snowmelt peaks are still present in the higher elevation bands as typically seen at Nervoll. The shift is least in the highest elevation band, but the snow melt flood tends to occur earlier and with smaller average peaks.

5.5 Projected changes of the streamflow in selected regions

5.5.1 River Trysilelv and upper River Glomma

5.5.1.1 Description of the basins

The upper River Glomma and River Trysilelv are situated close to the border with Sweden, and with some small parts of the upstream basins on the other side of the border. The region is fairly dry with cold winters, but the uppermost part of River Glomma is occasionally affected by weather systems over Trøndelag in Mid-Norway.

Scenarios are developed for three basins data in the region:

2.142 Knappom in River Flisa is mostly covered by forests.

311.6 Nybergsund in River Trysilelv comprises both forested and mountaneous areas within the basin. The basin comprises also a number of lakes, which attenuates floods, especially Lake Femunden.

2.111 Aursunden in River Glomma comprises the uppermost part of the Glomma basin. The basin comprises areas covered with mountain forests as well as low mountains plains. The basin is regulated, but naturalised flow series are available at the outlet of the basin.

5.5.1.2 Annual and seasonal mean streamflow

The projected change in annual and seasonal streamflow is shown in Figure 5.5.1. The changes are marginal in the annual streamflow, but show a well defined shift in the seasonal values. The winter streamflow is projected to increase by 55 to 80 % at Knappom, 10 to 50 % at Nybergsund and 25 to 65 % at Aursunden. The summer streamflow will decrease by 7-15 % at Knappom and increase by 5-35 while the autumn streamflow will decrease 2 to 18 % in the HadA2-scenario, remain unchanged in the HadB2-scenario at % in the two other higher basins. The summer streamflow will decrease by 15 to 42 % in all basins, Nybergsund and Knappom and increase by 17% at Aursunden. The ECHAM-B2-scenario projects an increase of 10-32% for all three basins.

The Knappom basin differs somewhat from the two other basins. This basin is situated at lower altitudes, and is dominated by forests. The observed weekly mean values and the weekly percentage change between the scenarios and the control period are shown in Figure 5.5.2 for the Aursunden basin and for the Knappom basin. The weekly statistics forms the basis for simulation of energy production.

5.5.1.3 Floods

Statistics of the annual flood show a decline or marginal change in most flood statistics within the region, as seen in Figure 5.5.3. The largest annual flood is usually the snowmelt flood in this region, although large rainfall floods can occur in the late summer linked to very warm events. The large event at Fulufjäll in Sweden 30.-31.august 1997 occurred at the eastern margin of this region. The maximum rainfall is estimated to more than 350 mm in the maximum zone, with a maximum of 150 mm on the Norwegian side of the border. This gave a 10-year flood at some stations in Trysilelv. More recently a severe rainstorm occurred 11.July at River Eltå, a tributary to Trysilelv. The most severe floods in the region, such as Storofsen in July 1789 and Vesleofsen in June 1995 were combined floods caused, both by snowmelt and rainfall.
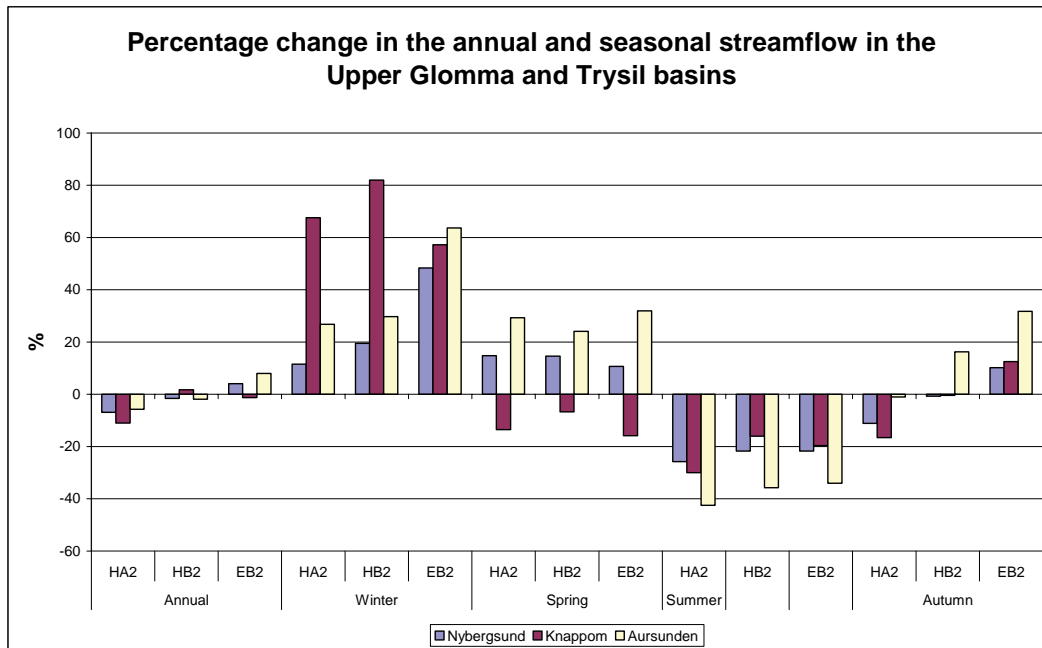
Figure 5.5.1   Projected percentage change in the mean seasonal streamflow in three basins in East Norway based on scenarios of the HadAm3H model (A2 and B2). Blue and red bars refer to basins draining to the east and south east, yellow and green bars to basins draining to the west.
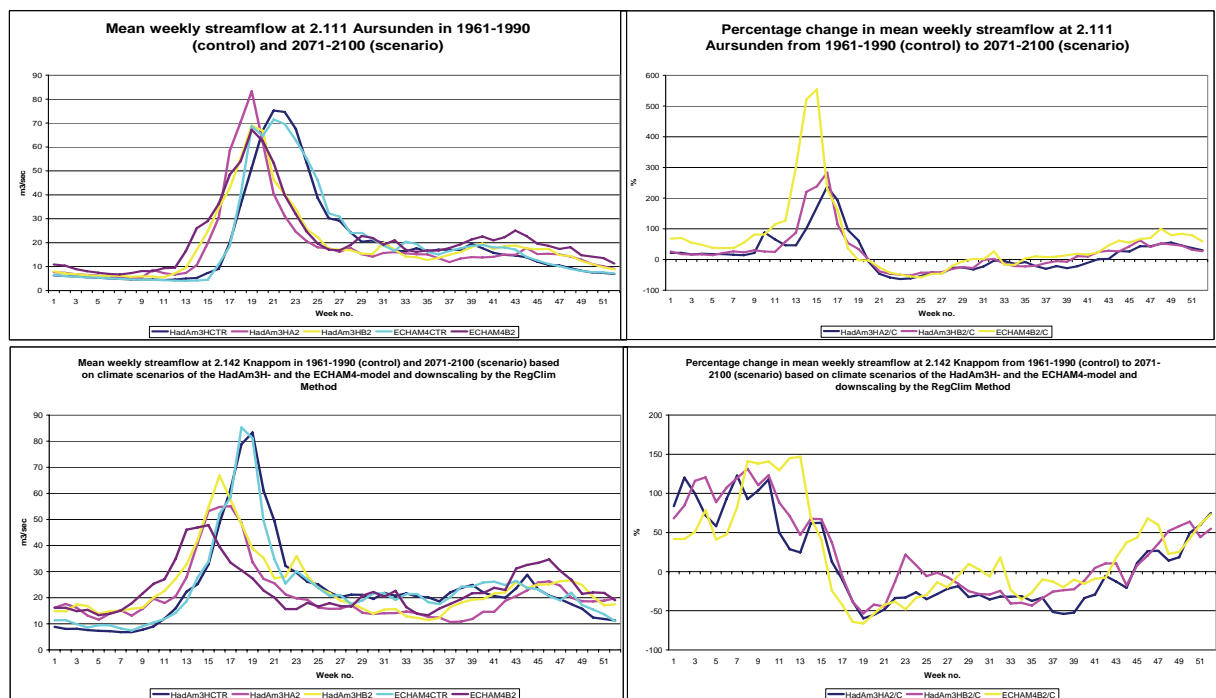
Figure 5.5.2 Weekly mean streamflow in the Aursunden basin (top left) and in the Knappom basin (bottom left) and projected percentage change in streamflow in the Aursunden basin (top right) and in the Knappom basin (bottom right) in the control period 1961-1990 and the scenario period 2071-2100.
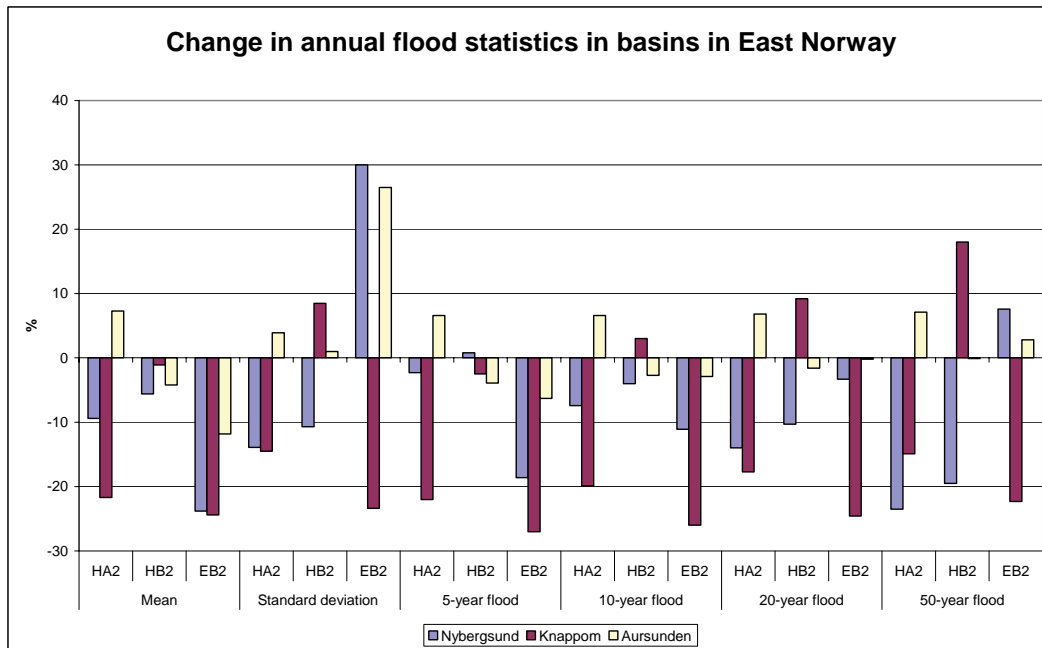
Figure 5.5.3 Projected change per decade in selected flood statistics for three basins in East Norway based on scenarios of the HadAm3H model (A2 and B2). Blue and red bars refer to basins draining to the east and south east, yellow and green bars to basins draining to the west.

The seasonal floods are projected to change more both in terms of timing of the flood and the flood magnitudes. The maximum flood in the winter will increase considerably, while the spring flood will decline in Trysilelv and remain unchanged in the Aursunden basin. The summer floods are projected to decline by 13 to 57 %, and the autumn flood will decline moderately in both HadAm3H-scenarios and increase by 21-53 % in the ECHAM4-scenario.

The mean annual flood will occur 17-19 days earlier at Nybergsund and Aursunden. The annual peak will occur from 13 days earlier to 20 days later at Knappom depending on the scenario. This reflects that snowmelt floods will be more reduced in the lower Knappom basin and that later rainfall floods will become more frequently the annual maximum. Figure 5.5.4 show the percentage of years with the maximum annual flood occurring in each month of the year for all scenarios. The figure show that the peak flood can occur in almost every month in the low Knappom basin, and that the spring flood tends to occur one month earlier in a warmer climate.
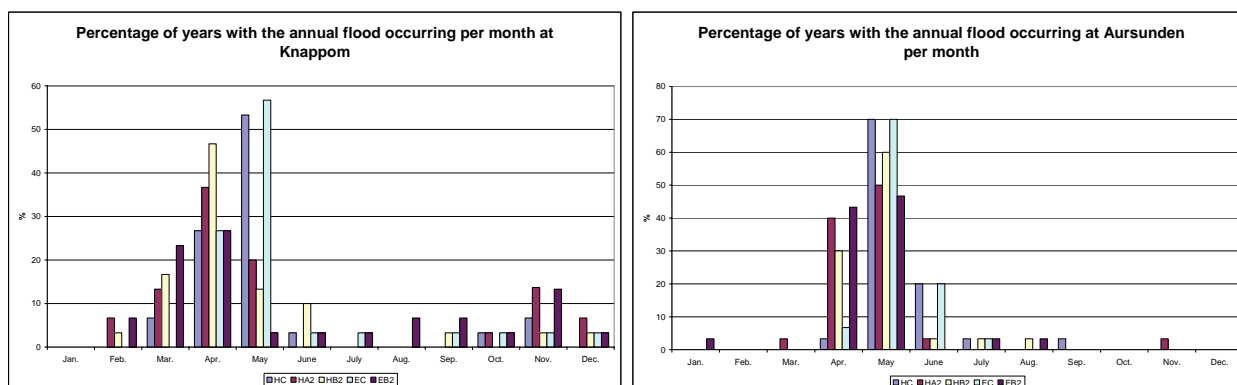
Figure 5.5.4   Percentage of years with the annual maximum flood occurring per month in the Knappom and Aursunden basin.

5.5.2 High alpine basins

5.5.2.1 Description of the region

There are three mountain regions with peaks exceeding 2000 m altitudes, ie Jotunheimen, Dovrefjell and Rondane. The study includes two basins: Sjodalsvatn in River Sjoa, which is situated on the east side of Jotunheimen and Risefoss in River Driva, which drains part of the central Dovrefjell area. The Sjodalsvatn basin reaches an elevation of 2362 m.a.s.l and is covered by 9.22 % glaciers, and has a lake percentage of 9.3 %. The Risefoss basin reaches an elevation of 2284 m, but has only 0.37 % glaciers, and very little attenuation of floods by lakes.
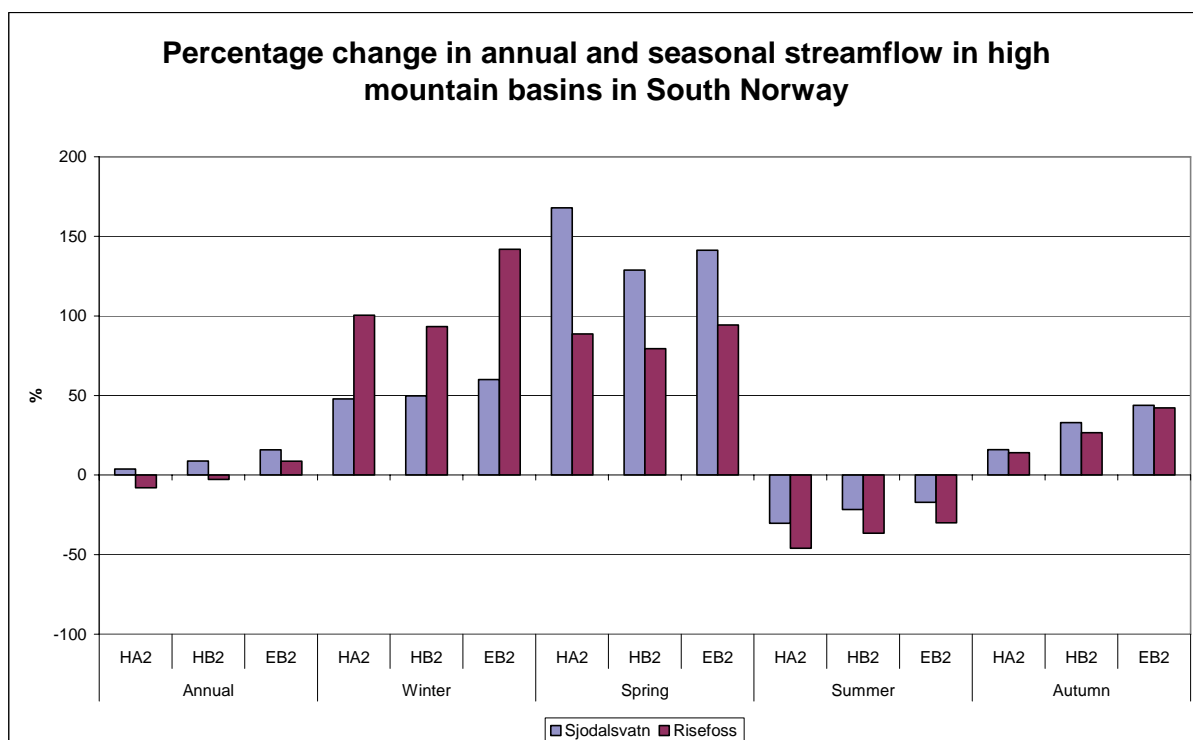
5.5.2.2 Annual and seasonal mean streamflow

The mean annual streamflow is projected to change marginally with an increase of 5 to 10 % at Sjodalsvatn and a smaller decrease or increase at Risefoss, see Figure 5.5.5. Changes in the seasonal streamflow is shown in Figure 5.5.6. The winter streamflow is projected to increase 50 to 60 % at Sjodalsvatn and 90 to 140 % at Risefoss. The spring streamflow will increase 130 to 160 % at Sjodalsvatn and 80 to 95 % at Risefoss. The autumn streamflow will increase by 15 to 45 % in both basins.

The large increase in the winter and spring streamflow reflects that winter streamflow is quite low under the climate of the control period. The snowmelt flood peaked usually in June, and the shift towards earlier snowmelt explains the shift in the seasonal means from a summer to a spring peak. The differences in magnitudes between the two basins reflects also that the Sjodalsvatn basin comprise more alpine areas and a much larger percentage of glaciers than the Risefoss basin.

Both basins are situated with high mountains to the west, well protected from the heavier precipitation closer to the coast. Scenarios have been developed for another basin close to Jotunheimen, Lalm at River Otta for the Climate and Energy project. The Lalm basin extends to the water divide and is less protected from precipitation from the west, especially in the western part. The annual streamflow is projected to increase by 14 to 18 % in the ECHAM4-scenarios, with increasing strength of the westerlies. The seasonal changes are fairly similar in the two basins, but with a tendency toward more autumn rainfall events in the western part of the Lalm basin.

Figure 5.5.5 Projected percentage change in the mean annual and seasonal streamflow in two high alpine basins in South Norway from 1961-1990 to 2071-2100 based on scenarios of the HadAm3H model (A2 and B2) and of the ECHAM4-model (B2).
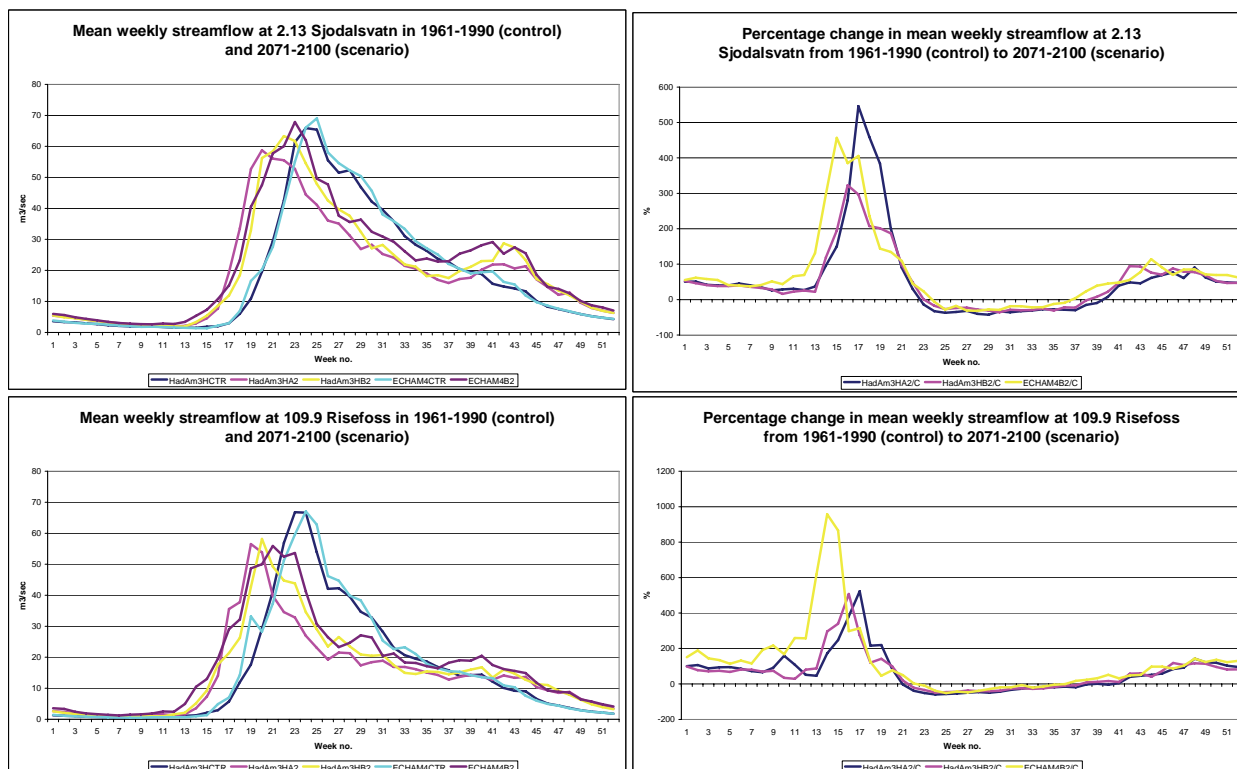
Figure 5.5.6 Projected weekly mean streamflow (right) and projected percentage change in streamflow (left) at Sjodalsvatn (top) and Risefoss (bottom) in the control period 1961-1990 and the scenario period 2071-2100.

5.5.5.3 Floods

The largest annual flood is usually the snowmelt flood in this region, although large rainfall floods can occur in the late summer linked to very warm events. Table 5.5.7 show projected changes in statistics of the annual maximum flood in the two basins. A moderate decline is projected in both basins. Sjodalsvatn has suffered from a few very large historical summer floods where heavy rainfall was main contributing factor to the flood, both Storofsen 21.-23.July 1789, the flood 15.-17.June 1860 and the flood 29.August-30.September 1938, which show that large rainfall floods can occur in this region as well. Risefoss has been affected by severe rainfall floods in 19.-20.July 1698, by Storofsen in July 1789 and by a large flood 8.July 1932, which was caused both by snowmelt and extreme rainfall. The western part of Jotunheimen including the Otta valley is in addition affected by weather systems penetrating from the west such as a large December thaw and flood 4.-5.December 1743.
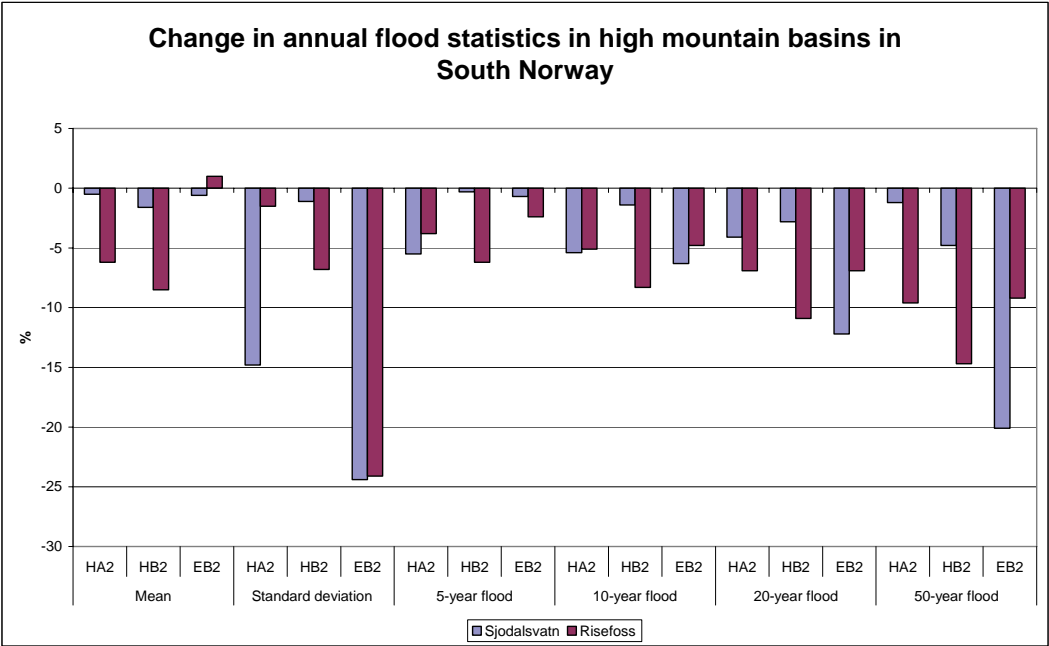

Figure 5.5.7   Projected change per decade in selected flood statistics for two basins in the high alpine region based on scenarios of the HadAm3H model (A2 and B2).
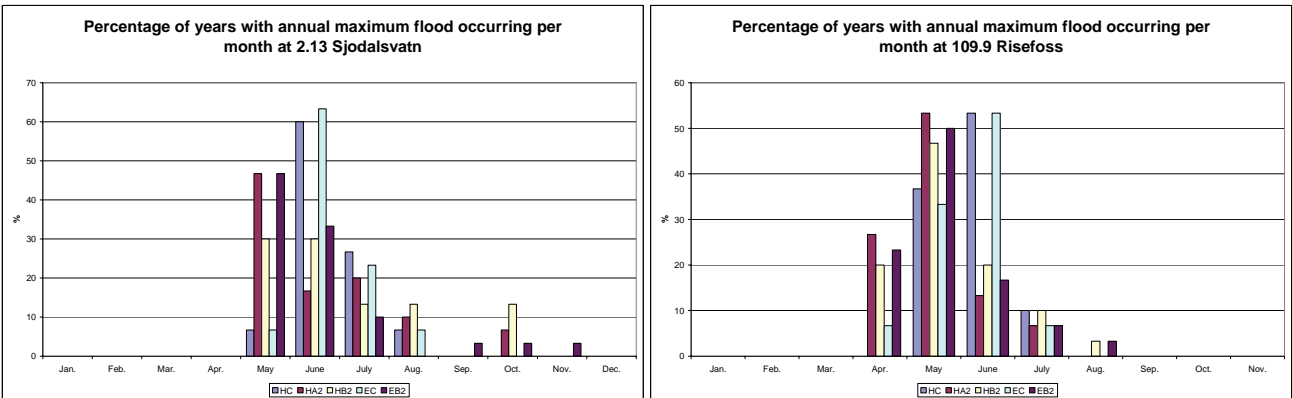

Figure 5.5.8   Percentage of years with the annual maximum flood occurring per month at Sjodalsvatn and Risefoss.

33

The frequency of years with the peak flood occurring per month is shown in Figure 5.5.8 for the two basins. The peak flood will both occur earlier than in the control period and with occasionally annual peaks later in the year
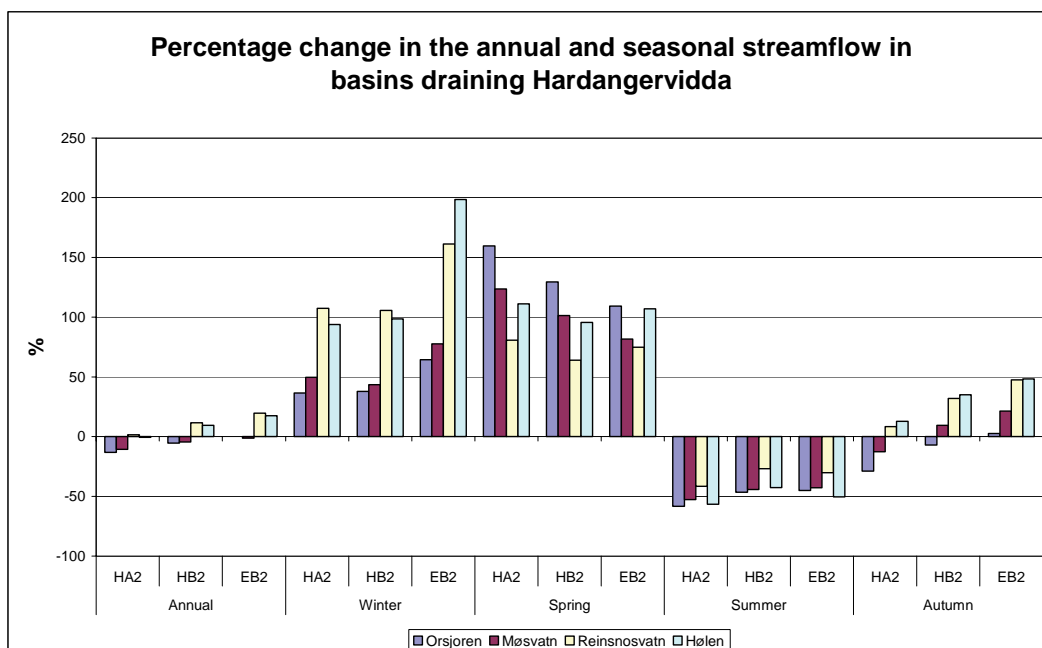
5.5.3 Basins around the Hardangervidda plateau

5.5.3.1 Description of the basins

The Hardangervidda plateau comprises some 12000 km2 of undulating mountains between 1000 and 1600 m altitude. Three of the major rivers in east Norway, River Drammenselv, Numedalslågen and Skienselv drain the plateau towards east and south east, while smaller rivers drains the plateau towards the west. Streamflow scenarios were developed for three basins, one in River Numedalslågen and two in rivers draining to the west. An additional basin has latter been added draining towards south east. The dominant flood is the spring or summer snowmelt flood, but intensive late summer floods occur in south east, and late autumn floods occur occasionally in the west. Three of the rivers are regulated with large reservoirs in River Numedalslågen and River Skienselv in the east and south east. Some of the rivers draining to the west are also regulated.

5.5.3.2 Annual and seasonal means

The projected change in the streamflow is quite marginal in annual values, although with a small decline in basins draining towards the east and a small increase in basins draining westward (Figure 5.5.9). The winter streamflow will increase by 40 to 75 % in rivers flowing eastward and 90 to 200 % in rivers flowing westward. The streamflow will increase in the spring by 60 to 160 % most in rivers flowing to the east. The HadA2-scenario produces the largest change in the spring. The summer streamflow is reduced by 30 to 50 % in all scenarios, while a small increase is indicated in the autumn except for the Orsjoren basin which is the driest of the four basins. The projected increase is largest in the west ranging from 10 to 50 %.

Figure 5.5.10 show weekly mean values and projected change in the weekly means for one basin draining to the east and one basin draining to the west. The peak is projected to occur earlier in both basins. The major difference between the east and west side of the plateau is the larger increase in the winter and autumn streamflow in the west.

Figure 5.5.9 **Projected percentage change in the mean seasonal streamflow in four basins around the Hardangervidda mountain plateau based on scenarios of the HadAm3H model (A2 and B2). Blue and red bars refer to basins draining to the east and south east, yellow and green bars to basins draining to the west.**
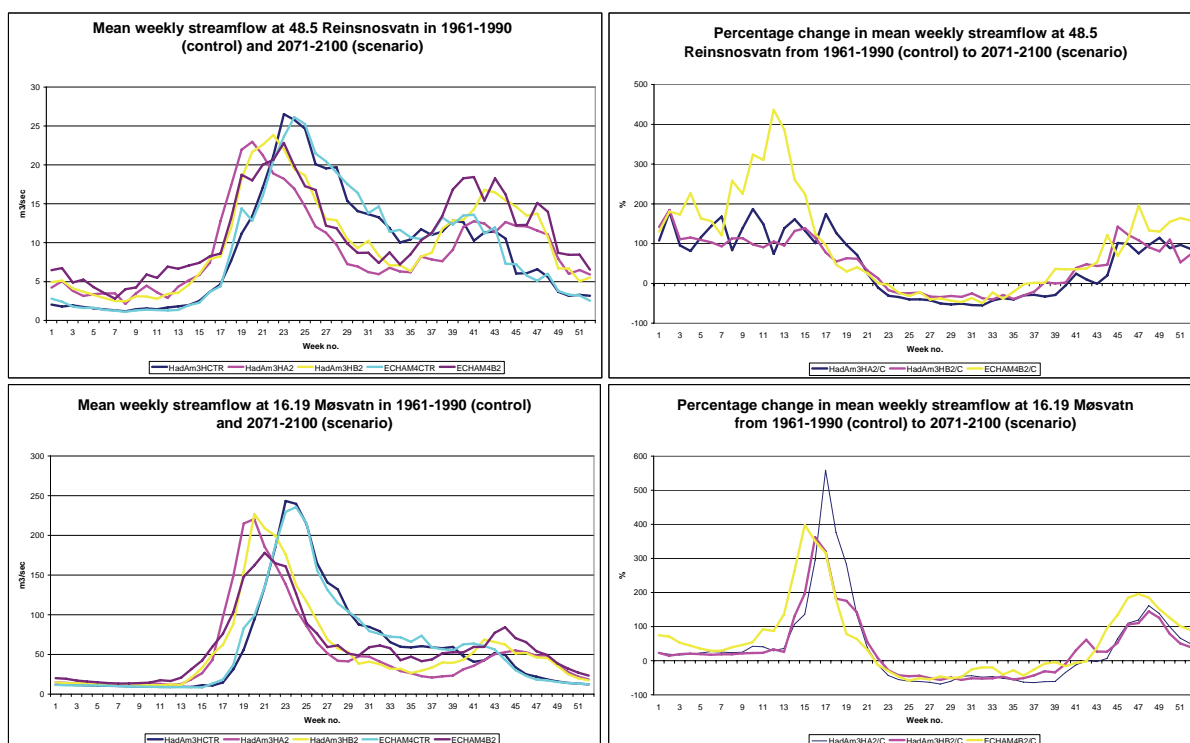
Figure 5.5.10 Weekly mean values for the control and scenario period and projected percentage change in the weekly mean streamflow between 1961-1990 to 2071-2100 for two basins on the Hardangervidda plateau. Reinsnosvatn (top) drains towards west Møsvatn (bottom) drains towards southeast.

5.5.3.3 Floods

The spring or early summer snowmelt flood occurs almost every year in the region, but the largest floods occur in the late summer or autumn. The largest floods on the eastern side occurred in August 1752, June 1860, late June 1927, August and September 1934 and August/September 1938. They were all caused by intensive rainfall. Some of the largest floods on the western side occurred in August 1719, December 1743, October 1918 and late November 1940. The autumn floods occur often as a combination of snow melting and heavy rainfall.

The differences in the projected change in the seasonal and weekly mean values on both sides of the mountain plateau are also reflected in the statistics of the projected annual flood shown in Figure 5.5.11. The eastern side with a dominance of snowmelt floods, but with intensive rainfall floods in some years, will have reduced 50 year floods, while the 50 year flood may increase in the west by up to 20 % if the ECHAM4B2 scenario is used.

Figure 5.5.11 Projected change per decade in selected flood statistics for four basins around the Hardangervidda mountain plateau based on scenarios of the HadAm3H model (A2 and B2). Blue and red bars refer to basins draining to the east and south east, yellow and green bars to basins draining to the west.
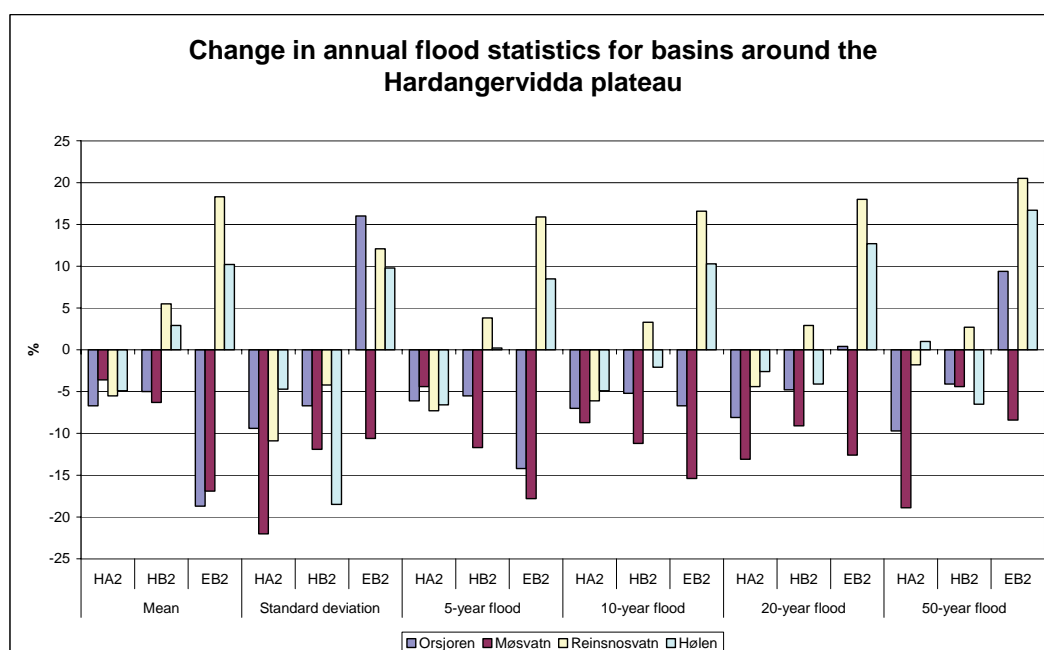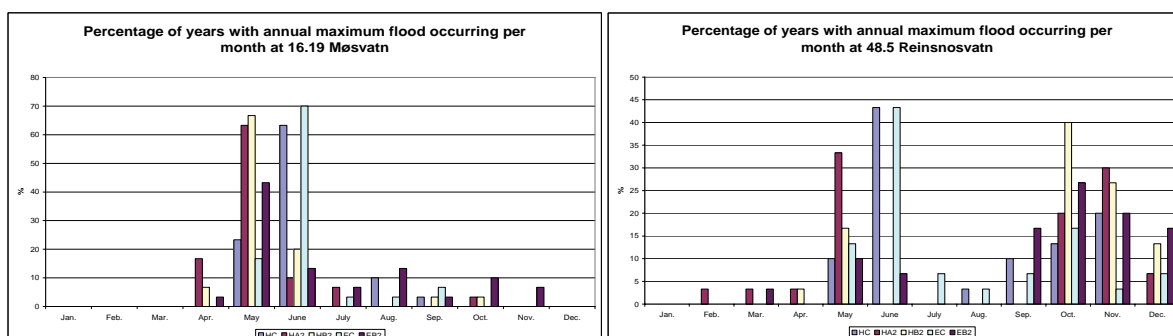

Figure 5.5.12 Monthly frequency of the time of the annual maximum flood in two basins of the Hardangervidda mountain plateau; Møsvatn (left) draining south east and Reinsnosvatn (right) draining westward.

The occurrence of the annual flood tends to occur later in a warmer climate, but can also occur in months without floods in the control period as shown in Figure 5.5.12.

5.5.4 Coastal basins in South Norway

5.5.4.1 Description of the region

Basins close to coast have some similarities in terms of seasonal distribution of the streamflow. The region comprises basins from the south coast to Nordland. The basins fall into two groups, extremely coastal basins such as 18.10 Gjerstad, 27.26 Hetland, 41.1 Stordalvatn, 107.3 Farstad as well as basins further from the coast, partly situated in the maximum precipitation zone, mostly with some parts of the basins situated in mountainous areas. The Gjerstad basin is in the on the east side of the southernmost part of Norway. Basins in the southwest tend to have a similar seasonal distribution, which differs somewhat from the basins further north along the west coast.
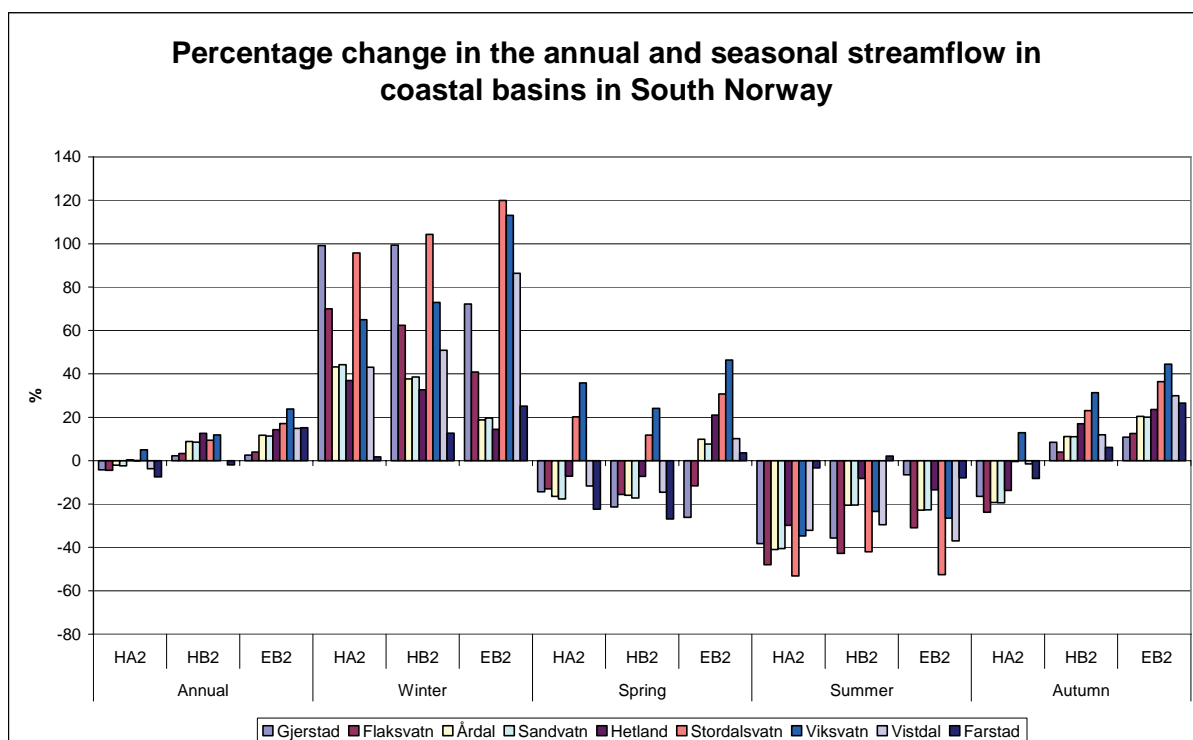
5.5.4.2 Changes in mean and seasonal streamflow

The easternmost basins are projected to have marginal changes in the annual streamflow, while basins in the southwest and west will have an increase of 10 to 25 % in the annual streamflow in the B2-scenarios (Figure 5.5.13). The winter streamflow is projected to increase by 20 to 120 %, most in the extreme coastal basins. The spring streamflow will decrease in most of the basins, except in the western basins in the ECHAM4-scenario. The spring streamflow is projected to increase by 10 to 45 % in the Viksvatn and the Stordalsvatn basin. Viksvatn is further inland than the other basins and have a little contribution to the streamflow from glacier melting. The summer streamflow will decline in all basins, and the autumn stream will decrease by 15 -25 % in most basins in the HadA2 scenario and increase by 5 to 45 % in the two B2-scenarios.
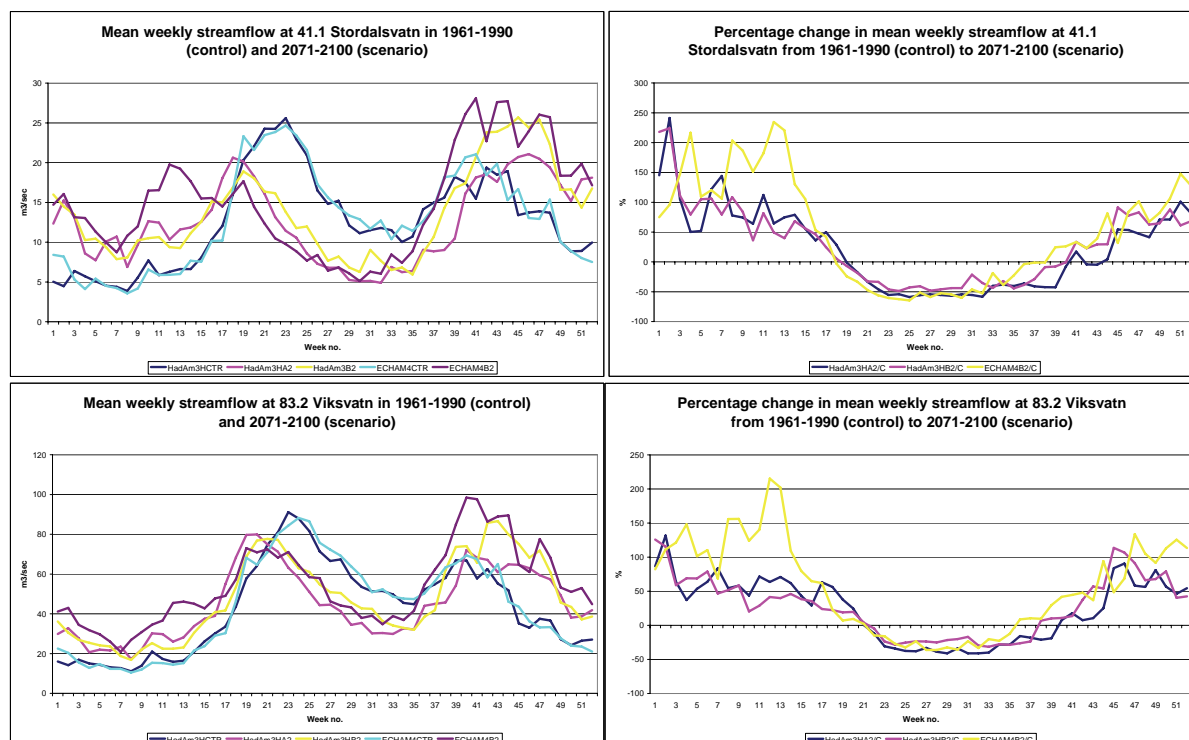
Figure 5.5.14 shows projected weekly means for the control period and the scenario period for both models and percentage change in the weekly values for the Stordalsvatn and Viksvatn basins. The seasonal regime at the coastal Stordalsvatn will change from a high flow period in the late spring and a smaller secondary wet period in the autumn, to a regime with a high flows in the autumn through the winter. The spring at Viksvatn will occur earlier, and the peak in the autumn will be as high or higher than the peak in the spring.

5.5.4.3 Floods

Large floods in coastal basins in West Norway are dominated by autumn flood caused by heavy or long duration rainfall events. The most severe events occurred in 1719, 1743, 1918 and 1940. The floods may occur after earlier snowfall, especially in the inner part of the region. Intensive rainfall can also cause severe flooding, such as the rainstorm in the Bergen region 10.-11.October 1953 with 311 mm rainfall observed at Samnanger. Recently some local flooding was caused by intensive rainfall caused by remnants of tropical hurricanes such as the flood near Bergen 14.-15.November 2005. Winter floods can cause local damages when heavy rainfall fall on frozen or snow covered ground. Mountainous basins in the inner fjords are more affected by spring snowmelt floods as mentioned in Sub-Section 5.5.3.3. Figure 5.5.15 show projected changes in selected statistics of the annual flood within the region.

Figure 5.5.13 Projected percentage change in the mean annual and seasonal streamflow in coastal basins in South Norway from 1961-1990 to 2071-2100 based on scenarios of the HadAm3H model (A2 and B2) and of the ECHAM4-model (B2).

Figure 5.5.14 Weekly mean values for the control and scenario period and projected percentage change in the weekly mean streamflow between 1961-1990 to 2071-2100 for two basins on the west coast of Norway. Stordalsvatn (left) is on the extreme coast while Viksvatn (right) is more inland.

The annual flood is projected to decrease in the two southernmost basins and increase elsewhere by 5 to 30 %. The winter flood is projected to increase by 12 to 78 % most in the HadA2-scenario in the south and southwest. The B2-scenarios will increase by 5 to 72 %, most in the ECHAM4-scenario in the west. The spring flood is projected to decrease by 13 to 23 % in the HadA2-scenario in the south and southwest, and increase in the west by 14 to 39 %. The spring flood will decrease by 0 to 13 % in the south and increase by 4 to 22 % in the rest of the region for the B2-scenario, most in the ECHAM4-scenario. The HadA2 and B2 scenario indicate reduced floods of 12 to 48 % in the summer, except in the Gjerstad basin. The ECHAM4-scenario indicates increased summer floods in the south and southwest of 8 to 49 % and small changes in the west. The autumn floods are projected to decrease by 6 to 17 % in the south and southwest in the HadA2 scenario. The two B2-scenarios indicate an increase of 0 to 29 % in all basins. The extreme coastal Farstad basin differs from the other basins within the region in terms of seasonal changes in the floods.

Figure 5.5.16 show the frequency of years with the annual flood occurring per month for Stordalsvatn and Viksvatn. The annual peak flood will occur more frequently in all winter months in a warmer climate.
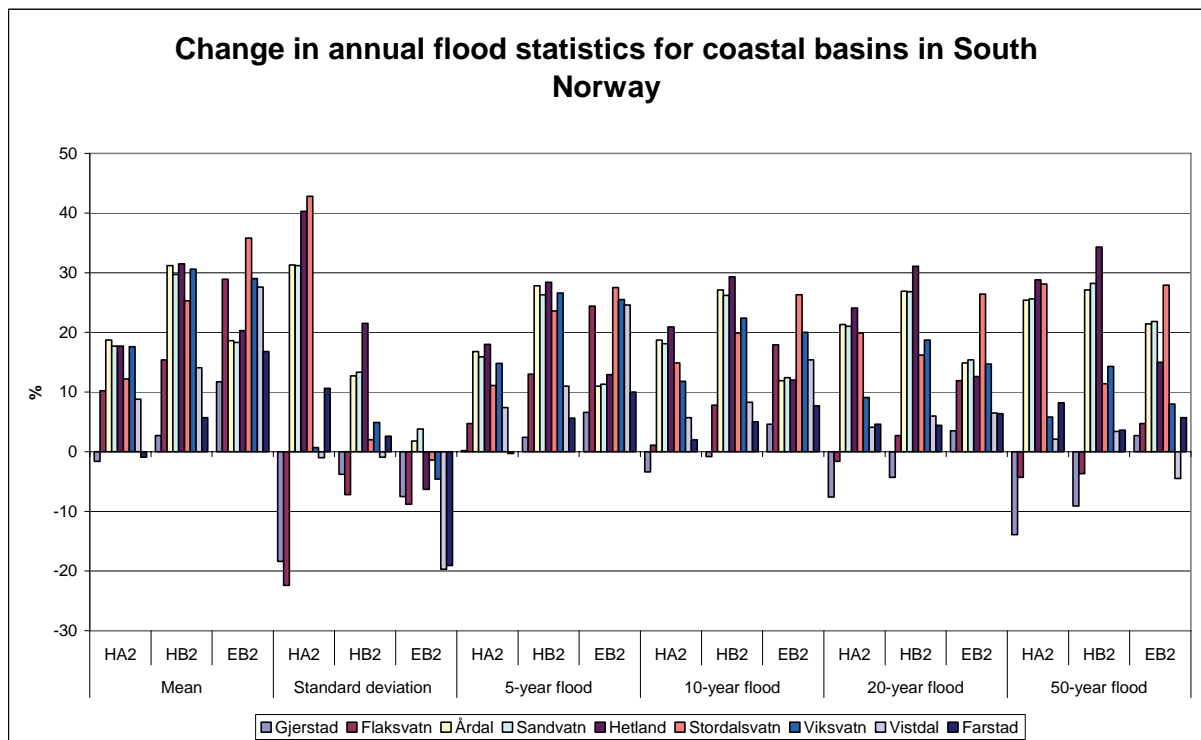
Figure 5.5.15 Projected change in selected flood statistics for coastal basins based on scenarios of the HadAm3H model (A2 and B2) and the ECHAM4 (B2).
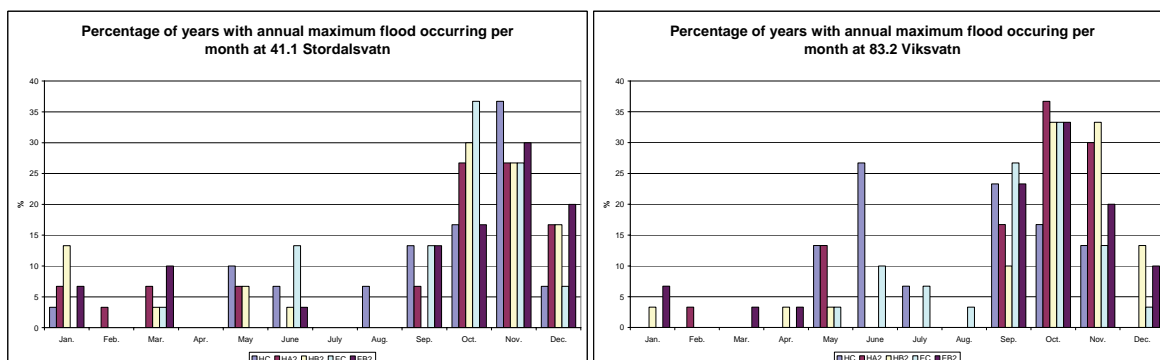
Figure 5.5.16 Frequency of the occurrence of the annual maximum flood per month at Stordalsvatn (left) and Viksvatn (right).

5.5.4 Basins in Trøndelag and North Norway

5.5.4.1 Description of the basins

The region comprises both inland basins with a dominating snowmelt regime and basins affected by a more coastal streamflow regime. Two basins have been included from Trøndelag, both in River Nea. The scenarios developed for the Climate and Energy project includes also basins in River Gaula, Stjørdalselv and Årgårdselv in Trøndelag. The region includes two basins from Nordland and one basin on Finnmarksvidda. The Kobbvatn basin is exposed to weather systems from the west, although the basin is fairly mountainous. The Nervoll basin is more sheltered, but has larger areas at low elevations. The elevation range of the Masi basin is quite small. The snowmelt occurs therefore simultaneously over much of the basin.

### 5.5.4.2 Annual and seasonal mean streamflow

The annual streamflow is projected to increase by 5 to 20 % except in the Masi basin, where the Hadley scenarios indicate a small decrease (Figure 5.5.17). The winter streamflow is projected to increase, most in the Nervoll basin. The change is from 40 to 200 % according to the ECHAM4-scenario. The change in the spring is small in the two basins in Trøndelag, but ranging from 35 to 70 % in the other basins. The summer streamflow will decrease from 10 to 55% in all basins. The autumn streamflow will increase by 10 to 55 %.

Figure 5.5.18 shows projected weekly means for the control period and the scenario period for both models and percentage change in the weekly values for the Kobbvatn and Masi basins. The high flow in the spring will be reduced and occur earlier at Kobbvatn. The spring flood will still be dominant at Masi, but the high flows will occur earlier than in the present climate.

Dankers (2002) has developed scenarios of the streamflow and other water balance elements for the Tana River basin. The study comprises partly of sensitivity modelling given temperature increase of 2 and 5 degrees and precipitation increase of 0 and 50 %. He applied also a distributed physically-based model with snow modelling based on an energy balance model and evotranspiration model based on the Penman-Monteith Model. The climate change scenarios were based on the ECHAM4-model with dynamical downscaling based on the regional HIRHAM4-model and the A2-emission scenario. The annual precipitation is projected to increase by 25 %, similar to the HadAm2-A2-scenario. The changes in various water balance elements are similar to those found for the Masi basin although the change in annual streamflow is higher in Tana than in Masi.
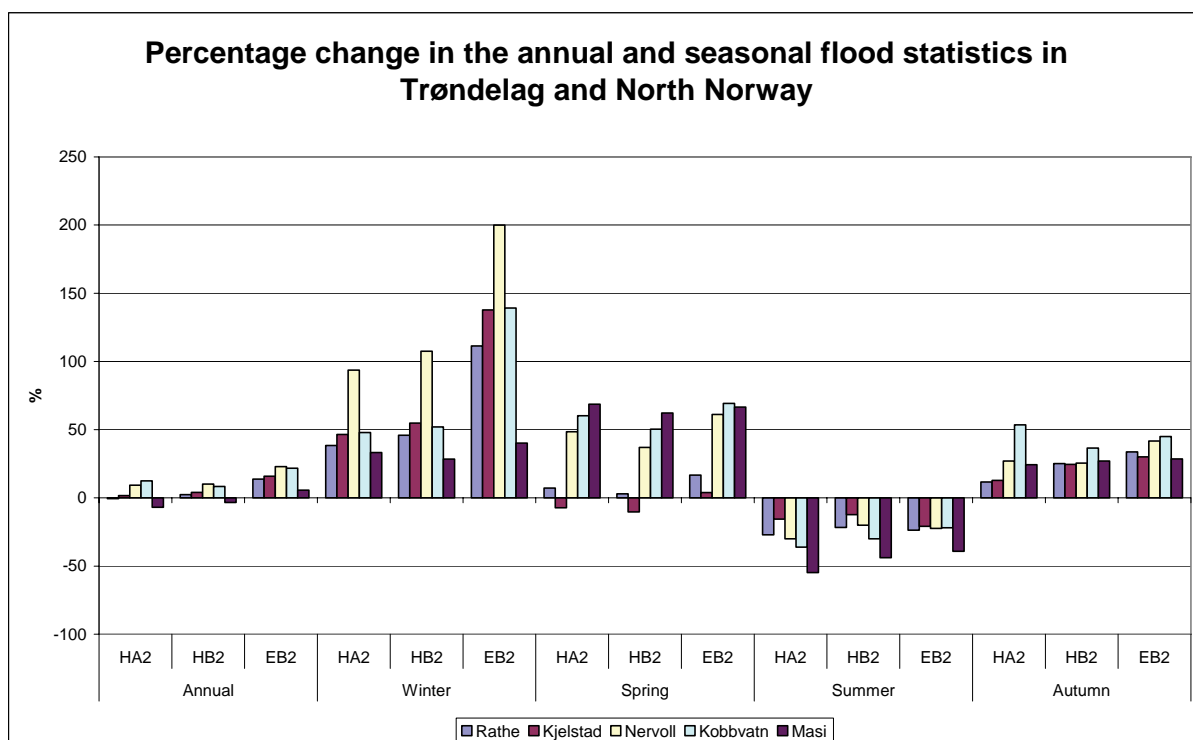
Figure 5.5.17 Projected percentage change in the mean annual and seasonal streamflow in basins in Trøndelag and North Norway from 1961-1990 to 2071-2100 based on scenarios of the HadAm3H model (A2 and B2) and of the ECHAM4-model (B2).
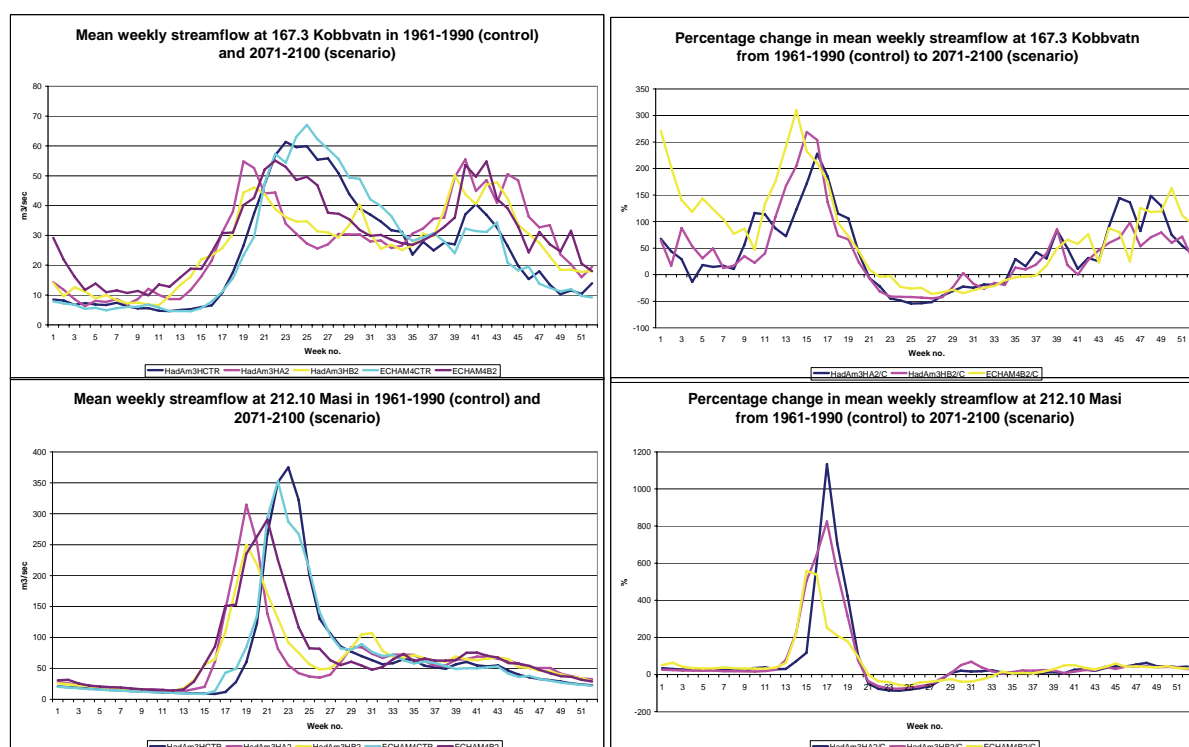
**Figure 5.5.18 Weekly mean values for the control and scenario period and projected percentage change in the weekly mean streamflow between 1961-1990 to 2071-2100 for two basins in North Norway. Kobbvatn is a mountain basin also strongly affected by the closeness to the coast, while the Masi basin drains parts of Finnmarksvidda.**

41

5.5.4.3 Floods

The dominant flood of the control period is the snowmelt flood for the basins included in the study in this region. Basins on the extreme coast of Trøndelag and Nordland have a flood regime as outer coastal basins on Vestlandet, with the annual flood occurring in most months of the year, although with a dominance in the autumn and winter. Intensive rainfall events have also occurred in this region. The 1789-flood caused extensive damages in Driva, Surna, Orkla and locally in Gaula. A severe rainstorm in August 1940 caused also extensive damages in Gaula. The large snowmelt floods in southern Norway occurred also in most of these basins in 1916, 1934, 1966 and 1995. Many coastal basins have often been affected by rainfall of more than 100 mm in a day, causing flooding in the rivers. The largest floods in North Troms and Finnmark are all snowmelt floods; the largest observed floods occurred in 1917, 1920 and 1996.

The annual streamflow is projected to increase in the Kobbvatn basin by 40 % according to the ECHAM4B2 scenario (Figure 5.5.19). The annual streamflow will change marginally in the other basins. The winter floods will increase by 15 to 44 % at Rathe. The increase will be in the range of 18 to 226 % further north, most in the Masi basin, where the winter flow is very low in the control period. The spring flood is projected to increase in the Kobbvatn basin in both Hadley scenarios by 24 to 40 % and at Masi in the ECHAM4-scenario by 13 %. The spring flood will otherwise decline from 1 to 18 % in the region. The summer flood will increase in Trøndelag and at Kobbvatn, especially in the HadA2-scenario by 2 to 26 %. The summer flood will decrease at Nervoll and Masi by 3 to 34 %. The autumn flood will decrease by 1 to 19 % at Rathe, Kjelstad and Nervoll, and increase by 5 to 151 % at Kobbvatn and Masi.

Figure 5.5.20 show the frequency of years with the annual flood occurring per month for Kobbvatn and Masi. Winter and early spring flood is likely to be more frequent at Kobbvatn, while rainfall floods may be more frequent as the annual flood at Masi.
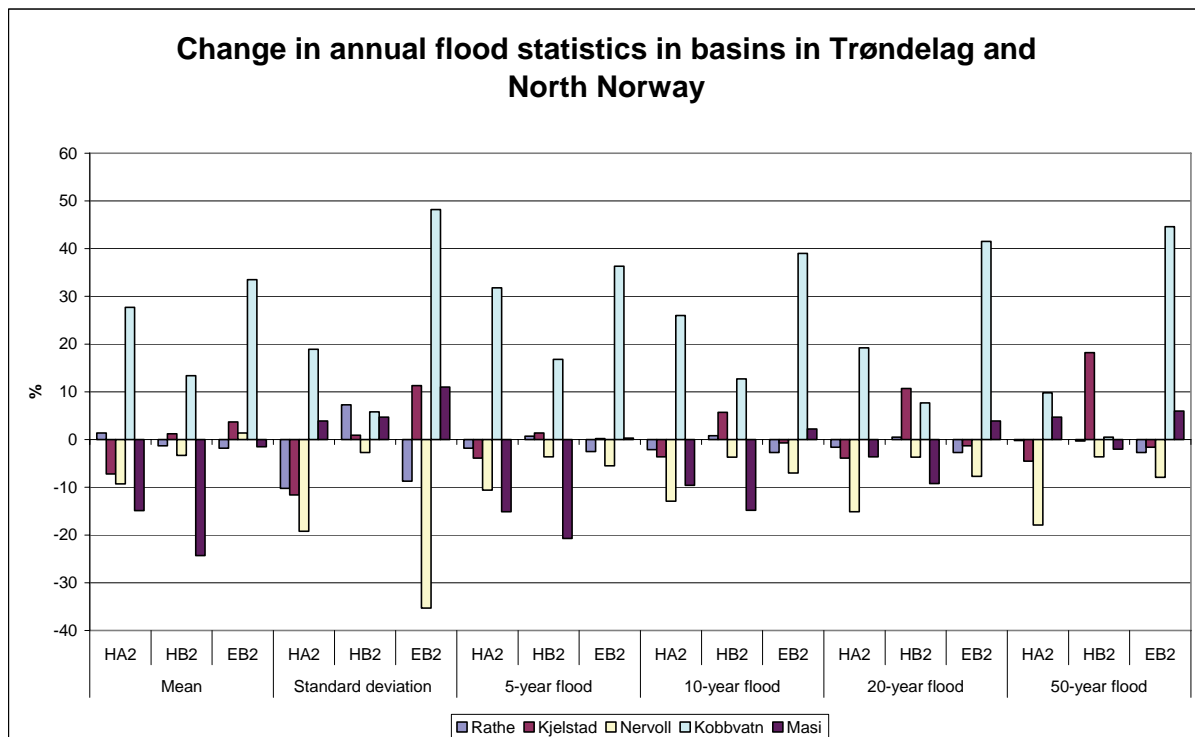
Figure 5.5.19 Projected change in selected flood statistics of basins in Trøndelag and North Norway based on scenarios of the HadAm3H model (A2 and B2) and the ECHAM4 (B2).
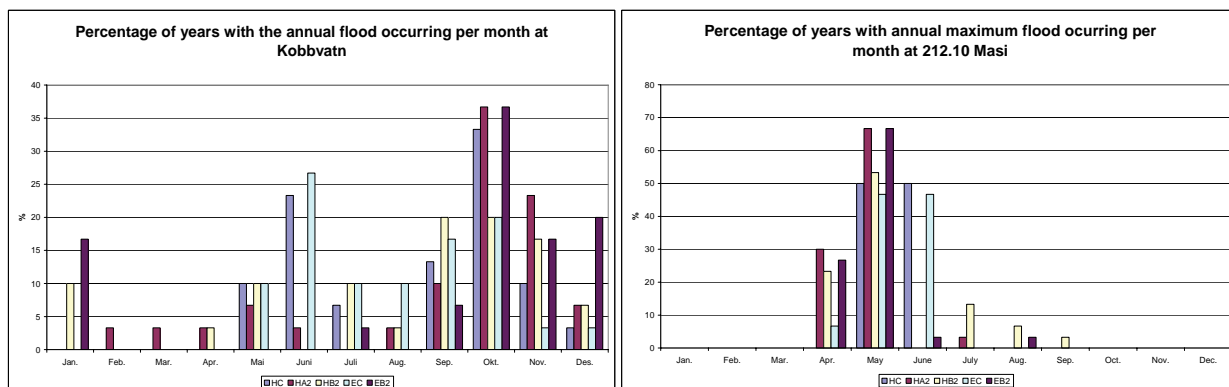
Figure 5.5.20 Frequency of the occurrence of the annual maximum flood per month at Kobbvatn (left) and Masi (right).

6 Projected changes in other water balance elements

The Norwegian landscape is dominated by boreal forests and mountains, with distinct topographic features such as valleys, hills, ridges and plateaus that were shaped beneath great Pleistocene ice sheets. Exposed bedrock and shallow till deposits interspersed with isolated glaciofluvial deposits cover the land surface. Streams, lakes and bogs are abundant, and glaciers are common in western and northern parts. This mosaic of terrain elements creates a heterogeneous lower boundary to the atmosphere with highly differing thermal, roughness and radiative properties. Small scale phenomena influence the exchanges of water and energy between the land surface and the atmosphere and the lateral redistribution of water through subsurface and surface flows. In view of the natural variability of the landscape and the non-linearity of the processes involved, hydrological models should apply a process-adequate areal discretization scheme, where individual model elements act as hydrological response units, i.e. patches in the landscape mosaic having a common climate, land use and pedological, topographical and geological conditions controlling their hydrological process dynamics. A physically realistic framework for regional modelling of land surface hydrology is therefore provided by models which integrate the contributions from several small scale elements. The hydrological model must account for the water balance of ungauged areas where no data are available for calibration. Model parameters must therefore be estimated using information about land surface properties and available hydrological data from other parts of the region of interest (Gottschalk et al., 2001). This procedure was applied for the hydrological modelling in this study, using a geographically transferable set of model parameters determined by Beldring et al (2003).

The parameter values assigned to the computational elements of the precipitation-runoff model should reflect that hydrological processes are sensitive to spatial variations in topography, soil properties and vegetation. As the Norwegian landscape is dominated by shallow surface deposits overlying a relative impermeable bedrock, the capacity for subsurface storage of water is small (Beldring, 2002). Areas with low capacity for soil water storage will be depleted faster and reduced evapotranspiration caused by moisture stress shows up earlier than in areas with high capacity for soil water storage (Zhu and Mackay, 2001). Vegetation characteristics such as stand height and leaf area index influence the water balance at different time scales through their control on evapotranspiration, snow accumulation and snow melt (Matheussen *et al.*, 2000). The following land use classes were used for describing the properties of the 1 km^2 landscape elements of the model: (i) areas above the tree line with extremely sparse vegetation, mostly lichens, mosses and grass; (ii) areas above the tree line with grass, heather, shrubs or dwarfed trees; (iii) areas below the tree line with subalpine forests; (iv) lowland areas with coniferous or deciduous forests; and (v) non-forested areas below the tree line. The model was run with specific parameters for each land use class controlling snow processes, interception storage, evapotranspiration and subsurface moisture storage and runoff generation. Lake evaporation and glacier mass balance were controlled by parameters with global values.

6.1 Water equivalent of the snow cover

6.1.1 Modelling the snow cover

Snow storage is described by a temperature index approach. Precipitation accumulates as snow when the daily mean air temperature falls below a threshold value. The accumulation is even to an accumulated snow storage of 20 mm. When the snow storage reaches this level, additional snow fall is

distributed according to a log-normal distribution. The actual form of the snow distribution is a function of vegetation type, with largest skewness for landscape elements with low vegetation and open terrain exposed to wind. Snow melt is a function of a degree-day index and the difference between the daily mean air temperature above a threshold value. Meltwater is retained in the snow pack until the amount of liquid water reaches a specified fraction of the snow water equivalent. Above this threshold meltwater leaves the snow pack and infiltrates into the soil moisture zone. When the daily mean temperature is below the threshold melt temperature, liquid water in the snow pack will refreeze, but at a lower efficiency than the snow melt. Simulated and observed time series of snow water equivalent at the snow pillow at Vauldalen in the Aursunden catchment are shown in Figure 6.1.1.
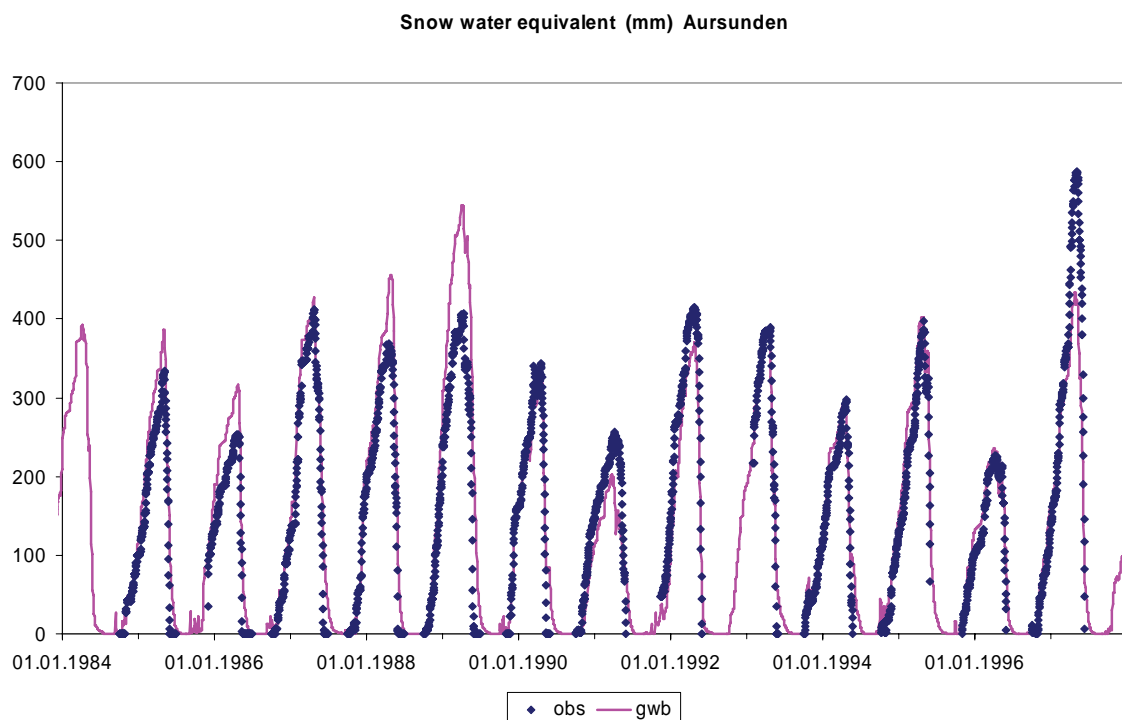
Figure 6.1.1   Observed and simulated snow water equivalent (mm) in the Aursunden catchment for period 1984-1997.

6.1.2 Changes in maximum snow storage and duration of snow cover

The seasonal change in the streamflow described in Chapter 5 is strongly linked to changes in the snow cover. The amount of snow is both dependent on the air temperature and the amount of precipitation accumulating as snow. The winter precipitation is projected to increase in many regions. Roald et al (2002) found that the snow storage could increase in high mountainous areas especially in the inland up to 2050. The scenarios indicate that the temperatures will increase more after 2050. Mild episodes will be more common in the winter and the accumulation season can be expected to become shorter. The gridded water balance model produces also series of daily snow water storage for each grid cell, and this can be averaged over selected basins as time series. The changes in the snow water storage were examined by determining the change in the total annual volume, the length of the season

with significant snow-cover, the change in the maximum snow-water equivalent and the time of the maximum value.

Figure 6.1.2 shows the distribution over Norway of maximum snow water equivalent during the control period and changes in the maximum snow water equivalent from the present to the three scenarios. Figure 6.1.3 shows the number of days per year with snow covering more the 50 % of the ground for each 1km^2 grid cell of the model for the present climate and changes from present to the three scenarios.
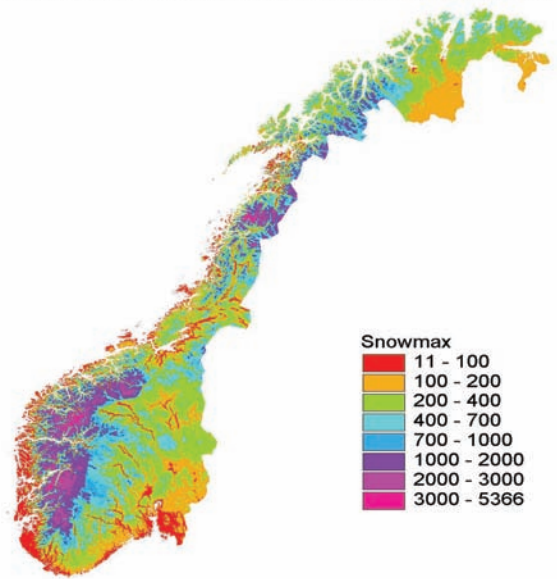
6.2 Evapotranspiration

6.2.1 Modelling evapotranspiration

Potential evapotranspiration is calculated by a temperature index approach which accounts for seasonal variations of biomass in the different land use/vegetation classes. For temperatures below the freezing point potential evapotranspiration is equal to zero. Only snow free areas are assumed to evaporate, an exception is intercepted snow. Maximum interception storage is specified for each vegetation type. The interception storage will lose water at the potential rate, regardless of whether the intercepted precipitation is rain or snow. Actual evapotranspiration from the soil moisture zone is equal to potential evapotranspiration as long as the soil moisture is above a threshold. Below this threshold, actual evapotranspiration is reduced linearly to zero as a function of soil moisture content. Water can be drawn from the groundwater zone to the soil moisture zone at a rate which is a function of the water content in the two zones. As long as water is present in the interception storage, the actual evapotranspiration from the soil moisture zone is reduced. Lakes are assumed to evaporate at a potential rate which is a function of air temperature and lake temperature. Lake temperatures are modelled by an autoregressive model which delays the effects of changes in air temperatures.

6.2.2 Changes in evapotranspiration

The temperature scenarios for 2071-2100 project an increase in annual mean temperatures for all parts of Norway. Annual precipitation is also expected to increase in most parts of the country. This surplus of energy and water compared to present conditions results in increased evapotranspiration as shown in Figures 6.2.1 and 6.2.2. The increase in evapotranspiration is larger in western parts of Norway than in eastern parts, following the pattern of precipitation increase. The temperature index approach may introduce a bias in evapotranspiration modelling for changed climate conditions, as plants have the ability to reduce their water losses when temperatures increase. Furthermore, increased CO_2 contents in the atmosphere may result in more efficient photosynthetic rates, resulting in reduced water loss from vegetation. However, these effects are uncertain and have not been taken into consideration in this study.

Figure 6.1.2 **Average of annual maximum snow water equivalent for 1961-1990 (mm) (upper left) and projected change from 1961-1990 to 2071-2100 (mm) for the HadAm3H-A2 scenario (upper right), the ECHAM4-B2 scenario (lower left) and the HadAm3H-B2 scenario (lower right).**
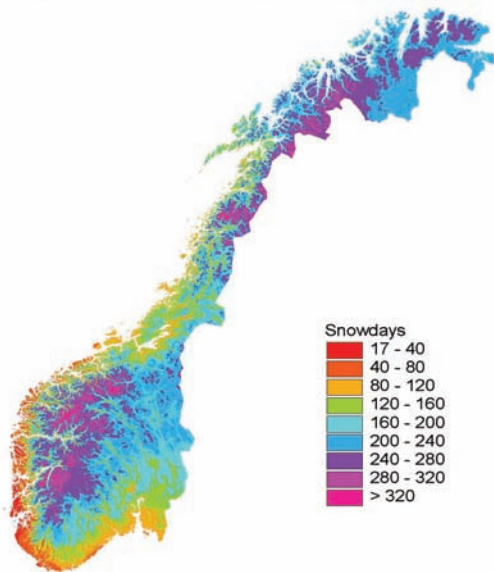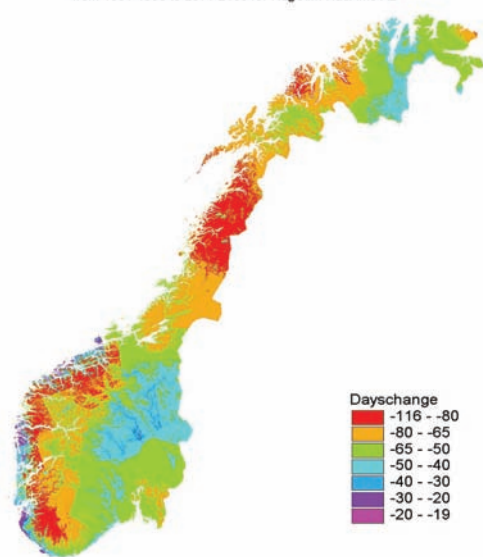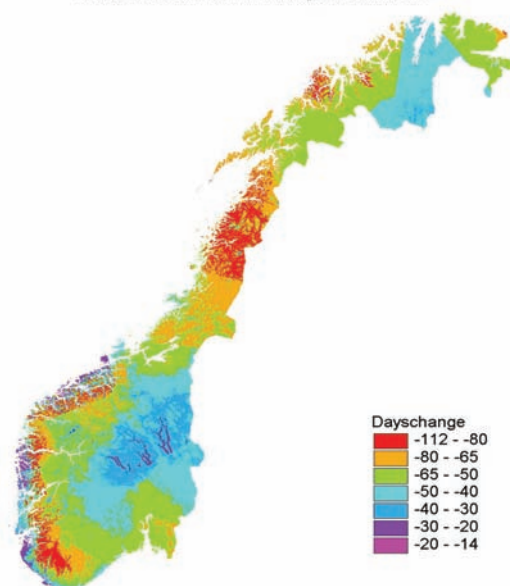
Figure 6.1.3 **Average number of days per year with snow covering more than 50 % of the ground for 1961-1990 (upper left) and projected change from 1961-1990 to 2071-2100 for the HadAm3H-A2 scenario (upper right), the ECHAM4-B2 scenario (lower left) and the HadAm3H-B2 scenario (lower right).**
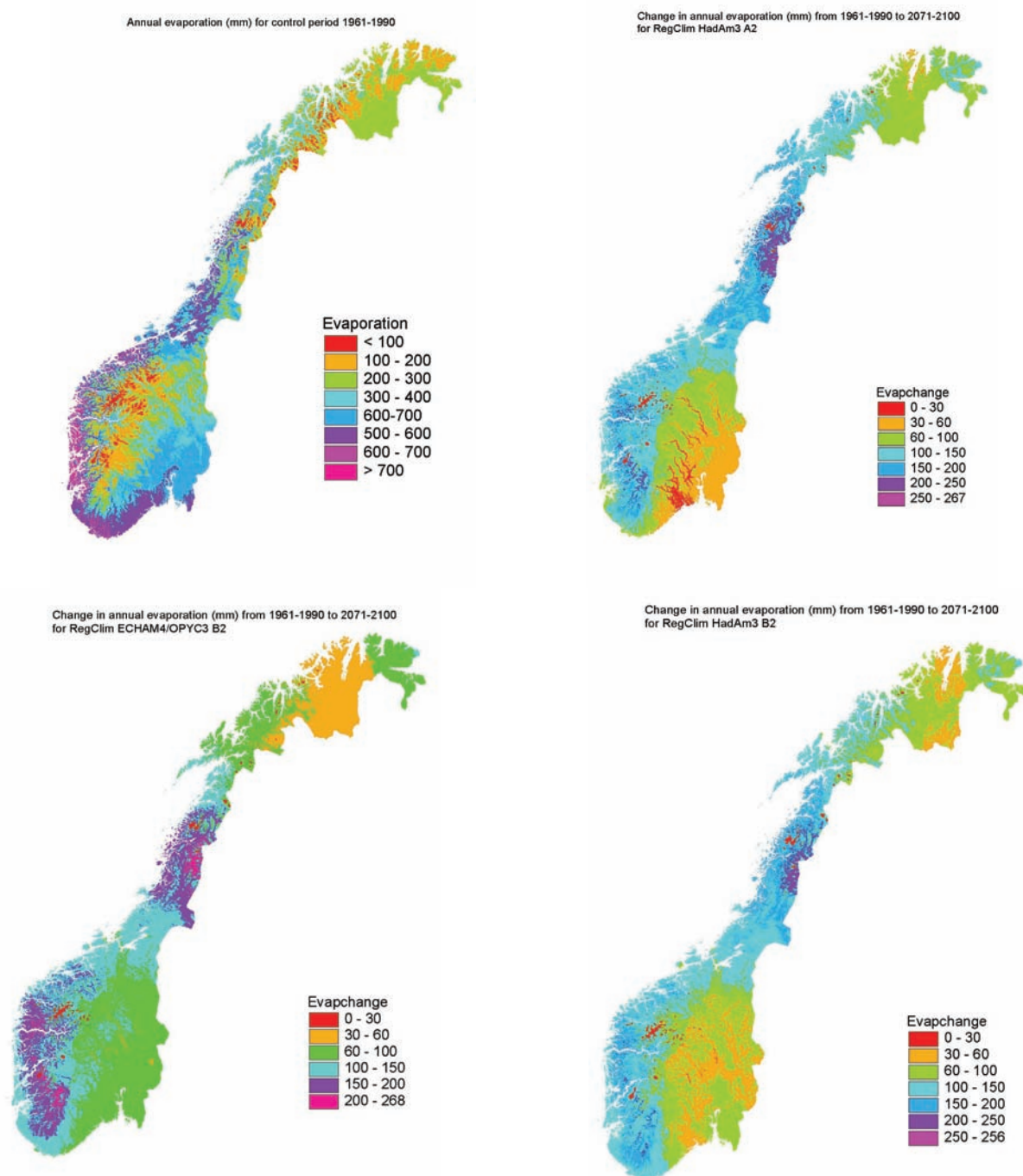
Figure 6.2.1 **Annual evapotranspiration for 1961-1990 (mm) (upper left) and projected change from 1961-1990 to 2071-2100 (mm) based on the HadAm3H-A2 scenario (upper right), the ECHAM4-B2 (lower left) and HadAm3H-B2 (lower right).**
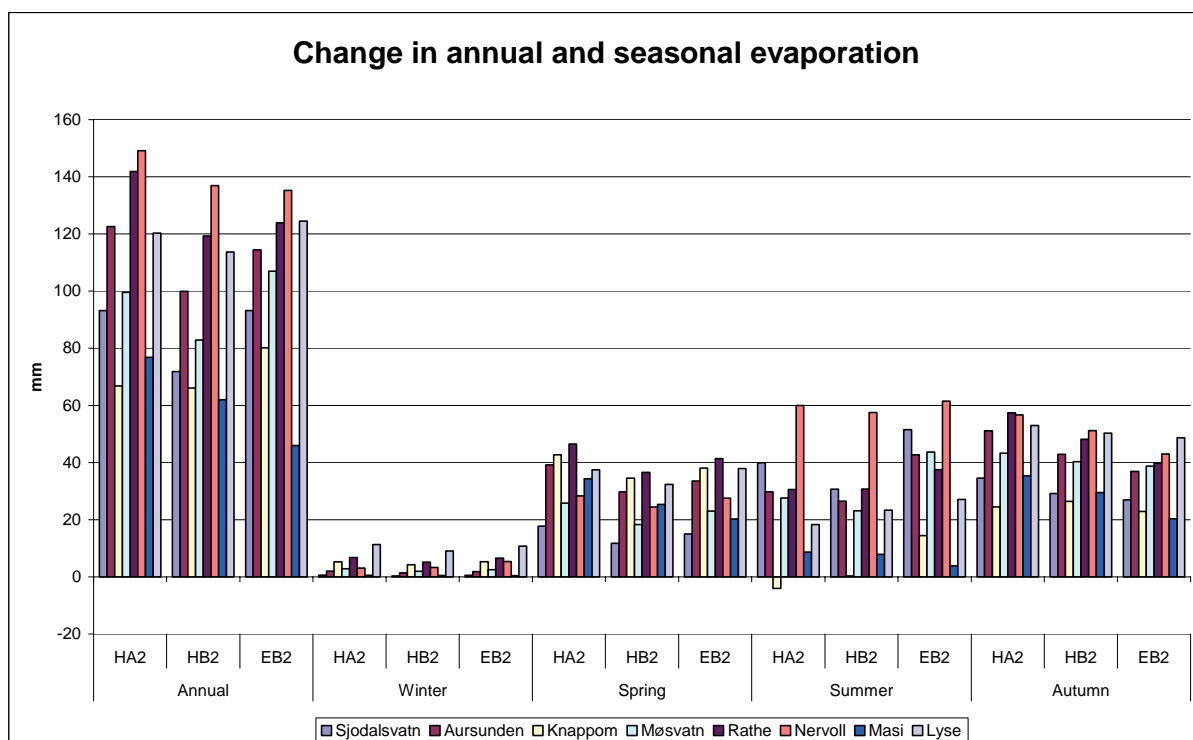
Figure 6.2.2   Projected change in the annual and seasonal basin average evapotranspiration in eight Norwegian basins from 1961-1990 to 2071-2100 (mm).

6.3 Groundwater volume

6.3.1 Modelling groundwater volume

Groundwater volumes are modelled as the sum of the water content in the two lower zones of the distributed GWB-model. Although these values may not be comparable to the total volume of groundwater, they describe the subsurface water which is involved in the hydrological cycle at annual and daily time scales. In order to compare model results to observed data, groundwater levels were determined using a storage coefficient and the depth to an impermeable base following the method described by Bergström and Sandberg (1983). This algorithm requires observed groundwater levels for calibration, and has therefore only been applied for two catchments, Aursunden and Møsvatn. Simulated and observed groundwater levels at Abrahamsvoll in the Aursunden catchment is shown in Figure 6.3.1.

6.3.2 Changes in groundwater volume

Changes in groundwater volumes have been determined for all catchments, as this is a part of the water balance calculations. Figure 6.3.2 shows changes in seasonal and annual groundwater volumes for 8 Norwegian basins.

Groundwater table depth (m) Aursunden
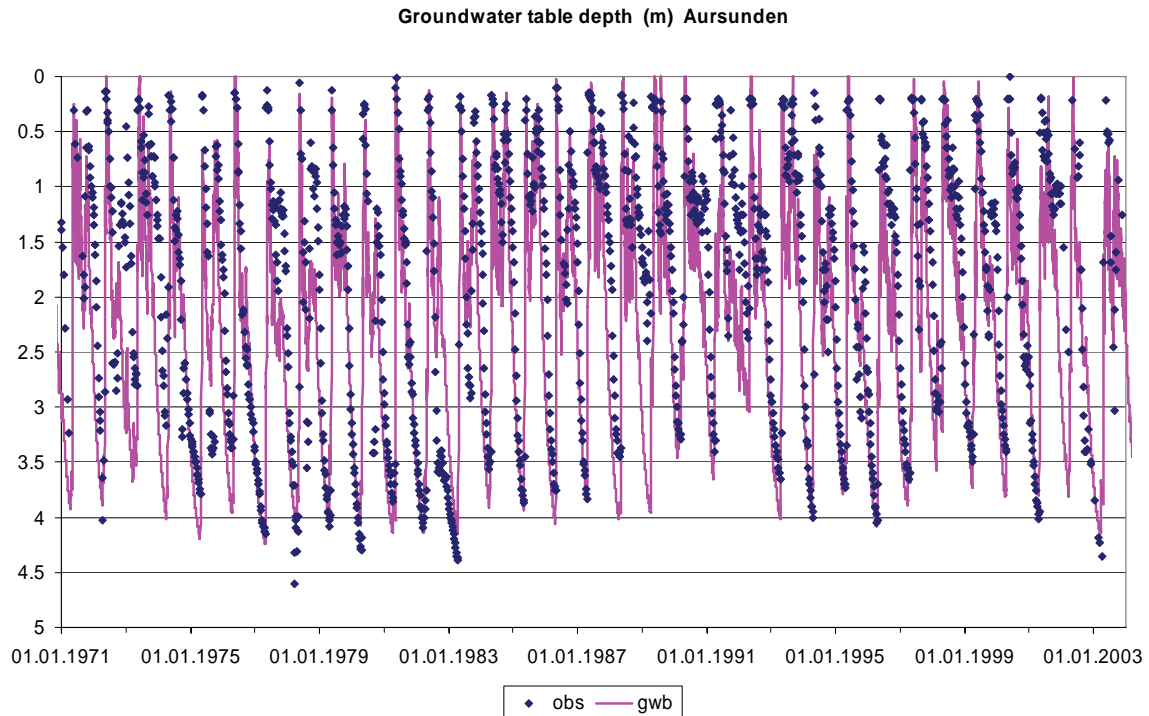
Figure 6.3.1   Observed and simulated groundwater levels (m) in the Aursunden catchment for period 1971-2003.
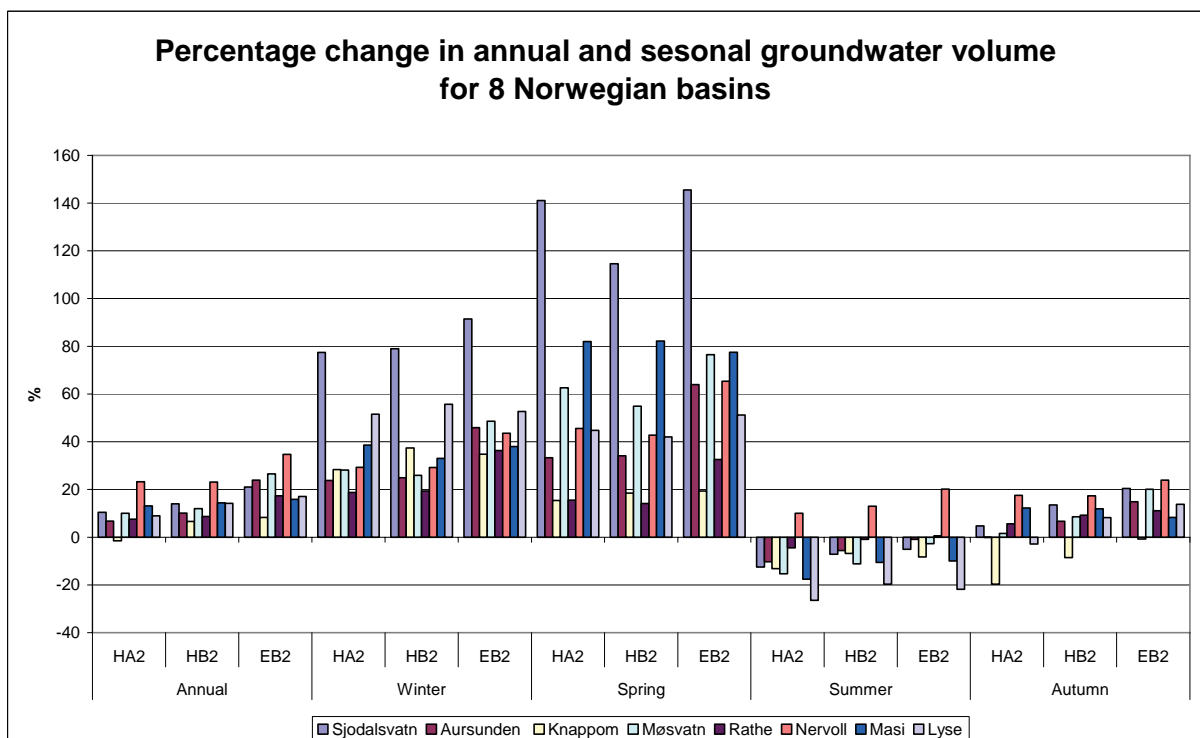
Figure 6.3.2   Projected change in the annual and seasonal basin average groundwater volumes (%) in eight Norwegian basins from 1961-1990 to 2071-2100.

6.4 Soil moisture deficit

6.4.1 Modelling soil moisture

The soil moisture zone receives meltwater from snow and glacier ice and rain on snow free areas. In addition water can be drawn up from the groundwater zone. Actual evapotranspiration and percolation to the groundwater zone is a function of the soil moisture content. The soil moisture deficit, the difference between the maximum soil moisture content and the actual soil moisture content is an indicator of the moisture state of the upper soil layer. Some of the water that infiltrates into the soil moisture zone is used to replenish the soil moisture deficit before runoff generation following rain or snowmelt events takes place. The fraction of infiltrated water used for runoff generation decreases when the soil moisture deficit increases.

6.4.2 Changes in soil moisture deficit

Changes in annual maximum soil moisture deficit compared to present conditions are shown in Figures 6.4.1 and 6.4.2. The maximum soil moisture deficit is expected to increase for almost all parts of Norway for all the three climate change scenarios. This result shows that although more subsurface water will be available for most seasons as shown by the groundwater volume scenarios, the interannual variability will be large and dry periods with low flow are expected to occur in the future.
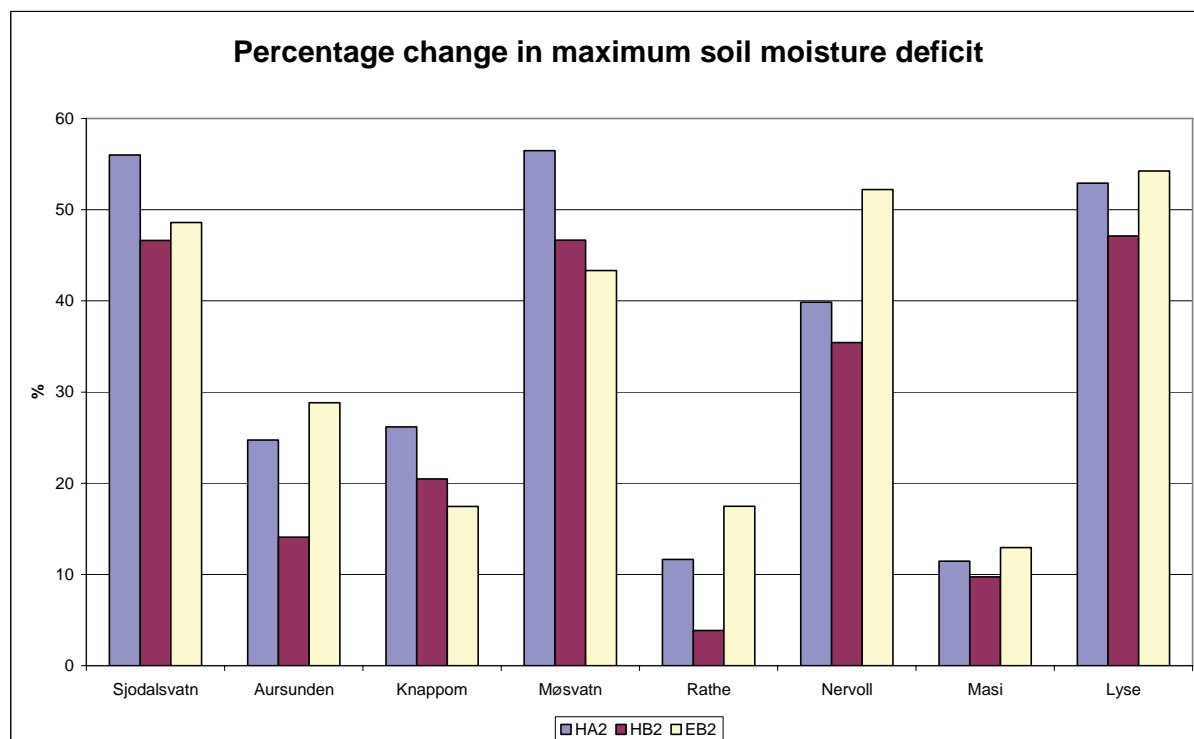
Figure 6.4.1   Projected change in the basin average annual maximum soil moisture deficit (%) in eight Norwegian basins from 1961-1990 to 2071-2100.
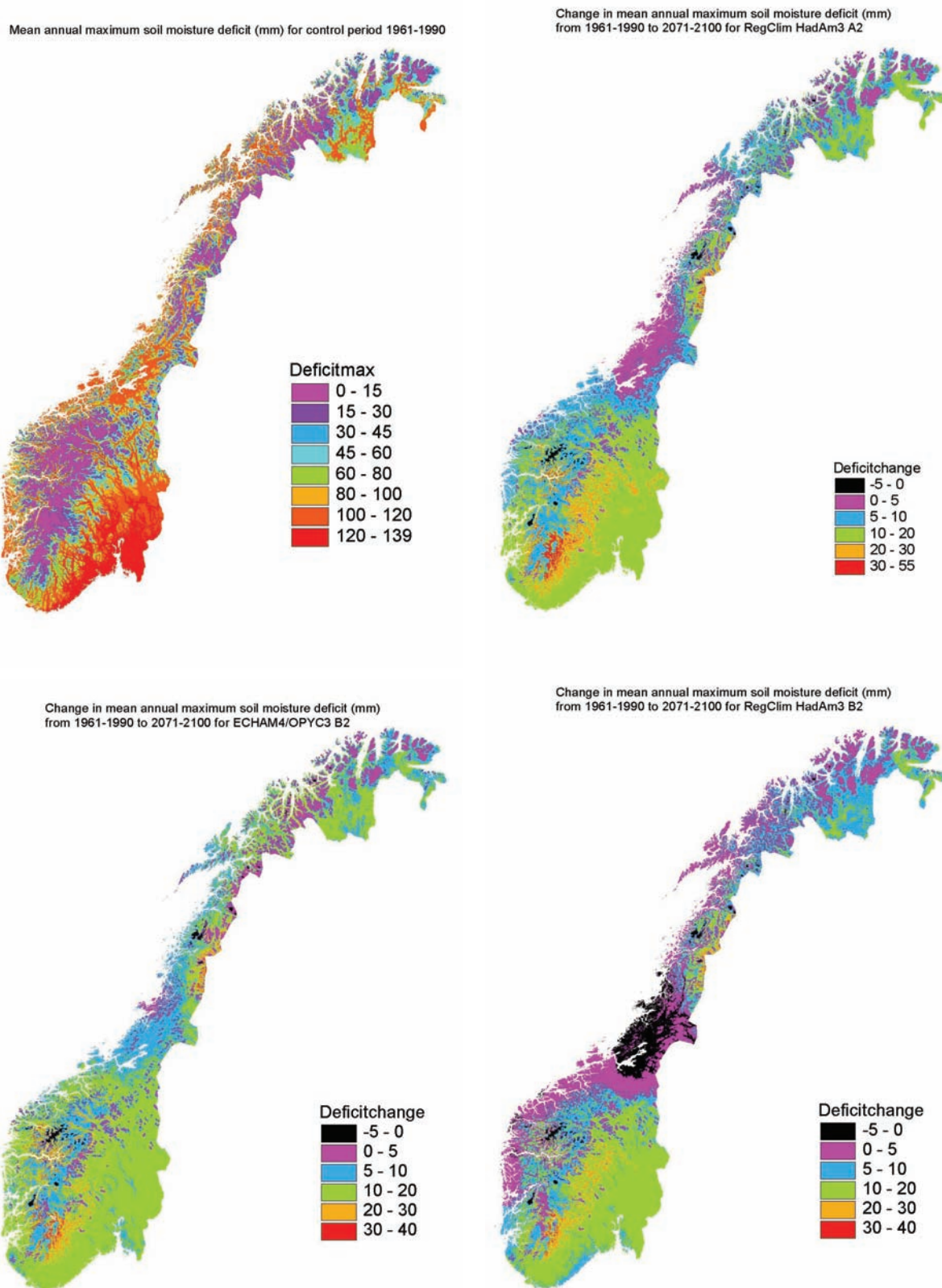
Figure 6.4.2   Average of annual maximum soil moisture deficit for 1961-1990 (mm) (upper left) and projected change from 1961-1990 to 2071-2100 (mm) based on the HadAm3H-A2 scenario (upper right), the ECHAM4-B2 (lower left) and HadAm3H-B2 (lower right).

6.5 Depth of frozen soil

6.5.1 Modelling soil frost depth

An algorithm for calculation of soil frost depth based on results from Vehviläinen and Motovilov (1989) has been introduced in the model. Snow depth is determined using a physical snow cover model and frost depth is calculated based on simulations of heat flux through the snow cover and soil. This algorithm requires observed frost levels for calibration, and has therefore only been applied for two catchments, Aursunden and Møsvatn. Simulated and observed frost depths at Abrahamsvoll in the Aursunden catchment are shown in Figure 6.5.1.
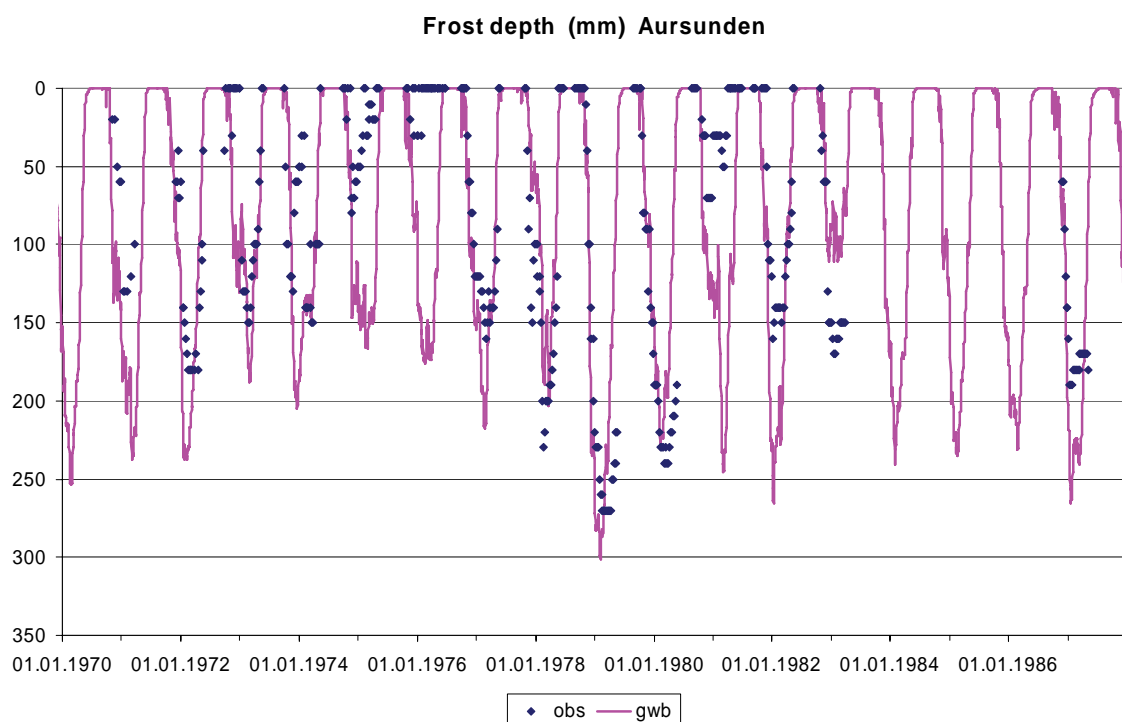
Figure 6.5.1   Observed and simulated soil frost depth (mm) in the Aursunden catchment for period 1970-1987.

6.5.2 Changes in soil frost depth

Frost depth simulations for future conditions based on the Hadley and ECHAM scenarios show minor reductions. Figure 6.5.2 show frost depth for present and future conditions for Abrahamsvoll in the Aursunden catchment.
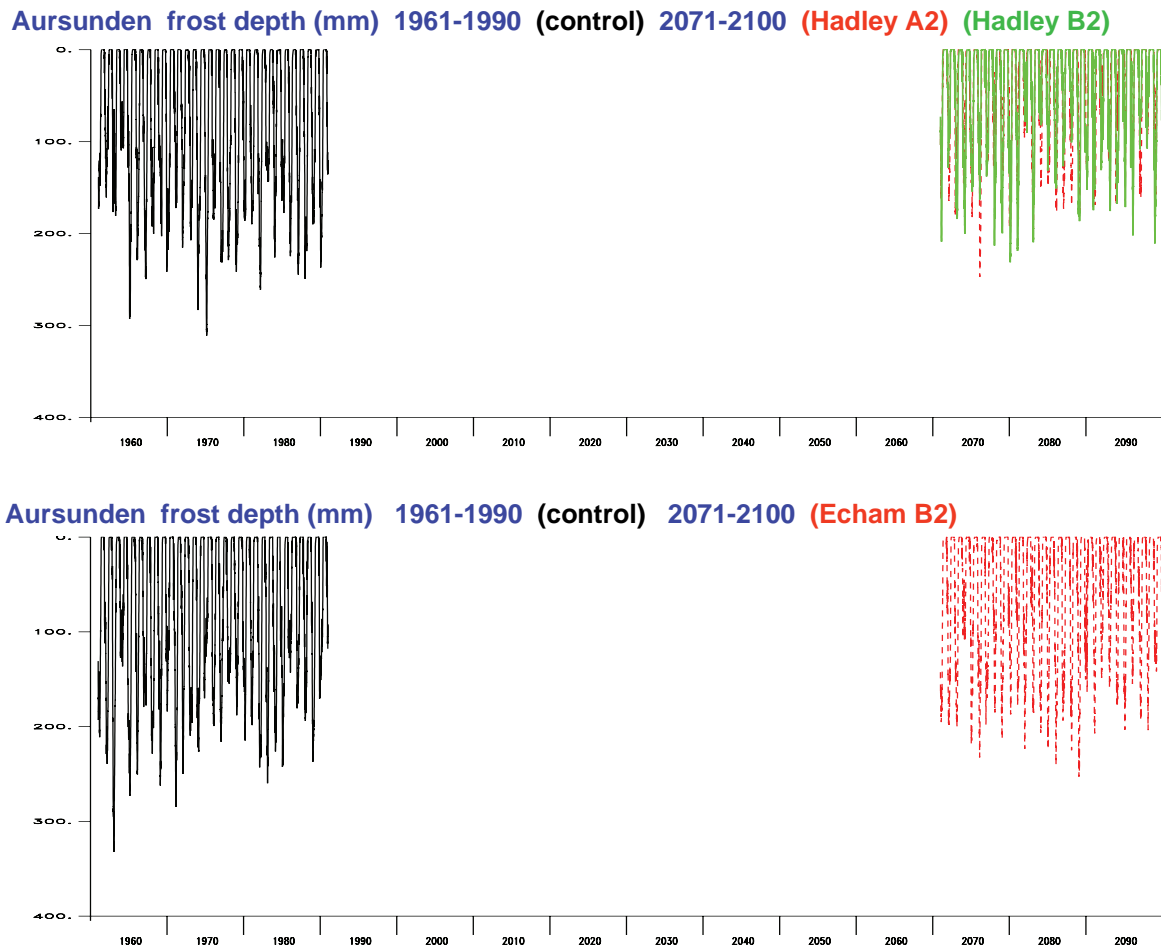
Figure 6.5.2 **Frost depth (mm) for control period 1961-1990 and scenario period 2071-2100 based on hydrological model simulations with input from the HadAm3H-model (control, A2, B2) (top) and ECHAM4-model (control, B2) (bottom).**

7 Uncertainties

7.1 Uncertainties in climate change

The modelling of climate involves a number of uncertainties as the understanding of the entire climate system with all relevant processes is incomplete. Furthermore, climate models cannot possibly account for every process at the very smallest scales explicitly. Hence, AOGCMs must approximate descriptions of a large number of processes that take place on a spatial scale unresolved by the model grid boxes. For instance, the description of cloud processes, ocean currents, and vapour/energy exchange between the atmosphere and the surface may vary with the location and can only be described by a general approximation. A variety of climate models exist and it has been shown that each model can give a different picture of the climate evolution (Cubash et al, 2001). An example is given of 16 different model projections to different sites in Norway for the period 2000-2050 in October (Figure 7.1.1). Even when a climate model is perfect there may be uncertainties associated with a simulated climate change. Benestad (2000) noted that the climate model spin-up process is important for the description of the local climatic evolution, and that there were regional differences between four simulations done with the HadCM2 model for different initial conditions. These differences were regarded as a result of the non-linear chaotic behaviour of climate, and hence part of the unpredictable natural variability (Benestad, 2001b). It is also evident that these natural fluctuations contaminate the climate change analysis such as for 30-year long time slices. Benestad (2003) argued that part of the natural variations are 'externally forced', by for instance volcanoes, solar activity or landscape changes, and will therefore not be captured by climate models only prescribed with emission data.
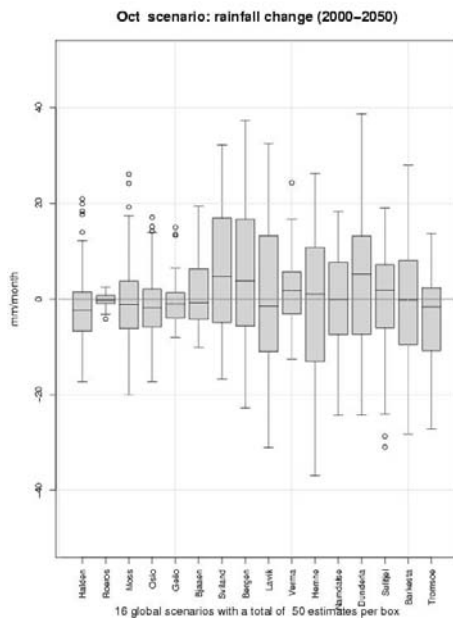
Figure 7.1.1   Projected mean monthly trend for October based on 16 different global scenarios for the period 2000-2050. The box shows the interquartile range (IQR:20-75 percentiles), the horizontal line gives the median value and the whiskers extend to the most extreme data points which is no more than |1.5| the quartile range from the Box (Benestad, 2002).

7.2 Uncertainties in dynamical downscaling

Regional climate models (RCMs) are promising tools to derive climate change scenarios on spatial scales that are represented too coarse by the AOGCMs. RCM simulations are frequently used as input data for climate impact studies (Wood et al. 2004; Bronstert, 2004) which require the representations of the present climate to be realistically reproduced by the RCM especially with respect to the variability, change and impacts on extreme events. The statistics of precipitation estimates, (mean, wet-day frequency, precipitation intensity and quantiles of the frequency distribution) based on five different RCMs are analysed by Frei et al (2003). They found considerable biases when comparing the statistics.

The time resolution of archived output from dynamically downscaled scenarios is typically on a 6 hourly basis. The spatial resolution (typically 50 x 50 km^2), however, is too coarse to be representative locally. The terrain in the regional climate models is smoothened, the sites elevation is thus wrongly represented, and the frequency of days with precipitation is overestimated (Charles et al., 1999). Observed climate of specific sites, especially in areas with complex topography, is therefore not well reproduced. The AOGCM is initially developed to capture the overall regional weather pattern of an area. Interpolation of temperature and precipitation data from RCMs to at site locations therefore requires special attention.

It is also important to note that the representation of a parameter in RCM may be either a point value or a mean value for a given grid box volume, and which of these representations are used in the model formulation may not always be obvious when bringing together a large variety of different models describing a range of processes over different scales.

7.3 Uncertainties in trend analysis

By adopting best-fit linear trend scenarios for sufficiently long time intervals (at least 60 years), the mean rate of change for the given period can be estimated and systematic biases between control integration and transient run can be ignored. The uncertainty in the trend estimate can easily be calculated. The length of time interval influences the sensitivity to natural variability of interannual and decadal time scales. The linear trend method is valid, even if the slow changes are non-linear, as long as we only want a measure for the mean climate change over a given time period. It may also be useful to use a polynomial trend model for cases where the evolution clearly is not linear (Benestad, 2003). This approach should not, however, be used for extrapolating outside the given time interval. It is important to stress the importance of evaluating the past climatic trends before making scenarios for the future, because there are no reason to believe that the GCMs will be able to provide a reliable prediction for the future if they cannot predict the past (Benestad, 2004, 2003, 2002).

7.4 Uncertainties in the hydrological modelling

The hydrological model represents a simplified description of the hydrological processes governing the streamflow generation in a basin. The model utilises furthermore data from a limited number of climate stations to estimate the streamflow as well as other water balance elements. Daily temperature and precipitation data are assigned to grid-cells of 1 km2 based on the three closest climate stations taking into account differences in altitudes and land use. The simplified description of the governing processes will introduce uncertainties in the simulated data. The uncertainty in the meteorological data driving the model both in terms of values and representativity of the data is probably a more important contribution to the uncertainties in the simulated streamflow and other water balance elements.
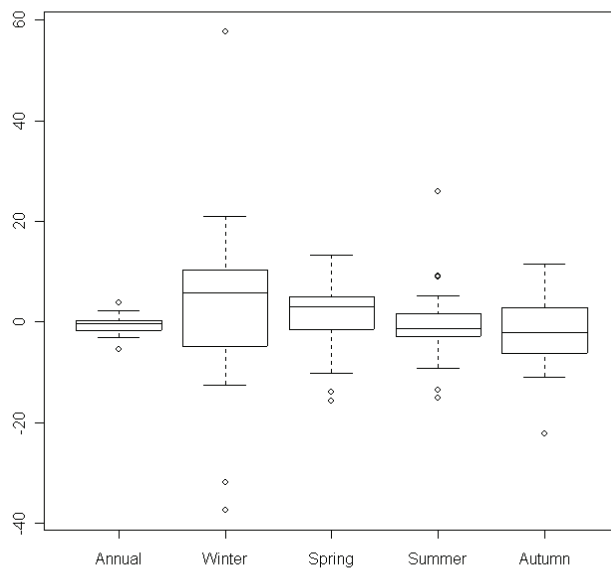
Figure 7.4.1 **Percentage differences between observed and simulated streamflow in the calibration period for 22 basins, shown a Box whiskers diagram. 1: Annual, 2: Winter, 3: Spring, 4: Summer, 5: Autumn means.**

The calibration of the model results in mostly good agreement between observed and simulated streamflow in the calibration period as shown in Figure 7.4.1. The average bias in annual means is -0.44 % for 22 basins. The average bias is 3.49 % in the winter, 1.34 % in the spring, -0.70 % in the summer and 1.9 % in the autumn. The winter streamflow is quite low in some of the basins, and the observations are also most unreliable at this time of the year. This explains the larger errors in the winter season. The model seems to capture the variability fairly well in most basins. The largest errors stem from the use of less representative precipitation data.

The change in the streamflow is calculated as the percentage change between the annual, seasonal or weekly means from the scenario period to the control period. The control series of streamflow is calculated using simulated and downscaled data from the regional climate model adjusted to station points, which again is based on two different global climate models. Percentage differences in the B2-streamflow scenario are shown in Figure 7.4.2 for projections based on the HadAm3H- and the ECHAM4-model. The average change in annual and seasonal values is of similar magnitude. The ECHAM4-model gives higher percentage increase than the HadAm3H-model for all seasons except in the summer. There are however regional differences as shown in Section 5.4. The large variability in the winter and spring is strongly linked to the topography and location of each basin controlling the accumulation and melting of snow.
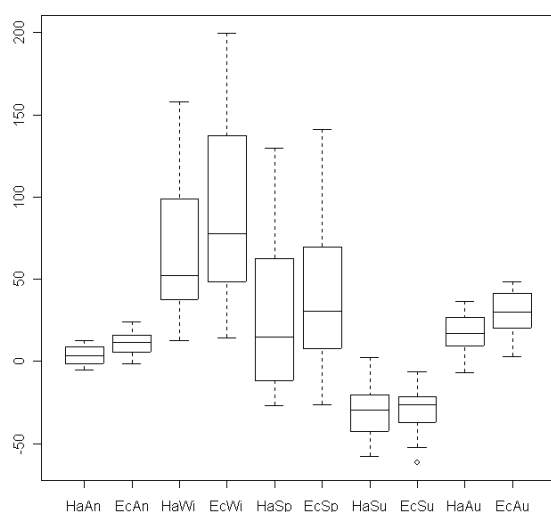
Figure 7.4.2   The percentage differences in projected change in the annual and seasonal streamflow based on scenarios of the HadAm3H- and the ECHAM4-models, shown as Box whiskers plot for the B2 emission scenario.

The scenarios are based on two different emission scenarios; the A2-scenario (high) and the B2-scenario (low). Figure 7.4.3 shows percentage differences of the 25 series for the two scenarios based on the HadAm3H-model. The projected change in winter and spring streamflow is quite similar for the two model. The variability between the stations are however quite large in these seasons. The change in the annual, summer and autumn streamflow is lower in the A2- than in the B2-scenario. A possible explanation is that the simulated evaporation are higher in the warmer A2-scenario.
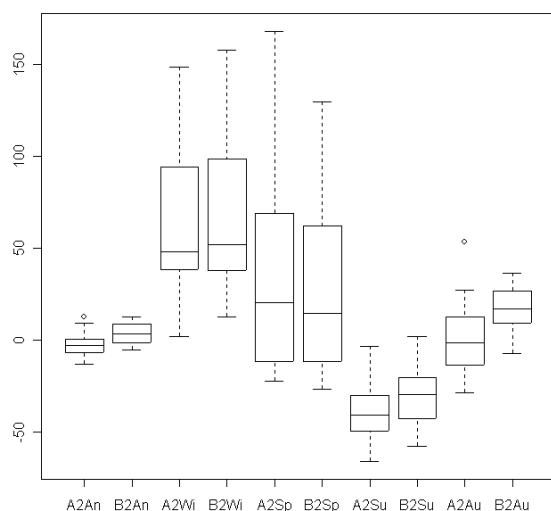
Figure 7.4.3   The percentage differences in projected change in the annual and seasonal streamflow based on scenarios of the HadAm3H-model for emission scenarios A2 and B2, shown as Box whiskers plot.

The scenario series of temperature and precipitation used in this study were based on downscaling by the RegClim method, described in Chapter 3. The Nordic Climate and Energy utilises however

simulated streamflow series for the control period directly based on observed data, which are available for more stations than those based on the RegClim Method. The scenario series is obtained using the Δ-change method based on corrections from a regional climate model. The projected changes are summarised in Figures 7.4.4 and 7.4.5. Weekly mean values are shown in Figure 7.4.6 for the control series based on the RegClim Method, and the control series based on the Rossby Center Method.
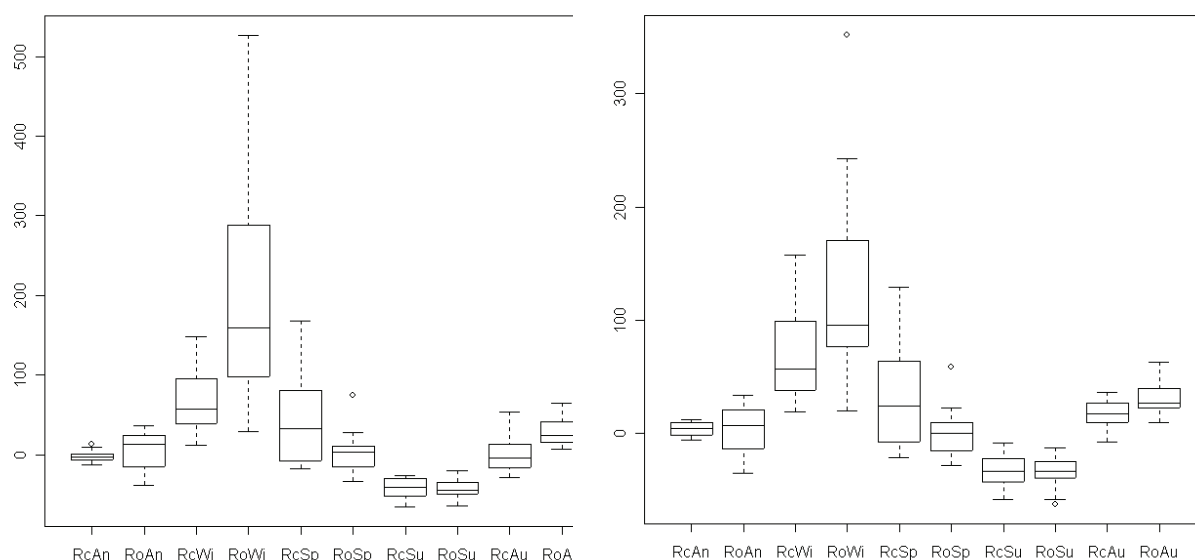
Figure 7.4.4   Percentage change in the annual and seasonal streamflow of 22 series based on the HadAm3-model and emission scenario A2 (left) and B2 (right) and downscaling based on the RegClim (Rc) and the Rossby Center (Ro) methods.
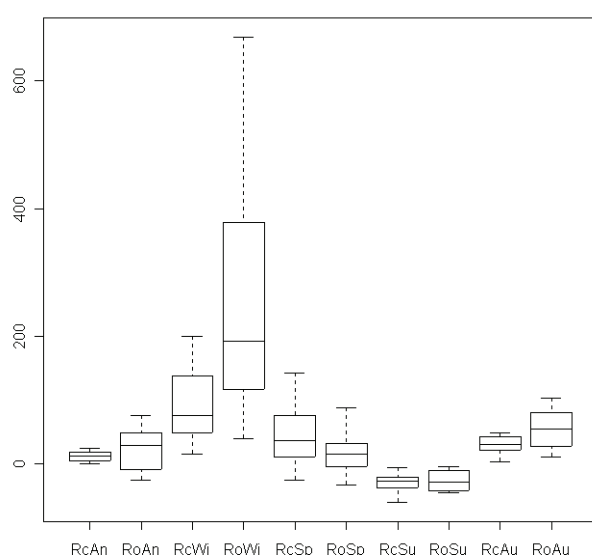
Figure 7.4.5   Percentage change in the annual and seasonal streamflow of 22 series based on the ECHAM4-model and emission scenario B2 and downscaling based on the RegClim (Rc) and the Rossby Center (Ro) methods.

60
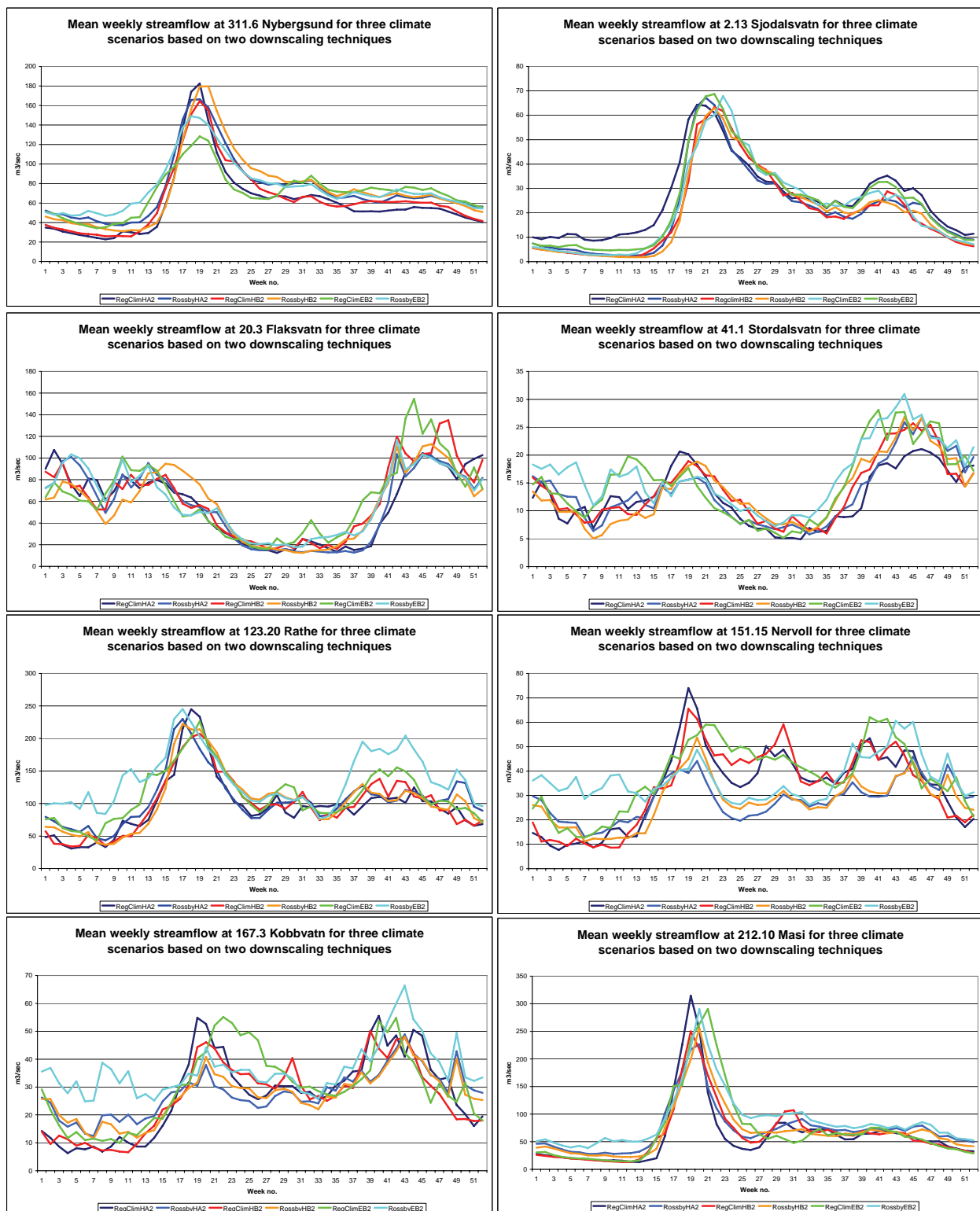
Figure 7.4.6   Comparison of weekly mean streamflow for all scenarios described in Chapter 5 for eight basins based on downscaling by the RegClim Method and the Rossby Center Method.

The changes in the weekly means agree fairly well for most of the scenarios with exception of the Rossby B2-scenario based on the ECHAM4-model.

8 Discussion

The projected changes in the streamflow differ between the various scenarios based on the ECHAM4 and the HadAm3H-models. Because of natural climate variability, the two models result in two different dominating circulation patterns, with increasing dominance from the west in ECHAM4 and a more easterly pattern in the HadAm3H-scenarios. With the topography of Norway, this results in different distributions of the precipitation and the streamflow (Tveito & Roald, 2005). The projected changes in the mean annual streamflow are moderate, but the changes in the seasonal streamflow are far larger and have implications for the operation of the Norwegian hydropower system if the scenarios are correct.

The change in the seasonal streamflow is strongly linked to changes in the snow regime. The snow cover will be more unstable in the winter season and more mild periods will cause occasional winter floods. The milder winters are also accompanied with more winter precipitation in some regions. The spring flood will occur three to four weeks earlier in the mountains. The spring flood, which now is mostly occurring in the early summer, will occur more frequently in the spring months, and this explains the increase in the spring in the mountainous basins in south Norway and in basins in North Norway.

The summer will be drier, and summer droughts may become more severe. This is partly caused by the shift in the time of the peak snow melt flood in mountainous basins, but also by an increased evapotranspiration in a warmer climate. The A2-scenarios project a moderately larger reduction in the streamflow than the B2-scenarios in the summer and autumn, as expected since the temperatures are projected to be higher in the A2-scenario. The models differ most in their projections of changes in the autumn streamflow. The rainfall peaks in the autumn in West Norway, where much of the hydropower plants are situated. While the ECHAM4-scenario indicates an increase in the west and in parts of North Norway, the HadAm3H-scenario indicates a large increase only in the southwest corner of Norway with some decrease further north.

The year to year variability is likely to be as high as under the present climate. This implies that dry years will also occur even if the long term means increase.

Given earlier snowmelt and reduced snow storage, the occurrence of large snowmelt floods is likely to become more seldom. The scenarios series does not include extreme rainfall as in some of the largest observed events, which are caused by quite rare atmospheric circulation patterns, as in 1789. Many of these events are comparatively small scale phenomena, and it cannot be expected that the climate models with their coarse resolution are able to model these events properly. Historical data show however an overabundance of intensive local rainfall floods in the warm 1930's. These floods can therefore become more severe because of increasing rainfall intensities in a warmer climate. These floods are potentially more dangerous in steep terrain, because they can cause landslides. Urban flood damage has increased considerably in recent years. This is as much an effect of increased vulnerability because of land use changes as of changes in the rainfall intensities.

The change in the seasonality of the average streamflow towards higher streamflow in the cold season will agree better with the seasonality of electricity consumption than during the control period. This can open for a changed operation of the reservoirs, but the large year to year variability in the future streamflow regime must be taken into consideration, when changes in the operation scheme is considered. The possible occurrence of large rainfall flood on full reservoirs has also implications for dam safety in the future.

There are many sources of uncertainties in the scenarios, in the climate modelling, the downscaling to climate stations and in the hydrological modelling. The uncertainty caused by the hydrological model

is of less importance than the uncertainties caused by the representativity of the meteorological data driving the model. The projection of water balance elements in a warmer climate is based on the assumption that the model parameters used to simulate streamflow under the present climate is still valid during a changed climate. The scenarios presented in this report are based on climate scenarios of two different global climate models, two emission scenarios and dynamical downscaling with subsequent statistical adjustment of temperature and precipitation series to climate stations. A comparison between the annual and seasonal streamflow based on the two models and one emission scenario show general similarities, especially when topography and location of the basins are considered. The difference in projected streamflow between the two scenarios is not very large, but there are differences in the warm season which can be explained by the warmer A2-scenario.

A comparison of the projected changes in the seasonality of the mean weekly streamflow between scenarios based on the RegClim and the Rossby Center downscaling techniques show fairly good agreement for most of the scenarios. The weekly scenarios of the Rossby Center method are used as input for modelling of the energy production in the Climate and Energy programme.

The review paper by Barnett et al (2005) summarises possible changes in water availability in four snow- dominated regions. They find that the most obvious change is changes in the seasonality induced by earlier snowmelt, which is controlled by the temperature. A problem in some regions will be a temporary increase in glacier meltwater, until the glaciers are melted back. This will cause shrinking availability of water in otherwise dry regions in the future. The projected changes in precipitation for Norway differ from the regions discussed in this review paper. The problems caused by lack of glacial meltwater will have less importance in the more maritime climate of Norway. Changes in the mass-balance of glaciers will also have effect on the streamflow in Norwegian rivers with a substantial fraction of glaciers in the basin. This is studied in more detail in the Climate and Energy project.

Hisdal et al (2004) have analysed annual and seasonal trends in 150 long-term streamflow series for the Nordic countries for three time slots. Trends have been found in a number of series for the winter, spring and summer, which agree with the projections presented in this report. Trends cannot be found in the autumn, when the climate models indicate a marked increase, especially in the late autumn.

9 Conclusions

Given the projected changes in air temperature and precipitation the stream flow regime will change in the following way:

Moderate change in the annual streamflow, with a decline in some basins in East Norway in some scenarios and increase in most basins exposed to westerly winds. The increase is dependent on the spatial distribution of the pressure fields as modelled by the two global climate models.

Significant changes in the seasonal distribution of the streamflow; increase everywhere in the winter, increase in mountainous basins and in North Norway in the spring and a moderate decline in low-lying basins in South and Mid- Norway. Decrease will occur everywhere in the summer. Increase in the autumn streamflow in almost every basin given the moderate B2-scenario, most in scenarios based on the ECHAM4-model. Decrease in low-lying basins in the east and south giving the more extreme A2-scenario.

The annual flood will be moderately reduced in basins in East Norway with a dominating snow melt flood regime under climate of the control. The annual flood will increase in basins close to the coast in West- and North Norway.

There will be more floods in the winter especially in the low-lying basins, and the spring flood will decrease and occur earlier. Late autumn floods are likely to become both more frequent and more severe, especially in basins in West- and North Norway. The period of the year in which large floods can occur, will be extended in a warmer climate, and some events may occur at a time of the year without large floods in earlier times.

The scenarios do not indicate an increase in summer floods, caused by intensive rainfall. This type of events is linked to fairly small scale weather phenomena, and is therefore not described satisfactory in the climate models. Provided that some summers may experience very hot events, even if the projected changes in the mean temperatures are least in the summer, it seems obvious that more flash floods can be expected in small rivers in steep terrain. This is also confirmed by historical data.

The snow storage may increase moderately in high mountainous basins in the first part of the 21st century. However, the rise in air temperature seem to cause the snow storage to decline even with increased winter precipitation in the latter part of the century..

The projected shift in the seasonal streamflow agrees with recent trends in the winter, spring and summer, but diverges in the autumn.

References

Barnett, T.P, Adam, J.C. and Lettenmaier, D.P. (2005). Potential impacts of a warming climate on water availability in snow-dominated regions. Nature, Vol 438|17 November 2005.

Beldring, S. (2002). Runoff generating processes in boreal forest environments with glacial tills. Nordic Hydrology, 33, 347-372.

Beldring, S., Engeland, K., Roald, L.A., Sælthun, N.R. and Voksø, A. (2003) Estimation of parameters in a distributed precipitation-runoff model for Norway. *Hydrology and Earth System Sciences 7*, 304-316.

Benestad, R.E. (2004). Tentative probabilistic temperature scenarios for northern Europe Tellus 56A, 89-101.

Benestad, R.E. (2003). What can present climate models tell us about climate change? Climatic Change Vol 59, 311-332.

Benestad, R.E. (2002). Empirically downscaled multi-model ensemble temperature and precipitation scenarios for Norway, Journal of Climate Vol 15, 3008-3027.

Benestad, R.E. (2001a). A comparison between two empirical downscaling strategies, Int. J. Climatology,Vol 21, Issue 13, pp.1645-1668. [DOI 10.1002/joc.703]

Benestad, R.E. (2001b). The cause of warming over Norway in the ECHAM4/OPYC3 GHG integration, Int. J. Clim. 15 March Vol 21 371-387.

Benestad, R.E. (2000). Future Climate Scenarios for Norway based on empirical Downscaling and inferred directly from AOGCM results, DNMI Klima, 23/00, pp.127

Bergström, S. (1995), The HBV model. In: Singh, V.P. (Ed.), Computer Models of Watershed Hydrology. Water Resources Publications, Highlands Ranch, 443-476.

Bergström, S., Sandberg, G. (1983). Simulation of groundwater response by conceptual models - three case studies. Nordic Hydrology, 14, 71-84.

Bjørge D., Haugen, J.E., and Nordeng, T.E. (2000). Future climate in Norway, Research Report No. 103, Norwegian Meteorological Institute, Oslo

Bronstert, A. (2004). Rainfall-runoff modelling for assessing impacts of climate and land-use change, Hydrol. Process.18:567-570.

Charles S., Bates, B.C., Whetton, P.H., and Hughes, J.P. (1999). Validation of downscaling models for changed climate conditions: case study of southwestern Australia, Clim Res 12:1-14

Cubash, U, Meehl, G.A., Boer, GJ, Stouffer, RJ and 5 others (2001). Projections of future climate change. In: Houghton JT, Ding Y., Griggs DJ, Noguer M, van der Linden PJ, Dai X, Maskell K, Johnson CA (eds) Climate change 2001: the scientific basis. Contribution of Working Group I to the

Third Assessment Report of International Panel on Climate Change. Cambridge University Press, Cambridge, p 583-638.

Daly, C., Neilson. R.P. and Phillips, D.L. (1994). A statistical-topographic model for mapping precipitation over mountainous terrain. Journal of Applied Meteorology, 33, 140-158.

Doherty, J., Brebber, L. and Whyte, P. (1998). PEST. Model independent parameter estimation. Watermark Computing, 185 pp.

Engen-Skaugen, T. (2004). Refinement of dynamically downscaled precipitation and temperature scenarios. Met.no report no. 15/2004 Climate.

Engen-Skaugen, T., Roald, L.A., Beldring, S., Førland, E.J., Tveito, O.E., Engeland K. & Benestad, R. (2005). Climate change impacts on water balance in Norway. Met.no report no.1/2005 Climate

Frei, C., Christensen, J.H., Déqué, M., Jacob, D., Jones, R.G. and Vidale, P.L. (2003). Daily Precipitation Statistics in Regional Climate Models: Evaluation and Intercomparison for the European Alps, J. Geophys. Res., 108, 10.1029/2002JD002287

Førland, E.J., Allerup, P., Dahlström, B., Elomaa, E., Jónsson, T., Madsen, H., Perälä, J., Rissanen, P., Vedin, H. and Vejen, F.: 1996, Manual for operational correction of Nordic precipitation data. Norwegian Meteorological Institute DNMI Klima Report 24/96, 66 pp.

Giorgi F., Hewitson, B., Christensen J.H., Hulme, M and 5 others (2001).`Regional climate information – evaluation and projections´. In: Houghton JT, Ding Y., Griggs DJ, Noguer M, van der Linden PJ, Dai X, Maskell K, Johnson CA (eds) Climate change 2001: the scientific basis. Contribution of Working Group I to the Third Assessment Report of International Panel on Climate Change. Cambridge University Press, Cambridge, p 525-582.

Gordon, C., Cooper, C., Senior, C.A., Banks, H., Gregory, J.M., Johns,T.C., Mitchell, J.B.F. and Wood, R.A. (2000). The simulation of SST, sea ice extents and ocean heat transport in a version of the Hadley Centre coupled model without flux adjustments, Clim.Dyn., 16,147-168.

Gottschalk, L., Beldring, S., Engeland, K., Tallaksen, L., Sælthun, N.R., Kolberg, S. and Motovilov, Y. 2001. Regional/macroscale hydrological modelling: a Scandinavian experience. Hydrological Sciences Journal, 46, 963–982.

Hisdal, H., Holmqvist, E., Kuusisto, E., Lindström, G. and Roald, L.A. (2004). Has streamflow changed in the Nordic countries? NHP Report No.48, Tartu, 2004.

Hosking, J. R. M. and Wallis, J. R. (1997). Regional frequency analysis: an approach based on L-moments. Cambridge University Press, Cambridge, U.K.

Killingtveit, Å., Hisdal, H., Roald, L.A., Skaugen, T. Væringstad, T. & Holmqvist, E. (2003) Tørrårsberegninger – Analyse av forløp, hyppighet og utbredelse av tørke i Norge og Sverige. NVE Oppdragsrapport B, 13 – 2003.

Lettenmaier, D.P., Wood, A.W., Palmer, R.N., Wood,E.F. and Stakhiv, E.Z. (1999). Water resources implications of global warming: A U.S. regional perspective, Climatic Change 43:537-579.

Matheussen, B., Kirschbaum, R.L., Goodman, I.A., O'Donnel, G.M. and Lettenmaier, D.P. 2000. Effects of land cover change on streamflow in the interior Columbia River Basin (USA and Canada). Hydrological Processes, 14, 867-885.

Middelkoop, H., Daamen,K., Gellens,D.,Grabs,W., Kwadijk, J.C.J., Lang, H., Parmet, B.W.A.H., Schädler, B., Schulla, J. and Wilke, K. (2001) Impact of climate change on hydrological regimes and water resources management in the Rhine basin, Climatic Change 49:105-128

Reynard, N.S., Prudhomme, C. and Crooks, S.M. (2001). The flood characteristics of large U.K.Rivers: Potential effects of changing climate and land use. Climatic change 48:343-359.

Roald, L.A., Skaugen, T.E., Beldring, S., Wæringstad,T., Engeset, R. and Førland, E.J. (2002) Scenarios of annual and seasonal runoff for Norway based on climate scenarios 2030-49. *NVE-report A 10/02, met.no Report 19/02 Klima.*

Roeckner E, Bengtsson L., Feichter J, Lelieveld J. and Rodhe H. (1999). Transient climate change si mulations with a coupled atmosphere-ocean GCM including the tropospheric sulphur cycle. J.Clim 12:3004-3032

Sælthun, N.R. (1996). The Nordic HBV model. Norwegian Water Resources and Energy Administration Publication 7, Oslo, 26 pp.

Sælthun, N.R., Aittonemi, P., Bergstrøm, S., Einarsson, K., Jòhannesson, T., Lindström, G., Ohlsson, P-E., Thomsen, T., Vehviläinen, B., and Aamodt, K.O. (1998). Climate change impacts on runoff and hydropower in the Nordic countries. Final report from the project "Climate Change and Energy Production". TemaNord 1998:552. ISBN 92-893-0212-7. ISSN 0908-6692. Copenhagen. 170 p.

Tveito, O.E. and Roald, L.A. (2005). Relations between long-term variations in seasonal runoff and large scale atmospheric circulation patterns. Met.no report no 7/2005 Climate

Vehviläinen, B., Motovilov, Y. (1989). Simulation of soil frost depth and effect on runoff. Nordic Hydrology 20, 9-24.

Węglarczyk, S. (1998) The interdependence and applicability of some statistical quality measures for hydrological models. Journal of Hydrology, 206, 98-103.

Wood, A.W., Leung, L.R., Sridhar, V. and Lettenmaier, D.P. (2004) Hydrologic implications of dynamical and statistical approaches to downscaling climate model outputs. Clim. Change 62: 189-216.

Zhu, A.X. and Mackay, D.S. 2001. Effects of spatial detail of soil information on watershed modeling. Journal of Hydrology, 248, 54-77.

APPENDIX I. Overview of simulated time series available on HydraII.

Data series have been stored on Hydra II as daily time series for the control period (1961-1990) and for the scenario period (2071-2100) of a number of basins. Each series can be identified by the HydraII key comprising the station no., a point number, a code describing the type of water balance variable and a version number. Streamflow data is identified by code 1001 (unit: m³/sec), temperature data by code 41, precipitation data by code 0, evaporation data by code 1, groundwater data by code 2000, soil moisture deficit by code 2001, snow water equivalent data by code 2003 and the depth of frozen soil by code 2004. The point number is set equal to the version number in the key of each series, with the exception of groundwater where groundwater volume is stored with the same point and version number, while groundwater depth is indicated by point number 0 and version number as given below. The scenario streamflow series for Nybergsund for the HadAm3H-model is therefore identified as 311.6.93.1001.93 since 93 is the version number of this scenario as shown in Table A1.

Table A1.1 gives an overview of data series with daily average streamflow data for all basins based on the RegClim method of downscaling.

Table A1.2a gives an overview of the subset of basins with streamflow data from different altitude zones. Since the size of each sub-basin varies considerably in each basin, streamflow data are both available in m3/sec (code: 1001) and in specific units as mm/day (code: 5000). These series are identified by other point and version numbers as given in Table A1.2b.

Table A1.3 summarises the subset of basins with basin average time series available for climatic variables and other water balance variables. These series are identified by their respective code and point and version numbers as given for the streamflow data in Table A1.1. Data are also available at Aursunden and Møsvatn for groundwater depth and depth of frozen soil. The identification of these series is: 2.111.0.2000.version and 2.111.point.2004.version respective for the Aursunden basin and 16.19.0.2000.version and 16.19.point.2004.version respective for the Møsvatn basin. The values of point and version are identical as given in Table A1.1.

Table A1.1   Basin average daily streamflow series and the version number used to identify each series.

Station no.	Name	River	Version	Observed		HadleyAm3H			ECHAM4	
				From	To	Control	A2	B2	Control	B2
311.6	Nybergsund	Trysilelv	0	1908	2005	92	93	94	97	99
2.142	Knappom	Flisa	1	1916	2004	92	93	94	97	99
2.111	Aursunden	Glomma	3*	1902	2004	92	93	94	97	99
2.13	Sjodalsvatn	Sjoa	0	1930	2004	92	93	94	97	99
15.79	Orsjoren	Numedalslågen	1*	1930	2004	92	93	94	97	99
16.19	Møsvatn	Måna	3*	1909	2004	92	93	94	97	99
18.10	Gjerstad	Gjerstadelv	1	1924	2004	92	93	94	97	99
20.2	Austenå	Tovdalselv	1	1924	2004	92	93	94	97	99
20.3	Flaksvatn	Tovdalselv	2*	1899	2004	92	93	94	97	99
26.20	Årdal	Sira	91	1970	2004	92	93	94	97	99
26.21	Sandvatn	Sira	91	1971	2004	92	93	94	97	99
27.26	Hetland	Bjerkreimselv	0	1915	2004	92	93	94	97	99
257.257	Lyse krv	Lyse	-	-	-	92	93	94	97	99
41.1	Stordalsvatn	Etneelv	1	1912	2005	92	93	94	97	99
48.5	Reinsnosvatn	Austdøla	1	1917	2005	92	93	94	97	99
50.1	Hølen	Kinso	1	1923	2004	92	93	94	97	99
83.2	Viksvatn	Gaular	1	1902	2005	92	93	94	97	99
104.23	Vistdal	Visa	1	1975	2004	92	93	94	97	99
107.3	Farstad	Farstadelv	1	1965	2004	92	93	94	97	99
109.9	Risefoss	Driva	1	1935	2005	92	93	94	97	99
123.20	Rathe	Nidelv	4*	1899	2004	92	93	94	97	99
123.31	Kjelstad	Garbergelv	1	1930	2003	92	93	94	97	99
151.15	Nervoll	Vefsna	1	1968	2004	92	93	94	97	99
167.3	Kobbvatn	Kobbelv	4*	1916	2004	92	93	94	97	99
212.10	Masi	Alta	1	1966	2004	92	93	94	97	99

*   The series are regulated and have been corrected for the effect of storage in reservoirs and diversions (tilsigsserier).

Table A1.2a.   Overview of streamflow series from different altitude zones in selected basins.

Station no.	Name	River	Altitude zone			
			0-500	500-1000	1000-1500	>1500
311.6	Nybergsund	Trysilelv	x	x	x	x
2.13	Sjodalsvatn	Sjoa		x	x	x
20.3	Flaksvatn	Tovdalselv	x	x	x	
83.2	Viksvatn	Gaular	x	x	x	x
123.20	Rathe	Nidelv	x	x	x	x
151.15	Nervoll	Vefsna	x	x	x	x
167.3	Kobbvatn	Kobbelv	x	x	x	
212.10	Masi	Alta	x	x		

Table A1.2b.   Overview of point and version numbers assigned to each scenario.

Altitude zone	Observed	HadleyAm3H			ECHAM4	
		Control	A2	B2	Control	B2
0-500	120	125	130	135	140	145
500-1000	121	126	131	136	141	146
1000-1500	122	127	132	137	142	147
>1500	123	128	133	138	143	148

The streamflow series in different altitude zones are available both as daily streamflow in m^3/sec (code 1001) and in specific units as mm/day (code 5000).

Table A1.3   Overview over basins with additional daily time series data of basin average climate data and water balance elements on Hydra II.

Station no.	Name	River	Precipitation	Evaporation	Temperature	Grw.vol	Soil moisture deficit	Snow water equivalent
			0	1	17	2000	2001	2003
2.13	Sjodalsvatn	Sjoa	x	x	x	x	x	x
2.111	Aursunden	Glomma	x	x	x	x	x	x
2.142	Knappom	Flisa	x	x	x	x	x	x
16.19	Møsvatn	Måna	x	x	x	x	x	x
123.20	Rathe	Nidelv	x	x	x	x	x	x
151.15	Nervoll	Vefsna	x	x	x	x	x	x
212.10	Masi	Alta	x	x	x	x	x	x
257.257	Lyse krv	Lyse	x	x	x	x	x	x

APPENDIX II. Overview of files with GIS-coverages.

Seasonal values

PRE_DJF.ASC	Mean of all years for total precipitation (mm) in winter (Dec., Jan., Feb.)
EVA_DJF.ASC	Mean of all years for total evaporation (mm) in winter (Dec., Jan., Feb.)
RUN_DJF.ASC	Mean of all years for total runoff (mm) in winter (Dec., Jan., Feb.)
SMD_DJF.ASC	Mean of all years for daily soil moisture deficit (mm) in winter (Dec., Jan., Feb.)
GWT_DJF.ASC	Mean of all years for daily groundwater storage (mm) in winter (Dec., Jan., Feb.)
TEM_DJF.ASC	Mean of all years for daily temperature (°C) in winter (Dec., Jan., Feb.)

Annual values

PREC.ASC	Mean annual precipitation (mm)
EVAP.ASC	Mean annual evaporation (mm)
RUNOFF.ASC	Mean annual runoff (mm)
MASSBAL.ASC	Mean annual glacier mass balance (mm)
TEMP.ASC	Daily mean daily temperature (°C)
SNOWMAX.ASC	Mean of maxima of yearly snow water equivalent (mm)
SNOWDAYS.ASC	Mean of number of days per year with more than 50 % of ground covered by snow
SMDEFMAX.ASC	Mean of maxima of yearly soil moisture deficit (mm)
GWTOTAL.ASC	Daily mean groundwater storage (mm)

APPENDIX III. Overview over reports from the project.

Førland, E.J., Roald, L.A., Tveito, O.E. & Bauer-Hanssen, I. (2000) Past and future variations in climate and runoff in Norway. *DNMI Report no. 19/00.*

Roald, L.A., Førland, E.J., Tveito, O.E. & Bauer-Hanssen, I. (2000) Annexes to Past and future variations in climate and runoff in Norway. *DNMI Report no. 20/00.*

Skaugen, T.E. and Tveito, O.E. (2002) Heating degree-days – Present conditions and scenario for the period 2021-2050. *DNMI Report No. 01/02 Klima.*

Roald, L.A., Skaugen, T.E., Beldring, S., Wæringstad,T., Engeset, R. and Førland, E.J. (2002) Scenarios of annual and seasonal runoff for Norway based on climate scenarios 2030-49. *NVE-report A 10/02, met.no Report 19/02 Klima.*

Skaugen, T., Astrup, M., Roald, L.A. and Skaugen, T.E. (2002) Scenarios of extreme precipitation of duration 1 and 5 days for Norway caused by climatic change. *NVE-report A 7/02.*

Skaugen, T.E. (2002) Bruk av GIS til å generere historiske tidsserier av temperatur og nedbør for vilkårlige punkt og avrenning for utvalgte nedbørfelt. *DNMI Report Nr. 25/02.*

Engen-Skaugen, T. (2004). Refinement of dynamically downscaled precipitation and temperature scenarios. *Met.no report no. 15/2004 Climate.*

Engeland, K., Skaugen, T.E., Haugen, J.E., Beldring, S., Førland, E.J. (2004). Comparison of evaporation estimated by the HIRHAM and GWB models for present climate and climate change scenarios. *Norwegian Meteorological Institute, met.no Report no. 17/2004 Climate*, 26 pp.

Engen-Skaugen, T., Roald, L.A., Beldring, S., Førland, E.J., Tveito, O.E., Engeland K. & Benestad, R. (2005). Climate change impacts on water balance in Norway. *Met.no report no.1/2005 Climate.*

Tveito, O.E. and Roald, L.A. (2005). Relations between long-term variations in seasonal runoff and large scale atmospheric circulation patterns. *Met.no report no 7/2005 Climate.*

Denne serien utgis av Norges vassdrags- og energidirektorat (NVE)

Utgitt i Oppdragsrapportserie A i 2006

Nr. 1   Lars A. Roald, Stein Beldring, Torill Engen Skaugen, Eirik J. Førland and Rasmus Benestad:
Climate change impacts on streamflow in Norway (74 s.)